

eman ta zabal zazu



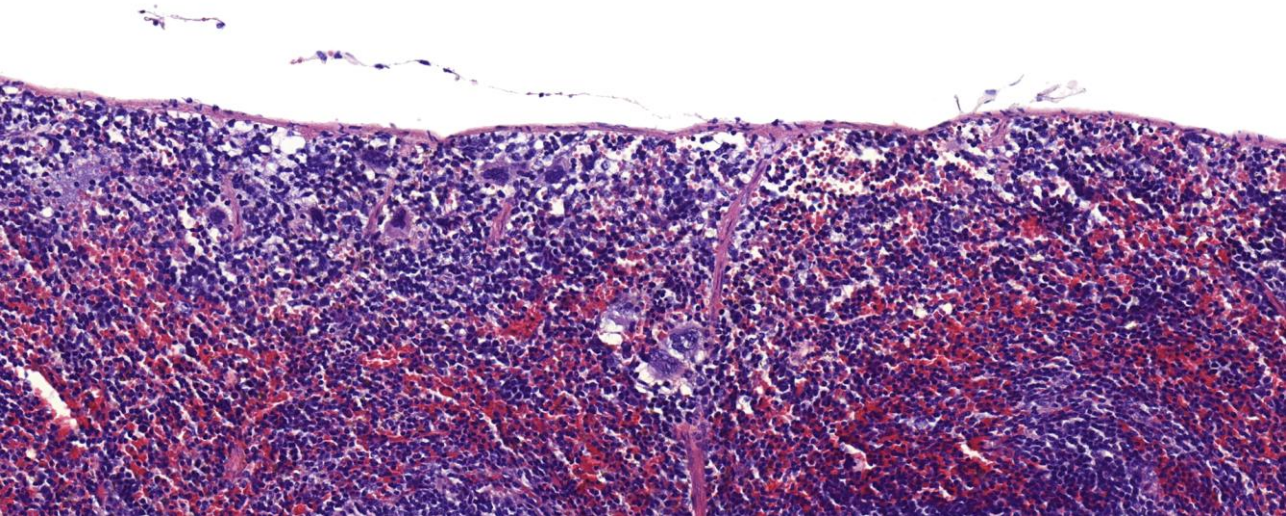
Universidad  
del País Vasco

Euskal Herriko  
Unibertsitatea

# Antibiotic-loaded nanostructured lipid carriers (NLCs) for multiresistant respiratory tract and wound infections

**CLAUDIA VAIRO**

Vitoria-Gasteiz  
2020



# Antibiotic-loaded nanostructured lipid carriers (NLCs) for multiresistant respiratory tract and wound infections

**CLAUDIA VAIRO**

Vitoria-Gasteiz, 2020

Laboratory of Pharmaceutics,  
NanoBioCel Group, School of Pharmacy  
University of the Basque Country (UPV/EHU)



*A journey of a thousand miles  
begins with a single step*

Lao Tzu



## **ACKNOWLEDGMENT FOR THE FINANCIAL SUPPORT**

*Claudia Vairo acknowledges the support provided by BioKeralty Research Institute AIE. This project has been partially funded by the Spanish Ministry of Economy and Competitiveness, in the framework of the TERFIQEC Project (IPT-2011-1402-900000). Also, by the Basque Government in the framework of NANOPLATFORM (KK-2015/0000036) and NANOGROW (ZE-2017/00014) projects, the latter also co-financed by the European Regional Development Fund (ERDF). Finally, her work has also been co-funded by the NANOGSKIN project (00108589), through the ERA-NET EuroNanoMed-III call.*

## **ACKNOWLEDGMENT TO THE EDITORIALS**

*Authors would like to thank the editorials for granting permission to reuse their previously published articles in this thesis. The links to the final version are the following:*

*Vairo C, et al. Nanomedicine. 2020;102259*

*<https://pubmed.ncbi.nlm.nih.gov/32619707/>*

*Pastor M, et al. Nanomedicine. 2019;18:101-111*

*<https://pubmed.ncbi.nlm.nih.gov/30849549/>*

*Vairo C, et al. Int J Pharm. 2019;569:118484*

*<https://pubmed.ncbi.nlm.nih.gov/31260785/>*

*The introduction of this doctoral thesis has been submitted to the International Journal of Antibiotic Agents with the following title: Colistin- and Amikacin-loaded lipid-based drug delivery systems for resistant gram-negative lung and wound bacterial infections (ID: IJAA-D-20-01603)*

## **ACKNOWLEDGMENT TO THE RESEARCH GROUP**

*The thesis has been carried out under a collaboration agreement between the NanoBioCel group of the School of Pharmacy (UPV/EHU) and BioKeralty Research Institute AIE. In addition, we would like to thank the groups that have participated in this project:*

- *Antimicrobial Resistance Laboratory, Vall d'Hebron Research Institute (VHIR). Department of Infectious Diseases, Hospital Universitari Vall d'Hebron, Passeig de la Vall d'Hebron, 119-129, 08035 Barcelona*
- *Department of Pathological Anatomy, Hospital Universitario de Álava (HUA), Vitoria-Gasteiz, Spain*
- *Department of Nuclear Medicine, Clínica Universidad de Navarra, Pamplona, Spain*
- *Small Animal Imaging Research Unit, Center for Applied Medical Research (CIMA) and Clínica Universidad de Navarra, Pamplona, Spain*
- *Department of Pharmacology and Toxicology, University of Navarra, 31008 Pamplona, Spain*
- *Toxicology Unit, Drug Development Unit University of Navarra (DDUNAV), 31008 Pamplona, Spain*

## **GLOSSARY**

**AD:** administered dose

**AMK:** amikacin

**AMR:** antimicrobial resistance

**ATP:** adenosine triphosphate

**CDC:** Center for Disease Control and Prevention

**CF:** cystic fibrosis

**CFU:** colony-forming units

**Chol-SO<sub>4</sub>:** sodium cholesteryl sulphate

**CLSI:** clinical and laboratory standards institute

**CMC:** carboxymethylcellulose

**CMS:** colistin methanesulfonate or sodium colistimethate

**CrCl:** creatinine clearance

**C<sub>ss</sub>:** steady-state plasma concentration

**CT:** computed tomography

**DLS:** dynamic light scattering

**DMSO:** dimethyl sulfoxide

**ECDC:** European Centre for Disease Prevention and Control

**EE:** encapsulation efficiency

**ELS:** electrophoretic light scattering

**EMA:** European Medicine Agency

**EU:** European Union

**EUCAST:** European Committee on Antimicrobial Susceptibility Testing

**FBS:** fetal bovine serum

**FDA:** Food and Drug Administration

**FTIR:** Fourier transform infrared

**GRAS:** generally recognized as safe

**HEPA:** high efficiency particulate air

**HPH:** high pressure homogenization

**HPLC:** high-performance liquid chromatography

**IDSA:** Infectious Disease Society of America

**IM:** intramuscular

**IP:** intraperitoneal

**IR-NLC:** infrared labeled NLC

**ITLC:** instant thin layer chromatography

**IV:** intravenously

**LAI:** liposomal amikacin for inhalation

**LBDDS:** lipid-based drug delivery system

**LPS:** lipopolysaccharide

**LSD:** least significant difference

**MBEC:** minimum biofilm eradication concentration

**MBIC:** minimum biofilm inhibitory concentration

**MBq:** megabecquerel

**MDR:** multidrug-resistant

**MHB:** Müeller Hinton broth

**MIC:** minimum inhibitory concentration

**MLST:** multilocus sequence typing

**modR:** moderate drug-resistant

**MTT:** 3-(4,5- dimethylthiazol-2-yl)-2,5-diphenyltetrazolium bromide

**NLC:** nanostructured lipid carrier

**PBS:** phosphate buffered saline

**PDI:** polydispersity index

**PII:** primary irritation index

**RLU:** relative luminescence units

**SCM:** colistin methanesulfonate or sodium colistimethate

**SD:** standard deviation

**SDS:** sodium dodecyl sulfate

**SI:** stimulation index

**SLS:** sodium lauril sulfate

**SLN:** solid lipid nanoparticle

**SnCl<sub>2</sub>:** stannous chloride

**SPECT:** single photon emission computed tomography

**SPECT/CT:** single photon emission computed tomography/computed tomography

**SPSS:** statistical package for social sciences

**TDM:** therapeutic drug monitoring

**TEM:** transmission electron microscopy

**TSA:** tryptic soy agar

**TSB:** tryptic soy broth

**UK:** United Kingdom

**UV-VIS:** ultraviolet-visible

**VOI:** volumes of interest

**XDR:** extensively drug resistant

**WHO:** World Health Organization

**2-MBT:** 2-Mercaptobenzothiazole

**<sup>99m</sup>Tc:** technetium-99m

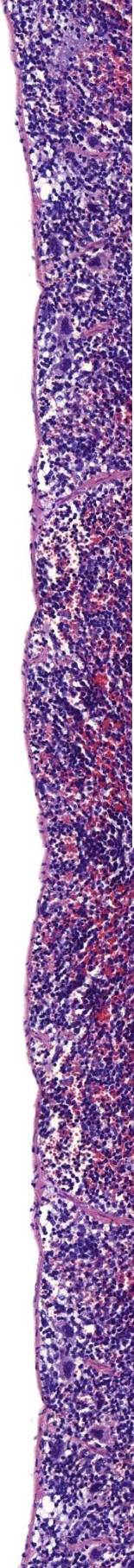
**<sup>99m</sup>TcO<sub>4</sub><sup>-</sup>:** technetium-99m pertechnetate

## INDEX

<b>Introduction</b>	1
<b>Objectives</b>	41
<b>Experimental work</b>	43
Chapter 1. <i>In vitro</i> and <i>in vivo</i> antimicrobial activity of sodium colistimethate and amikacin-loaded nanostructured lipid carriers (NLC)	45
Chapter 2. Safety and effectiveness of sodium colistimethate-loaded nanostructured lipid carriers (SCM-NLC) against <i>P. aeruginosa</i> : <i>in vitro</i> and <i>in vivo</i> studies following pulmonary and intramuscular administration	73
Chapter 3. Preclinical safety of topically administered nanostructured lipid carriers (NLC) for wound healing application: biodistribution and toxicity studies	103
<b>Discussion</b>	131
<b>Conclusions</b>	137
<b>Agradecimientos</b>	141



# Introduction





Antimicrobial resistance (AMR) or the ability of a microorganism to resist the action of an antimicrobial agent is an increasingly serious issue facing global public health that requires a drastic and immediate intervention of all government sectors and society [1]. AMR causes life-threatening infections such as wound and lung infections that lead to high costs to society and public health systems due to long hospital stays and expensive drug therapies [2]. Worryingly, AMR is reported to have recently increased in children [3].

Colistin and amikacin represent the antibiotics of choice to fight against gram-negative resistant wound and lung infections, but their use is greatly limited due to their high toxicity. Thus, new strategies should be investigated to provide safe and effective treatments. In this regard, lipid-based delivery systems, especially nanostructured lipid carriers (NLCs), could represent an interesting approach for their high drug intracellular uptake and controlled release [4]. Both phenomena could enable dose reduction and, consequently, drug toxicity may also decrease [5].

In this review, origin and consequences of AMR along with the general mechanisms of resistance of gram-negative bacteria (*Pseudomonas aeruginosa*, *Acinetobacter baumannii* and *Klebsiella pneumoniae*), classified as a global critical priority, will be described [6,7]. In addition, the fragile balance between efficacy and toxicity of colistin and amikacin, two of the antibiotics capable of tackling such difficult infections, will be analyzed. Besides, lipid-based drug delivery systems (LBDDSs), will be critically evaluated as novel and effective strategies for antibiotic delivery in wound and lung infections, highlighting NLCs as a promising approach to fight against AMR.

## 1. Origins and consequences of AMR

Antibiotics are the trigger of the current and problematic global AMR. It all started with the discovery of penicillin by Alexander Fleming in 1928, considered as a miracle drug revolutionizing medicine during the past half of the 20<sup>th</sup> century [8]. Nevertheless, first warning signs came to light soon when an *Escherichia coli* penicillinase was identified in 1940, a year before penicillin commercialization [9]. However, penicillin resistance quickly worsened from 1943, due to its extensive use. In 1945 four *Staphylococcus aureus* strains were found to overcome the action of

penicillin in hospitalized patients [10]. In 1955 it was already clear that the more antibiotics used the more resistant strains rapidly emerged, easily spreading within hospital or clinical settings by the frequency and the intimacy of contacts [11]. Notwithstanding such early warnings, antibiotics have been overused for the last 75 years, and it seems their use dated back to 2,000 years ago, since a recent study confirmed that some populations from Sudanese Nubia regularly consumed tetracycline, most likely within beer [12]. Besides, the Center for Disease Control and Prevention (CDC) has recently estimated that at least 30 % of all antibiotics prescribed in hospitals of United States are unnecessary or incorrectly prescribed [13]. For all these reasons, it is no surprise that AMR has spread worldwide at an ever-faster rate. Nowadays, antibiotic abuse is generating all sorts of antibiotic resistant bacteria and antibiotic resistant genes, significantly affecting humans directly and indirectly, since both can be frequently found in daily meals, in drinking water and even in the atmosphere [14-16]. Consequently, more resistant bacteria are constantly burgeoning, leading to the emergence of the so-called “superbugs”. The term superbug refers to microbes with multiple mutations endowing high levels of resistance to those antibiotics specifically recommended for their treatment. Superbugs are so widespread and complex that were classified depending on their resistance pattern so that epidemiological surveillance data could be collected and compared crosswise healthcare settings of several countries [17]. Consequently, these multidrug-resistant and extensively drug-resistant bacteria are considered as the most menacing factor for global mortality and morbidity. Moreover, it should be noted that the development of new effective antimicrobial agents is not as fast as the appearance of new resistant strains, perpetuating AMR as a serious threat for human health. It is discouraging how antibiotic discovery, always considered as one of the most significant health-related events of modern times, is turning into a double-edged sword, approaching today an apocalyptic scenario in which AMR is just as important as climate change [18]. Recent forecasts highlighted such alarming situation. In 2018, CDC estimated that annually two million people, in United States alone, were struck by antibiotic-resistant infections that led to 23,000 deaths [19]. In 2019, the World Health Organization (WHO) reported that 25,000 patients died every year in the European Union because of nosocomial serious resistant bacterial infections and at least 700,000 people perished worldwide for the same reason according to the most recent available data

[20-22]. Dame Sally Davies, the England Chief Medical Officer, considered the strong probability of AMR becoming a massive killer by 2040 and, if no action is taken, antimicrobial resistance will probably lead to 10 million deaths worldwide by 2050, surpassing cancer deaths and costing up to \$ 100 trillion [23-25]. Figure 1 shows a general overview of the current AMR situation [22]. The left side represents the global expected distribution of deaths associated to AMR by 2050, while, the right side illustrates the last reported data for casualties due to climate change, cancer and AMR [18,21,22,24].

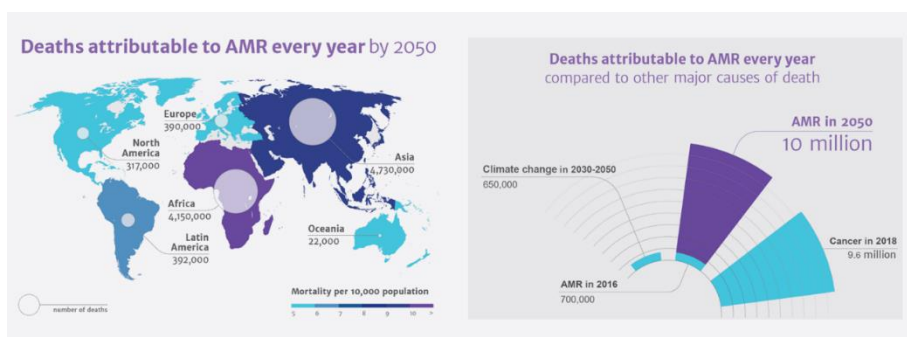


Figure 1. Global overview of AMR issue. Left side, global expected distribution of deaths associated to AMR by 2050; right side, last reported data for climate change, cancer and AMR related deaths. Reproduced and adapted from The Review on Antimicrobial Resistance chaired by Jim O'Neill (©2016) [22].

## 2. General mechanisms of resistance of gram-negative bacteria

Skin and respiratory tract have higher probability of infection being in direct contact with the external environment. Elderly and immunocompromised patients, as well as those with comorbidities, are at greater risk specially in a clinical environment where superbugs are easily found [26]. Once a resistant infection is established, bacteria create persistent and almost impossible-to-eradicate biofilm or more infiltrating infections, directly affecting epithelial integrity, cell migration and proliferation, and hampering the general wound repair mechanisms and the standard airway epithelial functions [26]. Over thousands of years, bacteria have developed different defense mechanisms as a natural process to survive the adversities [27]. Gram-negative mechanisms of resistance can be divided into three general groups, *i.e.* intrinsic, adaptive and acquired. However, the boundaries among them are not easily

identifiable as bacteria can use one, two or the three types of mechanisms simultaneously [28]. Intrinsic resistance is the natural ability of an organism to resist antimicrobial treatments by means of modulating both the permeability of the outer membrane and the non-specific drug efflux pumps, along with the production of antibiotic inactivating enzymes. Adaptive resistance arises from differential gene expression that allows bacteria to react to external stress, resulting in lifestyle changes such as formation of biofilms or persistent cells. Acquired resistance is the most common type of clinical AMR and consists of acquisition of mutations or genes to withstand a particular antibiotic by an antibiotic-sensitive organism (*e.g.* genes coding for  $\beta$ -lactamase enzymes or mutations in bacterial target proteins). Figure 2 summarizes the intrinsic, adaptive and acquired antimicrobial resistance mechanisms frequently arisen in gram-negative bacteria, such as *P. aeruginosa*, *K. pneumoniae* and *A. baumannii*, responsible for two-thirds of AMR related deaths in Europe [28].

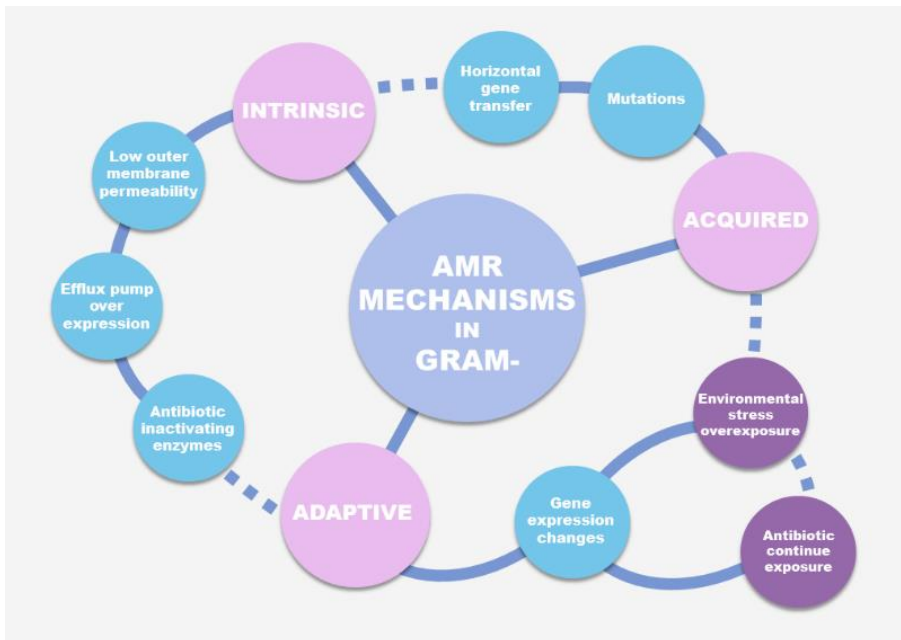


Figure 2. Schematic representation of intrinsic, adaptive and acquired antimicrobial resistance mechanisms in gram-negative bacteria. Intrinsic resistance consists of decreased outer membrane permeability, over-expression of efflux pump and production of antibiotic inactivating enzymes such as  $\beta$ -lactamases. Adaptive resistance occurs when the gene expression changes because of an overexposure to antibiotics and environmental stress. Acquired resistance is driven by mutation and horizontal gene transfer.

Bacteria can use two or three mechanisms simultaneously; thus, boundaries among them are not clearly distinguishable.

### 3. Colistin and Amikacin as effective but toxic antibiotics

Despite those problematic mechanisms of resistance, colistin and amikacin, both alone or in combination, have proven their high efficacy in clinical settings. Thus, their use has exponentially increased in the last years as an effective weapon against AMR [29]. Colistin, also known as polymyxin E, was isolated in 1947 from the bacterium *Paenibacillus polymyxa*. Colistin is a polycationic antibiotic, which targets the outer cell membrane of gram-negative bacteria. There, the  $\alpha,\gamma$ -diaminobutyric acid from colistin competitively displaces cations  $\text{Ca}^{2+}$  and  $\text{Mg}^{2+}$  placed in the phosphate groups of the lipopolysaccharide (LPS) lipid A region, causing LPS disruption, membrane permeability and consequent bacterial death [30]. Currently, colistin methanesulfonate (CMS), representing the colistin inactive prodrug, is the preferred form for parenteral route due to its lower toxicity compared to colistin [31]. On the other hand, amikacin, an aminoglycoside antibiotic, was introduced in 1977 and represents one of the most successful semisynthetic aminoglycosides synthesized by acylation with the 1-(-)- $\gamma$ -amino- $\alpha$ -hydroxybutyryl side chain at the C-1 amino group of the deoxystreptamine moiety of kanamycin A. Amikacin primary mechanism of action implies binding the bacterial 30S ribosomal subunits reducing ribosome proofreading capabilities and increasing mistranslation. This leads to impairment of protein synthesis and production of toxic or non-functional peptides [32]. It is noteworthy to mention that colistin and amikacin have broadly demonstrated their efficacy in chronic infections caused either by a single strain or by a combination of different bacteria. For instance, persistent wound infections are characterized by the ordinary presence of *S. aureus*, *P. aeruginosa*, *Proteus mirabilis*, *E. coli* and *Corynebacterium*. In addition, *S. aureus/P. aeruginosa* association shows the highest resistance to the majority of antibiotics used for gram-negative bacteria, for which the only effective treatment would be amikacin [33]. A study carried out in major burn wounds revealed that the top isolated multiresistant pathogen was *A. baumannii*, followed by *Pseudomonas*, both of them sensitive just to colistin and amikacin [34]. Regarding lung infections, *Streptococcus pneumoniae*, *Haemophilus influenzae*, *S. aureus*, *Mycobacterium tuberculosis*, *K. pneumoniae*, *P. aeruginosa* and *Moraxella*

### *Nanostructured lipid carriers (NLCs) for multiresistant infections*

*catarrhalis* have proven to be the most common causes of bacterial pneumonia in normal host [35,36]. In this regard, colistin and amikacin have been found promising in the treatment of resistant lung bacterial infections [37,38]. Therefore, the need for beating superbugs resulted in the recent re-introduction of colistin and amikacin into clinical practice, despite their replacement in the 1970s by less toxic antibiotics [39,40]. In fact, colistin and amikacin are both neurotoxic, although severe renal impairment is their worst reported side effect. Ototoxicity is also an added amikacin adverse effect. It is well known that related toxicity is dose-dependent and correlates with long exposure to therapy, usually becoming irreversible. The incidence of acute kidney injury ranges from 16.2 % to 77.5 % for colistin and 56,7 % for amikacin, probably depending on the general patient health condition prior to the infection outbreak [41,42]. Instead, ototoxicity associated to amikacin reported incidences between 15 % and 47 % [43,44], depending on age, genetic mutations or the concomitant use of other ototoxic drugs [45]. Therefore, physicians are currently bound to juggle safe and effective doses, aided by the Sanford Guide to Antimicrobial Therapy [46]. However, even then, the rate of premature treatment interruption to avoid potentially serious health risks is really high. As a matter of fact, acute kidney injury has reported to usually appear within the first 72 hours after colistin treatment [47]. A retrospective study carried out in a tertiary care medical center showed that 21 % of patients had to stop colistin therapy due to significant nephrotoxicity [48]. Another retrospective study revealed that around 36 % of patients suffering pulmonary infection had to stop amikacin treatment due to toxic adverse effects [49]. Figure 3 summarizes the last reported data regarding colistin and amikacin nephro- and ototoxicity and the consequential prevalence of treatment interruption.

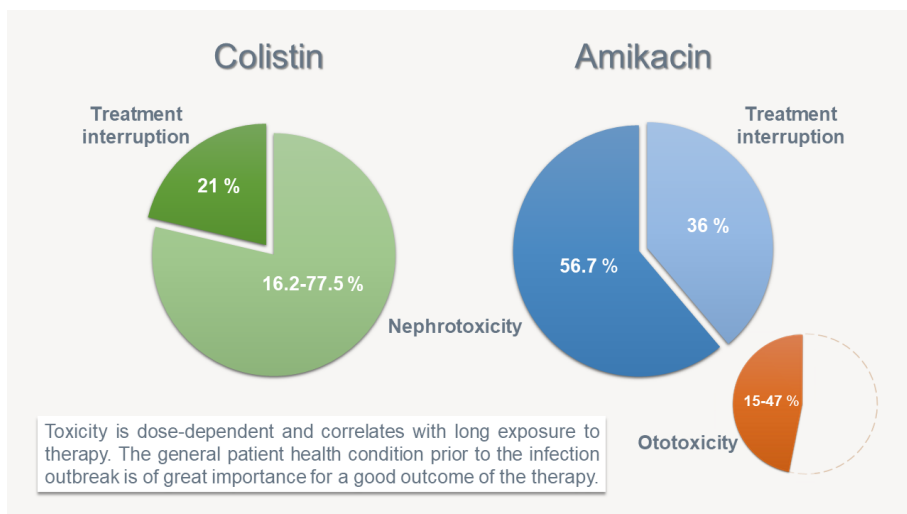


Figure 3. Colistin and amikacin toxicity overview and prevalence of treatment interruption.

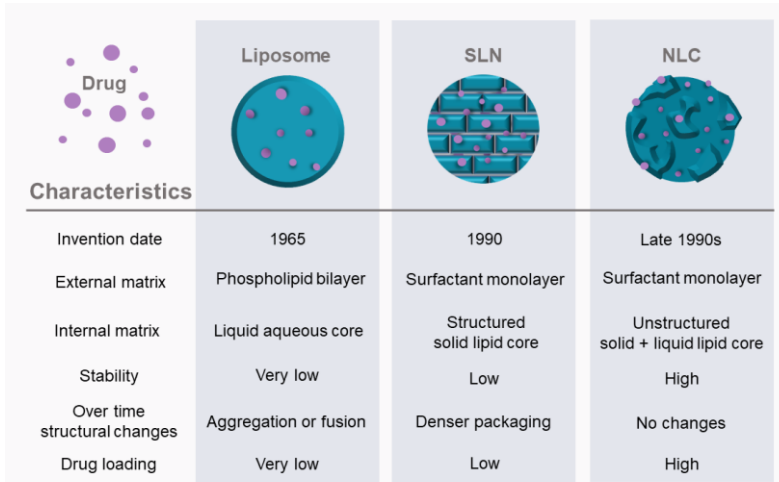
#### 4. Preventive, corrective measures and current clinical strategies against AMR

Colistin and amikacin are effective for defeating gram-negative resistant infections; however, their high toxicity represents a major drawback and limits their use against AMR. Thus, both preventive and corrective measures must be considered together with effective clinical strategies to appropriately tackle AMR. As preventive measures, one of the most recent global efforts is represented by “the AMR Challenge”, in which countries from all over the world are committed to fight together against antimicrobial resistance [50]. Besides, a strict control of daily antibiotic use, education of clinicians, antibiotic rotation/combination, vaccines and prediction tools for future bacterial mutations have been taken into account during the last years [51-53]. In addition, corrective measures, such as the creation of several global funds to enhance the infrastructure for public health surveillance or the improvement of identifying resistant bacteria, have significantly progressed in the last years. In the same line, alternative novel products, such as metal nanoparticles, vaccines together with genetically engineered bacteria and photodynamic therapy, among others, have been developed [54-56]. However, so far, dose adjustment and combination therapy are the most used approaches in clinical settings, both established taking into account pharmacokinetic parameters, such as patient creatinine clearance (CrCl) and drug target plasma concentration. Finding the correct antibiotic dose represents a major

drawback in critically ill patients since a variety of alterations, such as increased volume of distribution, modification of serum protein levels and binding, organ dysfunction and variation in clearance, are common and lead to relevant pharmacokinetic changes [57]. For these reasons, clinically desirable colistin average steady-state plasma concentration ( $C_{ss}$ , 2 mg/L) and amikacin peak serum concentration (64 mg/L) cannot be easily reached in critically ill patients [57-59]. In this regard, substantial interpatient variation in the colistin average  $C_{ss}$  was observed even in those patients with similar CrCl [60]. Two studies clarified that standard colistin administration schedule was not effective, leading to suboptimal plasma concentrations [61,62]. A recent study in critically ill elderly patients also showed that standard amikacin dose (15 mg/kg/day) was not sufficient to achieve the desired peak serum concentration and just 40 % of patients receiving the highest dose (25 mg/kg/day) reached the target level [63]. Those results were confirmed by another study, in which a 30 mg/kg/day dose was tested revealing that only 76 % of critically ill patients reached the target concentration [64]. In this respect, therapeutic drug monitoring (TDM) appeared as an essential technique to avoid sub-therapeutic dosing and, consequently, the appearance of antibiotic resistance and therapeutic failure [65]. In fact, Ehrentraut *et al.* confirmed that the absence of TDM might be unsafe and guideline adherence did not ensure efficient colistin target levels in critically ill patients [66]. In contrast, TDM involvement resulted in a successful adjustment of antibiotic therapy in patients with severe infection [67,68]. It should be noted that when there are no risk factors, combination therapy represents another interesting approach to bypass TDM and reduce health care cost. A prospective, randomized, single-blind study performed in a group of 152 patient showed that TDM exclusion could significantly decrease direct cost of about 235,410 € per 1000 patients/year when amikacin was combined with other antibiotics [69]. In the case of multidrug resistant *A. baumannii*, colistin and amikacin combination was necessary to avoid patient death [70]. However, similar studies in severe ill patients are still lacking, mostly because colistin needs to be used cautiously, especially when combined with other nephrotoxic agents, such as amikacin, and the risk-benefit ratio is not so favorable.

## **5. Lipid-based drug delivery systems as a new successful strategy**

As previously indicated, total eradication of AMR appears to be some way off. Novel and better tools are required, regarding not only design or discovery of new drugs, but also administration methods of existent effective antibiotics, such as colistin and amikacin. In this sense, the main focus is not only to improve treatment efficacy, but also and most important to reduce their toxicity. To this end, novel drug delivery systems allow drug release in a controlled and localized manner. Accordingly, it seems that nanocarriers, as nanotechnology-based formulations, represent an excellent choice for overcoming limitations associated with antibiotic drug therapy, especially referring to toxicity [71]. Among nanocarriers, lipid-based drug delivery systems (LBDDSs), such as liposomes, solid lipid nanoparticles (SLNs) and nanostructured lipid carriers (NLCs), are considered as the most promising approach due to their biocompatibility, safety and capability to improve lipophilic drug disposition. Liposomes were invented in 1965 and have been used for pharmaceutical and cosmetic applications for several years despite their limited stability and poor encapsulation efficacy. It was only in 1990 that SLNs and NLCs were identified as improved substitutes to liposomes. SLNs are composed of solid lipids, are more stable and suitable for high scale production but their crystalline structure lead to a low drug incorporation rate. Instead, NLCs were developed at the end of the 1990s as a response to SLN drawbacks and represent the ultimate enhanced version of LBDDSs. NLCs are composed of a blend of solid and liquid lipids, forming an irregular structure, which confers high stability, enhanced loading capacity and prevents drug expulsion during storage. All of the abovementioned LBDDSs have already shown improved efficacy compared to free antibiotic administration, showing that lower doses of colistin- and amikacin-encapsulated LBDDSs are just as effective as higher doses of free antibiotics [72]. Hence, LBDDSs represent a valuable strategy for toxicity reduction mainly due to the use of lower amounts of drug. Figure 4 represents an overview of LBDDS most important features. In the following sections, the most relevant studies about liposomes, SLNs and NLCs loaded with colistin or amikacin with intended use against resistant strains for lung and wound infections are reported and critically discussed.



	Liposome	SLN	NLC
<b>Characteristics</b>			
Invention date	1965	1990	Late 1990s
External matrix	Phospholipid bilayer	Surfactant monolayer	Surfactant monolayer
Internal matrix	Liquid aqueous core	Structured solid lipid core	Unstructured solid + liquid lipid core
Stability	Very low	Low	High
Over time structural changes	Aggregation or fusion	Denser packaging	No changes
Drug loading	Very low	Low	High

Figure 4. LBDDS most important characteristics. Liposomes present an external phospholipid bilayer and a liquid aqueous core. Their major drawbacks are a very low physical stability, due to aggregation or fusion upon storage, along with a very low drug loading. SLNs consist of an external surfactant monolayer and a solid lipid core that can be compared to a “symmetric brick wall”. Their stability is low due to important structural reorganizations over time, which lead to a denser packaging and a low drug loading. NLCs represent the last improved version of LBDDSs. They are composed of an external surfactant monolayer and an internal matrix containing both solid and liquid lipids, with a structure similar to a “welsh natural stone”. This type of matrix confers high stability, since no structural changes occur over time, which also guarantees high drug loading.

## 6. Colistin LBDDSs for resistant lung and wound infections

Although colistin and liposomes were both available in 1965, it was in the last decade when the first investigations were carried out to develop colistin-loaded liposomes for lung infections. In 2012, Wallace *et al.* studied the interactions between colistin and the liposome matrix in order to anticipate any possible limitation for pulmonary inhalation [73]. Results showed a low encapsulation efficiency (EE) of approximately 50 %, confirming the need to improve the formulation. Thus, some authors tried to enhance colistin-bilayer electrostatic attraction modifying liposomes with sodium cholesteryl sulphate (Chol-SO<sub>4</sub><sup>-</sup>) [74]. As expected, EE reached 86 % compared to 60.7 % of the control formulation. This optimized formulation was also administered by intratracheal instillation resulting in improved therapeutic efficacy in a murine pulmonary *P. aeruginosa* infection model compared to the colistin solution [75]. This research group also performed the first intravenous biodistribution study demonstrating that liposomal colistin-Chol-SO<sub>4</sub><sup>-</sup> needed to be PEGylated to avoid

lung embolism [76]. Worryingly, colistin-Chol-SO<sub>4</sub><sup>-</sup> formulation showed significant lung affinity and a rapid and extremely high accumulation early after injection producing aggregation. Therefore, PEGylation achieved prolonged blood circulation and homogeneous distribution among lungs, kidneys and spleen avoiding this undesirable effect (Figure 5).

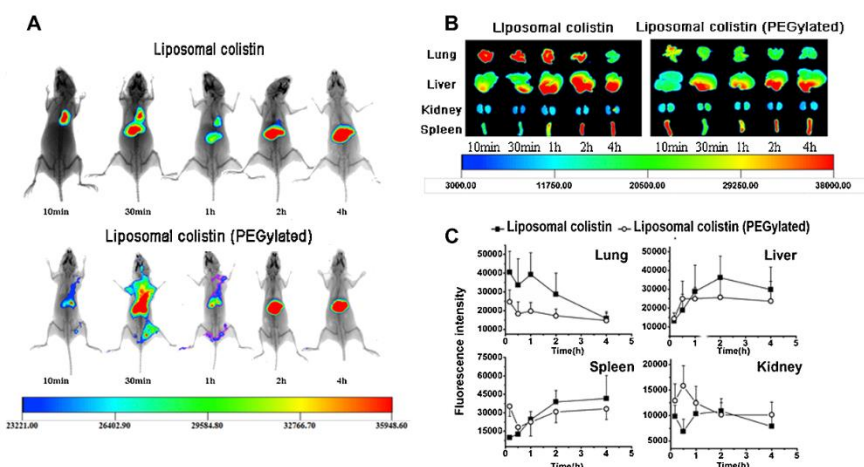


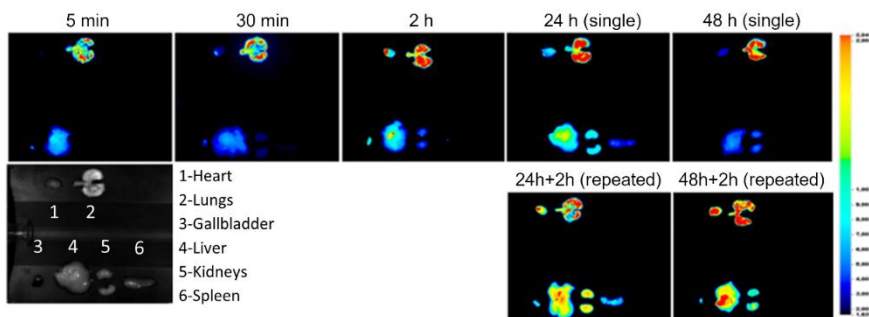
Figure 5. (A) *in vivo* and (B) *ex vivo* fluorescence imaging of Balb/c nude mice after intravenous administration of DiR-labeled liposomal colistin-Chol-SO<sub>4</sub><sup>-</sup> and its PEGylated form; (C) semi-quantitative results for fluorescence signal from lung, liver, spleen and kidney at different time points after both DiR-labeled formulation injection. PEGylation achieved prolonged blood circulation and homogeneous distribution, avoiding liposome aggregation in lungs. Reproduced and adapted from Joseph Li *et al.* (©2016)[76].

Taking advantage of its membrane permeabilizing ability, colistin has been also loaded in liposomes along with azithromycin. Consequently, when colistin was incorporated into the formulation, azithromycin release raised from 4.9 to 30 % enhancing azithromycin effectiveness [77]. Colistin has also been combined with ciprofloxacin for liposomal co-delivery. This combined liposomal formulation showed *in vitro* safety and achieved the same *in vitro* antimicrobial activity against multidrug resistant *P. aeruginosa* as those of monotherapies [78]. An *in vitro* evaluation in a human lung epithelial cell model also revealed that colistin and ciprofloxacin liposomal combination could enhance drug retention on the lung epithelial surfaces [79]. In addition, an inhalable powder of colistin and ciprofloxacin co-loaded liposomes displayed superior antibacterial activity against two clinical

isolates of *P. aeruginosa* compared to each antibiotic *per se* [80]. Therefore, this combined formulation represents a promising approach to treat multidrug resistant *P. aeruginosa* respiratory infections although further *in vivo* preclinical safety studies are required. Regarding other LBDDSs, colistin had also been encapsulated into SLNs and NLCs. Colistin-SLNs proved enhanced efficacy against *P. aeruginosa* clinical isolates from cystic fibrosis (CF) patients eradicating biofilm compared to the free drug and a similar activity when tested with planktonic bacteria [81]. Other investigation focused on the treatment of *P. aeruginosa* revealed that SLNs and NLCs loaded with CMS presented the same *in vitro* efficacy against mucoid *P. aeruginosa* strains isolated from CF patients; nonetheless, CMS-NLCs showed interesting advantages such as superior EE, increased drug release and lower toxicity compared to CMS-SLNs [82]. Likewise, stability regarding both CMS-NLC antibacterial activity and physico-chemical properties were maintained over a year at 5 and 25 °C with 60 % relative humidity [83]. Besides, spatiotemporal dependence of *P. aeruginosa* biofilm viability analyzed after colistin-NLC treatment showed 75 % of cell death vs 20 % for free colistin in just 20 min [84]. These results are consistent with our study proving preclinical safety and effectiveness of CMS-NLCs [5]. Briefly, CMS-NLCs administered following pulmonary and intramuscular (IM) routes in an acute mouse pneumonia model showed on the one hand to be safe, even when doubling the dose and, on the other hand, to be as effective as free CMS when used at 10-fold and 50-fold lower doses for pulmonary and IM administration, respectively. Moreover, biodistribution studies of infrared labeled NLCs (IR-NLCs) administered by the pulmonary route showed that IR-NLCs were mainly biodistributed in lungs and to a lesser extent in liver, maintaining the signal in lungs high and homogeneous after 48 h. When repeated doses were administered at 24 and 48 h, signal in lungs increased. IR-NLC IM administration initially revealed the highest signal at the injection site and then transferred to other organs, such as the liver and gallbladder. When repeated doses were administered, signal increased following the former distribution. Biodistribution images of IR-NLCs are represented in Figure 6. In addition, our recent *in vivo* study revealed that intraperitoneal (IP) CMS-NLC administration showed superior efficacy than the intramuscular route using 40-fold lower CMS total dose in a pulmonary infection model produced by an extensively drug-resistant *A. baumannii* strain [85]. Such results are extremely promising considering the high toxicity of free

colistin. Thus, such dose reduction by means of NLC formulation could be a potential strategy to achieve safer and more affordable treatments against multiresistant gram-negative lung infections.

#### A IR-NLCs, Pulmonary



#### B IR-NLCs, IM

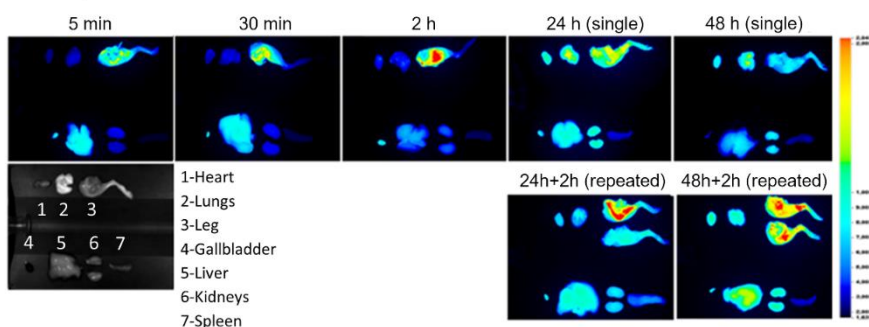


Figure 6. Biodistribution study. (A) IR-NLC distribution after nebulization by Microsprayer® aerosolizer. (B) IR-NLC biodistribution after IM administration. Reproduced and adapted from Marta Pastor *et al.* (©2019) [5].

Oddly enough, no studies regarding colistin LBDDSs for wound infections have been published so far, although it will be only a matter of time. In fact, our research group has already performed preliminary safety studies for topical administration of blank NLCs, both on intact and impaired skin, demonstrating safety for such type of application [86]. In essence, colistin-NLC topical administration for infected wounds could represent an interesting niche opportunity to be exploited.

A summary of all reported colistin LBDDSs for pulmonary infections is provided in Table 1.

*Nanostructured lipid carriers (NLCs) for multiresistant infections*

Table 1. Summary of colistin-loaded LBDDs used for pulmonary infections.

LBDDS	Antibiotic	Type of study	Bacteria	Administration route	Results	Ref.
Liposomes	Colistin CMS	<i>in vitro</i>	-	-	Both colistin- and CMS-loaded liposomes were considered unsuitable for <i>in vivo</i> pulmonary inhalation due to their <i>in vitro</i> colloidal instability and rapid antibiotic release.	[73]
	Colistin	<i>in vivo</i>	-	Intravenous	Colistin-entrapped liposomes of Chol-SO <sub>4</sub> <sup>-</sup> and coated Chol-SO <sub>4</sub> <sup>-</sup> /colistin complex liposomes improved colistin EE and enhanced pharmacokinetics compared to a free colistin solution. Pegylated colistin-entrapped liposomes of Chol-SO <sub>4</sub> <sup>-</sup> reduced aggregation and transient embolism in lung capillaries. The pegylated formulation significantly increased the maximum-tolerated dose, prolonged blood circulation and decreased colistin distribution in kidney.	[74,76]
	Colistin	<i>in vivo</i>	-	Intratracheal instillation	Colistin-entrapped liposomes of Chol-SO <sub>4</sub> <sup>-</sup> presented an enhanced antibiotic EE. In addition, a superior therapeutic efficacy was achieved due to a higher colistin retention in lungs and a consequent lower systemic biodistribution.	[75]
	Colistin Azithromycin	<i>in vitro</i>	-	-	Azithromycin liposomes and colistin-azithromycin liposomes were successfully produced. Azithromycin liposomes showed high EE (> 98 %) but a slow drug release (4.9-22 %). Colistin co-encapsulation did not change azithromycin EE; but considerably accelerated its release, probably due to the colistin permeabilizing ability, enhancing azithromycin effectiveness.	[77]
	Colistin Ciprofloxacin	<i>in vitro</i>	<i>P. aeruginosa</i>	-	Colistin and ciprofloxacin liposomes showed an EE of 67 % and 85.2 %, respectively. Incorporation of colistin significantly accelerated ciprofloxacin release. <i>In vitro</i> cytotoxicity assays confirmed that liposomes were safer than a	[78,79]

					free antibiotic solution, presenting an improved <i>in vitro</i> activity compared to the monotherapies. No toxicity was found in an <i>in vitro</i> lung epithelial model and, in addition, liposomes tended to be trapped within the mucus or on the cell monolayer, which could improve the drug retention time at the infection sites further promoting antibiotic sustained release.	
	Colistin Ciprofloxacin	<i>in vitro</i>	<i>P. aeruginosa</i>	-	An inhalation dry powder formulation comprising colistin and ciprofloxacin co-loaded liposomes was prepared by the ultrasonic spray-freeze-drying technique. The optimized formulation containing 5 µg/mL colistin and 20 µg/mL ciprofloxacin was not cytotoxic in A549 epithelial alveolar cells. In addition, liposomal formulation displayed superior antibacterial activity against clinical isolates of <i>P. aeruginosa</i> compared to each antibiotic <i>per se</i> .	[80]
SLNs and NLCs	Colistin	<i>in vitro</i>	<i>P. aeruginosa</i>	-	Colistin-SLNs and colistin-NLCs were tested against different <i>P. aeruginosa</i> clinical isolates from CF patients in planktonic cultures and biofilm. Colistin-SLCs were less active than colistin-NLCs, which also showed the same <i>in vitro</i> antimicrobial activity as the free drug against planktonic bacteria, but a considerably higher effectiveness eradicating biofilm.	[81,84]
	CMS	<i>in vivo</i>	<i>P. aeruginosa</i>	Pulmonary nebulization	Nebulization through a mesh vibrating nebulizer did not affect CMS-SLN and CMS-NLC integrity. Both nanoparticles appeared to be less toxic than free CMS in cell culture. <i>In vivo</i> biodistribution studies showed that nanoparticles, especially NLCs, spread homogeneously through the lung and that no lipid nanoparticle migration occurred to other organs. Only CMS-NLCs maintained the antibacterial activity and suitable physico-chemical properties over a year.	[82,83]

*Nanostructured lipid carriers (NLCs) for multiresistant infections*

NLCs	CMS	<i>in vivo</i>	<i>P. aeruginosa</i>	Pulmonary Intramuscular	CMS-NLCs were effective in a mouse acute pneumonia model. No toxicity was reported and nanoparticles distributed efficiently through the lung and liver after both pulmonary or intramuscular administrations.	[5]
	CMS Amikacin	<i>in vivo</i>	<i>P. aeruginosa</i> <i>K. pneumoniae</i> <i>A. baumannii</i>	Intraperitoneal Intramuscular	Both CMS-NLCs and amikacin-NLCs were successfully produced through high pressure homogenization. The <i>in vivo</i> study carried out in a neutropenic mouse acute pneumonia model infected with <i>A. baumannii</i> demonstrated that CMS-NLCs achieved the same effect as free CMS with a 10-fold dose reduction and a considerably more spaced administration (6mg/kg q24h vs 60mg/kg q6h).	[85]

## 7. Amikacin LBDDSs for resistant lung and wound infections

First evidence of successfully developed amikacin-loaded liposomes against *P. aeruginosa* dates back to 1995 [87]. Three years later their ability to reduce antibiotic oto- and hepatic toxicity was already proved [88]. In this regard, two formulations reached clinical trials and one of them managed to be registered and commercialized. In the late 1980s, the Californian company Vestar Inc. (later merged with NeXagen Inc. to form NeXstar Pharmaceuticals until its acquisition by Gilead Sciences Inc.) already mastered liposome technology and developed Mikasome<sup>®</sup>, a small (50 nm) unilamellar low-clearance liposome formulation containing amikacin for intravenous and extravascular administrations. The company started a Phase I clinical trial in 1993 to evaluate Mikasome<sup>®</sup> renal safety and five years later a Phase II clinical trial in patients with hospital-acquired pneumonia and bacterial infections related to CF [89,90]. After intravenous and extravascular administrations, Mikasome<sup>®</sup> showed prolonged plasma residence (half-life > 24 h), sustained efficacy in gram-negative infection models and an increased drug presence in all tissues compared to conventional amikacin; thus, allowing an extended dosing interval [91,92]. Specifically, a pharmacokinetic study in rhesus monkeys determined that Mikasome<sup>®</sup> could be safely administered at prolonged intervals ranging from 2 to 7 days, maintaining the desired effect [93]. Despite these promising results, Mikasome<sup>®</sup> has not yet been commercialized. Instead, Arikayce<sup>®</sup> (previously Arikace<sup>®</sup> from Transave Inc. before being acquired by Insmed Inc.) represents the first and only commercialized sustained-release liposomal amikacin for inhalation (LAI) featuring about 75 % EE and 260 nm particle size [94]. Shrenik *et al.* published the first LAI optimization study regarding the influence of fine excipient particles on performance of dry powder inhaler [95]. Thus, the company characterized liposome lung deposition according to the droplet size by means of an Andersen cascade impactor, showing that almost all formulation was homogeneously distributed within the lungs [96]. Successive *in vivo* studies demonstrated that Arikayce<sup>®</sup> easily penetrated into *P. aeruginosa* rat lung biofilms and infected mucus, releasing amikacin in a slow, sustained manner and being orders of magnitude more effective than inhaled free amikacin [97]. Additionally, LAI proved to be taken up by macrophages when administered in healthy rats and easily eliminated at the end of the treatment,

preserving macrophage function [98]. Optimization of  $^{99m}\text{Tc}$ -labeled LAI was also successfully carried out for future clinical studies [99]. Indeed, LAI lung deposition and clearance studies performed in healthy male volunteers by means of a gamma scintigraphy confirmed that inhalation of a single dose of liposomal amikacin (120 mg) was well tolerated [100]. In the light of the above, Arikayce<sup>®</sup> resulted to be an interesting therapeutic option for the treatment of CF patients with *P. aeruginosa* pulmonary infections being more effective than free amikacin due to the enhanced lung disposition. The first pharmacokinetic and pharmacodynamic evaluation in 24 CF patients showed LAI antibacterial efficacy when administered in a single dose of 500 mg/day and supported dose selection for further clinical studies [101]. With that in mind, other clinical trials also confirmed that 560 mg Arikayce<sup>®</sup> once-daily was safe and effective in CF patients with *P. aeruginosa* infection [102,103]. In addition, Bilton *et al.* compared once-daily dose of 590 mg LAI with a twice-daily dose of 300 mg of a commercially available tobramycin inhalation solution, confirming that a single administration was just as effective as a double dose of tobramycin [104]. In essence, initial Phase I and II clinical studies demonstrated that Arikayce<sup>®</sup> was a safe formulation capable of improving lung function after 14-28 days of treatment; besides, a Phase III study compared to inhaled tobramycin revealed similar results between the two formulations with one second increase in forced expiratory volume at the end of the treatment. Notwithstanding these good results in gram-negative bacteria, currently, Arikayce<sup>®</sup> is commercially available in 590 mg/vials for single use as the first and only Food and Drug Administration approved medication for gram-positive *Mycobacterium avium* complex lung disease, necessarily used in combination with other antibiotics to limit amikacin toxicity. Clearly, LAI enabled sustained amikacin release and an increased drug disposition in the lungs; however, the high administration dose (590 mg) remains the main responsible for its nephro-, neuro- and ototoxicity; therefore, other LBDDSs should be investigated. The first amikacin-SLNs were developed and optimized in the last decade. Varshosaz *et al.* achieved an improved particle size of about 150 nm and 90 % EE along with a suitable polydispersity index. These spherical SLNs had a drug release for up to a week without significant burst effect [105]. The same authors later improved amikacin-SLN suspension stability through lyophilization using sucrose, dextran or mannitol as cryoprotectants [106]. Results demonstrated that 12 % sucrose limited nanoparticle

aggregation after reconstitution, although particle size increased about 100 nm post-lyophilization. Moreover, these lyophilized SLNs showed a 2-fold improved activity compared to free amikacin against a pathogenic *P. aeruginosa* strain and higher stability compared to nanoparticles in suspension [107]. Finally, amikacin-SLN *in vivo* biodistribution studies demonstrated that pulmonary administration was safer than the intravenous route since negligible SLN amount reached kidneys, limiting amikacin nephrotoxicity [108]. Based on these results, our research group followed the LBDDS trend to achieve safer amikacin delivery and developed various amikacin-NLC formulations, which proved to be effective against a significant amount of clinical *P. aeruginosa*, *K. pneumoniae* and *A. baumannii* strains [85]. Further studies should be performed to evaluate the real NLC suitability to reduce amikacin toxicity, nonetheless future looks promising.

Several works have been published regarding amikacin LBDDSs for wound skin infections. A study published in 1995 indicated that amikacin liposomes fully protected collagen from adherence of 27 clinical *P. aeruginosa* strains, suggesting that its application could be advantageous in injured tissues in which extracellular matrix structures, such as collagen type I, became exposed [109]. Amikacin liposomes also showed enhanced efficacy compared to the free antibiotic when tested in human dermis matrix infected with *P. aeruginosa* strains isolated from burn wounds [110]. Finally, it is noteworthy to mention a special LBDDS developed in the late 1990s called DepoFoam<sup>®</sup> (SkyePharma Inc., now Pacira Pharmaceuticals Inc.). DepoFoam<sup>®</sup> is a honeycomb of multivesicular liposomes releasing encapsulated drug over several weeks after non-vascular administration due to erosion and reorganization of lipid membranes. Local application of DepoFoam<sup>®</sup> on the surface of prosthetic grafts has been proposed to prevent post-surgical infections [111]. Certainly, this formulation could pave the way to an unexplored area of nanotechnology, extremely useful for infected surgical fields and capable of massively reducing sepsis and second unscheduled surgeries, especially because DepoFoam<sup>®</sup> has proven sustained therapeutic levels of amikacin at a target site and reduced systemic toxicity [112]. Figure 7 shows DepoFoam<sup>®</sup> macroscopical aspect. There is no evidence of amikacin-SLN use in infected wounds; nonetheless, our research group has already shown safety of blank NLCs, as an improved version of liposomes and SLNs, for topical

### *Nanostructured lipid carriers (NLCs) for multiresistant infections*

application as already mentioned in the previous section [86]. In addition, our group has recently developed NLCs loaded with amikacin that could be further redirected towards the field of infected wounds [85]. NLCs as carriers for amikacin with intended use against wound infections represent an interesting forward-looking approach waiting to be exploited.

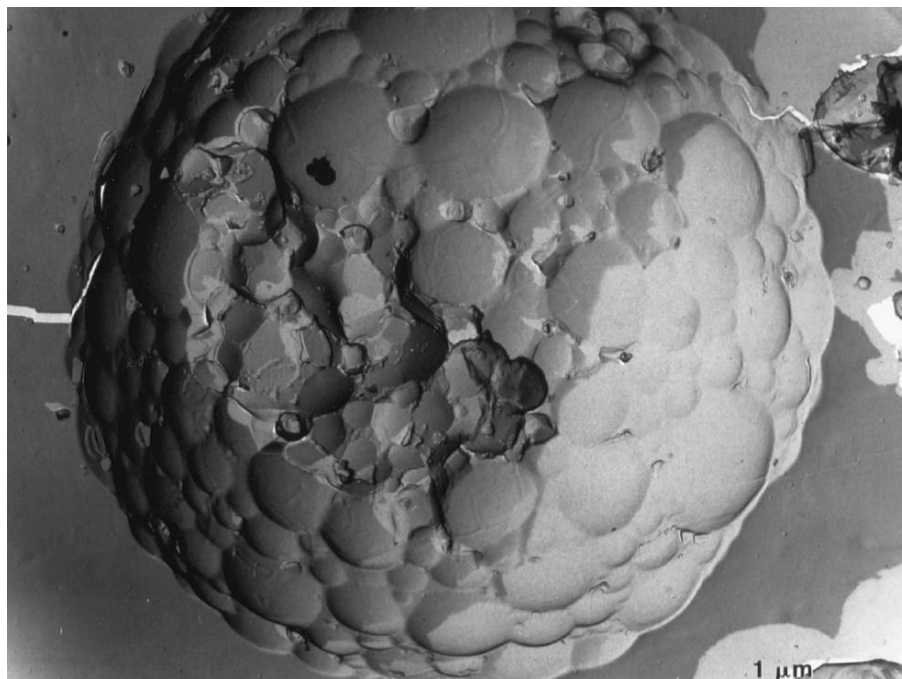


Figure 7. Scanning electron micrograph of a DepoFoam<sup>®</sup> particle (courtesy M. B. Sankaram, DepoTech Corporation). Each lipid particle (10 μm) contained several individual chambers, each bounded by a lipid bilayer. Amikacin can be found in the internal aqueous matrix. Reproduced and adapted from Joseph Huh *et al.* (©1998) [111].

A summary of all amikacin LBDDSs cited in this section, both for pulmonary and wound infections, is provided in Table 2.

Table 2. Summary of amikacin-loaded LBDDs used for pulmonary and wound infections.

LBDDS	Antibiotic	Type of study	Bacteria	Administration route	Results	Ref.
Liposomes	Amikacin Netilmicin Tobramycin	<i>in vitro</i>	<i>P. aeruginosa</i>	-	Cationic liposomes were successfully produced and presented a slightly better EE compared to anionic liposomes. No significant differences were found in drug release or antimicrobial activity.	[87]
	Amikacin Amphotericin B	-	-	-	Oto- and hepatic toxicity can be limited by liposome vectors allowing the use of higher doses of amikacin for longer periods.	[88]
	Amikacin (Mikasome®)	Clinical	-	-	Mikasome® produced a significant killing effect so that liposomal technology may reduce amikacin toxicity.	[89]
	Amikacin (Mikasome®)	Clinical	-	-	Mikasome® was successfully tested in 30 patients with complicated urinary tract infections and also in patient with hospital-acquired pneumonia and bacterial infections related to cystic fibrosis.	[90]
	Amikacin (Mikasome®)	<i>in vivo</i>	-	Intravenous Intraperitoneal Intramuscular Subcutaneous	Mikasome® increased and prolonged amikacin exposure in plasma, local tissues and lymph nodes, suggesting that an extended dosing interval could be possible (from 2 to 7 day) for chronic or prophylactic therapy to achieve high levels of liposomal amikacin with minimal exposure to free amikacin.	[91-93]

*Nanostructured lipid carriers (NLCs) for multiresistant infections*

				Intratracheal instillation		
Amikacin (Arikayce®)	-	<i>P. aeruginosa</i>	Pulmonary	Liposomal amikacin administered by inhalation enhanced drug delivery and drug retention in CF patients' airways. Arikayce® allowed once-daily dosing, mucus and biofilm penetration and potentially prolonged off-drug periods.	[94]	
Amikacin	<i>in vitro</i>	-	-	Different factors, such as liposomal charge, addition of fines and order of mixing fines, can have a significant effect on <i>in vitro</i> deposition of liposomal amikacin dry powder.	[95]	
Amikacin (Arikayce®)	<i>in vitro</i>	-	-	Formulation was aerosolized with an eFlow® nebulizer, coupled to an Andersen cascade impactor and analyzed for lipid-to-drug ratio, amikacin retention and liposome size. Results showed that liposomes were homogenously distributed within the lungs.	[96]	
Amikacin (Arikayce®)	<i>in vivo</i>	<i>P. aeruginosa</i>	Pulmonary	Liposomal amikacin was released in a slow and sustained manner in normal rat lungs, penetrated readily into biofilms and was significantly more effective than inhaled free amikacin in infected lungs. In addition, Arikayce® proved to be taken up by macrophages in a dose-dependent manner, and easily eliminated at the end of the treatment, preserving macrophage function.	[97,98]	
Amikacin	Clinical	-	Pulmonary	Liposomes were successfully radiolabeled with <sup>99m</sup> Tc. The aerosol droplet size distribution, gravimetrically determined, was similar to that measured by radioactivity. In addition, the high labelling efficiency and stability were adequate to evaluate the deposition and	[99,100]	

					clearance in the lung by clinical gamma scintigraphy. 120 mg of nebulized liposomal amikacin resulted in prolonged retention in the lungs of healthy volunteers. The treatment was well tolerated.	
Amikacin	Clinical	<i>P. aeruginosa</i>	Pulmonary		Preliminary pharmacokinetic and pharmacodynamic studies administrating 500 mg/day of liposomal amikacin demonstrated a significant LAI antibacterial activity just in some patients, suggesting that larger doses may be required.	[101]
Amikacin (Arikayce®)	Clinical	<i>P. aeruginosa</i>	Pulmonary		Arikace® was tested once-daily at different doses. The highest dose (560 mg) demonstrated acute tolerability, safety, biologic activity and efficacy in CF patients with <i>P. aeruginosa</i> infection.	[102,103]
Amikacin Tobramycin	Clinical	<i>P. aeruginosa</i>	Pulmonary		Once-daily liposomal amikacin (590 mg) and twice-daily tobramycin solution (300 mg) administrations showed similar results in terms of antibacterial activity.	[104]
Amikacin Polymyxin B	<i>in vitro</i>	<i>P. aeruginosa</i>	Topical		Amikacin liposomes completely removed 27 clinical <i>P. aeruginosa</i> strains from collagen type I, being a good choice for injured tissues in which extracellular matrix structures become exposed. In addition, liposomal formulation presented enhanced effectiveness removing <i>P. aeruginosa</i> microcolonies growing on dermal matrix compared to the free antibiotics.	[109,110]
Amikacin (DepoFoam®)	<i>in vivo</i>	<i>S. aureus</i>	Topical		Amikacin sustained-release applied to infected contaminated grafts increased survival and decreased postoperative graft infections.	[111]
Amikacin (DepoFoam®)	Clinical	-	Injectable		DepoFoam® effectively extended amikacin half-life, showing prolonged duration of therapeutic drug concentrations.	[112]

*Nanostructured lipid carriers (NLCs) for multiresistant infections*

SLNs	Amikacin	<i>in vitro</i>	-	-	Improved SLNs were successfully developed following predictive models by central composite design, a mathematical approach for product and process optimization. Amount of lipid phase, the drug/lipid ratio and volume of aqueous phase were the most important affecting variables. The optimized particle size was $149 \pm 4$ nm and $88 \pm 5$ % EE.	[105]
	Amikacin	<i>in vitro</i>	<i>P. aeruginosa</i>	-	SLNs were active against <i>P. aeruginosa</i> strains <i>in vitro</i> . MIC and MBEC of amikacin-SLNs was about two-fold lower compared to the free drug. SLN stability was increased using sucrose, dextran or mannitol as cryoprotectants. Lyophilization with sucrose maintained a sustained release behavior and produced a burst effect in the first 2 h. Also, pulmonary delivery caused higher drug concentration in lungs than kidneys, limiting its nephrotoxicity.	[106-108]
NLCs	Amikacin CMS	<i>in vitro</i>	<i>P. aeruginosa</i> <i>K. pneumoniae</i> <i>A. baumannii</i>	-	Amikacin-NLCs were active <i>in vitro</i> against a large number of <i>P. aeruginosa</i> , <i>K. pneumoniae</i> , <i>A. baumannii</i> clinical strains and displayed size values around 100 nm and a high EE of about 92 %.	[85]
	-	<i>in vitro</i>	-	Topical	Blank-NLCs were safe when administered on intact skin and may potentially exert a local effect after topical administration on wounds since no systemic absorption was shown. NLCs remained on the wound at least for 24 hours, avoiding a systemic absorption.	[86]

## 8. Conclusions

AMR represents a serious problem that needs to be addressed nowadays. Colistin and amikacin are the last available weapons to fight against multiresistant gram-negative bacterial infections due to their high neuro- and nephrotoxicity. Therefore, clinicians are forced to choose between an effective and safe dose, mostly leading to treatment failure. In this regard, LBDDSs represent a captivating strategy to reduce drug toxicity, capable of releasing antibiotics in a sustained manner and allowing dose reduction. Among LBDDSs, liposomes are the most popular systems due to their early development. Nevertheless, their limitations paved the way to SLN development and finally to NLCs, representing the last and improved version of lipid-based carriers. Colistin LBDDSs have been widely studied in lung infections; liposomes, SLNs as well as NLCs have been tested *in vivo* in pneumonia models with promising results, achieving a significant dose reduction, enhanced efficacy and a presumable lower toxicity. In contrast, no evidences have been found in the field of infected wounds, which represents a great opportunity to be exploited in the near future. On the contrary, amikacin liposomes reached the market several years ago, both for lung and wound infections. However, the administered amikacin dose for lung infections is still very high and necessarily needs improvement. Both amikacin-SLNs and NLCs, but especially NLCs being the latest improved version of LBDDSs, could represent a promising approach for amikacin administration in lung and wound infections due to their enhanced properties. In essence, NLCs could be the ultimate safe strategy for colistin and amikacin delivery to fight against gram-negative lung and wound infections.

## 9. Acknowledgments

This research was partially funded by the Centre for the Development of Industrial Technology (CDTI) through the 8<sup>th</sup> Joint Transnational Call within the framework of the ERA-NET EuroNanoMed-III [EXP: 00108589]; and co-funded by the Basque Government as part of the Hazitek program [EXP: ZE-2017/00014] and by the European Regional Development Fund (ERDF).

## 10. References

- [1] Podolsky SH. The evolving response to antibiotic resistance (1945–2018). Palgrave Communications 2018;4:124.
- [2] Mauldin PD, Salgado CD, Hansen IS, Durup DT, Bosso JA. Attributable Hospital Cost and Length of Stay Associated with Health Care-Associated Infections Caused by Antibiotic-Resistant Gram-Negative Bacteria. *Antimicrob Agents Chemother* 2010;54:109-115.
- [3] Medernach RL, Logan LK. The Growing Threat of Antibiotic Resistance in Children. *Infect Dis Clin North Am* 2018;32:1-17.
- [4] Abed N, Couvreur P. Nanocarriers for antibiotics: a promising solution to treat intracellular bacterial infections. *Int J Antimicrob Agents* 2014;43:485-496.
- [5] Pastor M, Basas J, Vairo C, Gainza G, Moreno-Sastre M, Gomis X, Fleischer A, Palomino E, Bachiller D, Gutiérrez FB, Aguirre JJ, Esquisabel A, Igartua M, Gainza E, Hernandez RM, Gavaldà J, Pedraz, JL. Safety and effectiveness of sodium colistimethate-loaded nanostructured lipid carriers (SCM-NLC) against *P. aeruginosa*: *in vitro* and *in vivo* studies following pulmonary and intramuscular administration. *Nanomedicine* 2019;18:101-111.
- [6] Tacconelli E, Carrara E, Savoldi A, Harbarth S, Mendelson M, Monnet DL, *et al.* Discovery, research, and development of new antibiotics: the WHO priority list of antibiotic-resistant bacteria and tuberculosis. *Lancet Infect Dis* 2018;18:318-327.
- [7] Tacconelli E, Magrini N. Global priority list of antibiotic-resistant bacteria to guide research, discovery, and development of new antibiotics. 2017; Available at: [https://www.who.int/medicines/publications/WHO-PPL-Short\\_Summary\\_25Feb-ET\\_NM\\_WHO.pdf?ua=1](https://www.who.int/medicines/publications/WHO-PPL-Short_Summary_25Feb-ET_NM_WHO.pdf?ua=1).
- [8] Bushak L. A Brief History Of Antibiotic Resistance: How A Medical Miracle Turned Into The Biggest Public Health Danger Of Our Time. 2016; Available at: <https://www.medicaldaily.com/antibiotic-resistance-history-373773>.
- [9] Abraham EP, Chain E. An enzyme from bacteria able to destroy penicillin. *Rev Infect Dis* 1988;10:677-678.

- [10] PLOUGH HH. Penicillin resistance of *Staphylococcus aureus* and its clinical implications. *Am J Clin Pathol* 1945;15:446-451.
- [11] Dowling HF, Lepper MH, Jackson GG. Clinical significance of antibiotic-resistant bacteria. *Jama* 1955;157:327-331.
- [12] Nelson ML, Dinardo A, Hochberg J, Armelagos GJ. Brief communication: Mass spectroscopic characterization of tetracycline in the skeletal remains of an ancient population from Sudanese Nubia 350-550 CE. *Am J Phys Anthropol* 2010;143:151-154.
- [13] Centers for Disease Control and Prevention. Antibiotic use in the United States: progress and opportunities. 2017; Available at: <https://www.cdc.gov/antibiotic-use/stewardship-report/pdf/stewardship-report.pdf>.
- [14] Li J, Cao J, Zhu Y, Chen Q, Shen F, Wu Y, *et al.* Global Survey of Antibiotic Resistance Genes in Air. *Environ Sci Technol* 2018;52:10975-10984.
- [15] Sanganyado E, Gwenzi W. Antibiotic resistance in drinking water systems: Occurrence, removal, and human health risks. *Sci Total Environ* 2019;669:785-797.
- [16] Centers for Disease Control and Prevention. Food and Food Animals. 2018; Available at: <https://www.cdc.gov/drugresistance/food.html>.
- [17] Magiorakos AP, Srinivasan A, Carey RB, Carmeli Y, Falagas ME, Giske CG, *et al.* Multidrug-resistant, extensively drug-resistant and pandrug-resistant bacteria: an international expert proposal for interim standard definitions for acquired resistance. *Clin Microbiol Infect* 2012;18:268-281.
- [18] Parncutt R. The Human Cost of Anthropogenic Global Warming: Semi-Quantitative Prediction and the 1,000-Tonne Rule. *Frontiers in Psychology* 2019;10:2323.
- [19] Centers for Disease Control and Prevention. About Antimicrobial Resistance. 2018; Available at: <https://www.cdc.gov/drugresistance/about.html>.

*Nanostructured lipid carriers (NLCs) for multiresistant infections*

[20] World Health Organization Europe. Antibiotic resistance. 2019; Available at: <http://www.euro.who.int/en/health-topics/disease-prevention/antimicrobial-resistance/antibiotic-resistance>.

[21] World Health Organization. New report calls for urgent action to avert antimicrobial resistance crisis. 2019; Available at: <https://www.who.int/news-room/detail/29-04-2019-new-report-calls-for-urgent-action-to-avert-antimicrobial-resistance-crisis>.

[22] O'Neill J. The Review on Antimicrobial Resistance. Tackling Drug-Resistant Infections Globally: Final Report and Recommendations. 2016; Available at: [https://amr-review.org/sites/default/files/160525\\_Final%20paper\\_with%20cover.pdf](https://amr-review.org/sites/default/files/160525_Final%20paper_with%20cover.pdf).

[23] O'Neill J. Review on Antimicrobial Resistance: Tackling a crisis for the health and wealth of nations. 2014; Available at: [https://amr-review.org/sites/default/files/AMR%20Review%20Paper%20-%20Tackling%20a%20crisis%20for%20the%20health%20and%20wealth%20of%20nations\\_1.pdf](https://amr-review.org/sites/default/files/AMR%20Review%20Paper%20-%20Tackling%20a%20crisis%20for%20the%20health%20and%20wealth%20of%20nations_1.pdf).

[24] World Health Organization. Cancer. 2018; Available at: <https://www.who.int/en/news-room/fact-sheets/detail/cancer>.

[25] Davies S. Annual Report of the Chief Medical Officer, 2018. 2018; Available at: [https://assets.publishing.service.gov.uk/government/uploads/system/uploads/attachment\\_data/file/767549/Annual\\_report\\_of\\_the\\_Chief\\_Medical\\_Officer\\_2018\\_-\\_health\\_2040\\_-\\_better\\_health\\_within\\_reach.pdf](https://assets.publishing.service.gov.uk/government/uploads/system/uploads/attachment_data/file/767549/Annual_report_of_the_Chief_Medical_Officer_2018_-_health_2040_-_better_health_within_reach.pdf).

[26] Ruffin M, Brochiero E. Repair Process Impairment by *Pseudomonas aeruginosa* in Epithelial Tissues: Major Features and Potential Therapeutic Avenues. *Front. Cell. Infect. Microbiol.* 2019;9:182.

[27] Morehead MS, Scarbrough C. Emergence of Global Antibiotic Resistance. *Prim Care* 2018;45:467-484.

[28] Arzanlou M, Chai WC, Venter H. Intrinsic, adaptive and acquired antimicrobial resistance in Gram-negative bacteria. *Essays Biochem* 2017;61:49-59.

- [29] Chung ES, Ko KS. Eradication of persister cells of *Acinetobacter baumannii* through combination of colistin and amikacin antibiotics. *J Antimicrob Chemother* 2019;74:1277-1283.
- [30] Aghapour Z, Gholizadeh P, Ganbarov K, Bialvaei AZ, Mahmood SS, Tanomand A, *et al.* Molecular mechanisms related to colistin resistance in *Enterobacteriaceae*. *Infect Drug Resist* 2019;12:965-975.
- [31] Bergen PJ, Li J, Rayner CR, Nation RL. Colistin methanesulfonate is an inactive prodrug of colistin against *Pseudomonas aeruginosa*. *Antimicrob Agents Chemother* 2006;50:1953-1958.
- [32] Ramirez MS, Tolmasky ME. Amikacin: Uses, Resistance, and Prospects for Inhibition. *Molecules* 2017;22:2267.
- [33] Bessa LJ, Fazii P, Di Giulio M, Cellini L. Bacterial isolates from infected wounds and their antibiotic susceptibility pattern: some remarks about wound infection. *Int Wound J* 2015;12:47-52.
- [34] Abesamis GMM, Cruz JJV. Bacteriologic Profile of Burn Wounds at a Tertiary Government Hospital in the Philippines-UP-PGH ATR Burn Center. *J Burn Care Res* 2019;40:658-668.
- [35] Speert DP. Bacterial infections of the lung in normal and immunodeficient patients. *Novartis Found Symp* 2006;279:42-51; discussion 51-5, 216-9.
- [36] Pahal P, Rajasurya V, Sharma S. Typical Bacterial Pneumonia. StatPearls Publishing; 2020.
- [37] Gurjar M. Colistin for lung infection: an update. *J Intensive Care* 2015;3:3-015-0072-9.
- [38] Li Bassi G, Motos A, Fernandez-Barat L, Aguilera Xiol E, Chiurazzi C, Senussi T, *et al.* Nebulized Amikacin and Fosfomycin for Severe *Pseudomonas aeruginosa* Pneumonia: An Experimental Study. *Crit Care Med* 2019;47:e470-e477.

*Nanostructured lipid carriers (NLCs) for multiresistant infections*

[39] Li J, Nation RL, Turnidge JD, Milne RW, Coulthard K, Rayner CR, *et al.* Colistin: the re-emerging antibiotic for multidrug-resistant Gram-negative bacterial infections. *Lancet Infect Dis* 2006;6:589-601.

[40] Zhang JP, Yang XS, Chen J, Peng YZ, Huang YS. Clinical assessment of colistin in treating infections caused by multidrug-resistant gram-negative bacillus in patients with severe burn. *Zhonghua Shao Shang Za Zhi* 2009;25(5):372-376.

[41] Oliveira JF, Silva CA, Barbieri CD, Oliveira GM, Zanetta DM, Burdmann EA. Prevalence and risk factors for aminoglycoside nephrotoxicity in intensive care units. *Antimicrob Agents Chemother* 2009;53:2887-2891.

[42] Inci A, Toker MK, Bicer IG, Derbent A, Salihoglu Z. Determination of colistin-related nephrotoxicity and risk factors in intensive care unit. *North Clin Istanb* 2018;5:120-124.

[43] Xie J, Talaska AE, Schacht J. New developments in aminoglycoside therapy and ototoxicity. *Hear Res* 2011;281:28-37.

[44] Black RE, Lau WK, Weinstein RJ, Young LS, Hewitt WL. Ototoxicity of amikacin. *Antimicrob Agents Chemother* 1976;9:956-961.

[45] Gambôa I, Carneiro de Sousa P, Duarte D, Oliveira N. Amikacin Ototoxicity: Case Report and Literature Review. *Otolaryngology Online Journal* 2018.

[46] Gilbert D, Chambers H, Eliopoulos G, Saag M, Pavia A. *The Sanford Guide to Antimicrobial Therapy* 2019. 49<sup>th</sup> ed. perryville, VA, USA:Antimicrobial Therapy, Inc.; 2019.

[47] Miano TA, Lautenbach E, Wilson FP, Guo W, Borovskiy Y, Hennessy S. Attributable Risk and Time Course of Colistin-Associated Acute Kidney Injury. *Clin J Am Soc Nephrol* 2018;13:542-550.

[48] Hartzell JD, Neff R, Ake J, Howard R, Olson S, Paolino K, *et al.* Nephrotoxicity Associated with Intravenous Colistin (Colistimethate Sodium) Treatment at a Tertiary Care Medical Center. *Clin Infect Dis* 2009;48:1724-1728.

- [49] Aznar ML, Marras TK, Elshal AS, Mehrabi M, Brode SK. Safety and effectiveness of low-dose amikacin in nontuberculous mycobacterial pulmonary disease treated in Toronto, Canada. *BMC Pharmacology and Toxicology* 2019;20:37.
- [50] Centers for Disease Control and Prevention. The AMR challenge. 2019; Available at: <https://www.cdc.gov/drugresistance/intl-activities/amr-challenge.html>.
- [51] Hughes D, Andersson DI. Evolutionary Trajectories to Antibiotic Resistance. *Annu Rev Microbiol* 2017;71:579-596.
- [52] Hwang AY, Gums JG. The emergence and evolution of antimicrobial resistance: Impact on a global scale. *Bioorganic & Medicinal Chemistry* 2016;24:6440-6445.
- [53] Henriques-Normark B, Normark S. Bacterial vaccines and antibiotic resistance. *Ups J Med Sci* 2014;119:205-208.
- [54] Sánchez-López E, Gomes D, Esteruelas G, Bonilla L, Lopez-Machado AL, Galindo R, *et al.* Metal-Based Nanoparticles as Antimicrobial Agents: An Overview. *Nanomaterials (Basel)* 2020;10:292.
- [55] Lobanovska M, Pilla G. Penicillin's Discovery and Antibiotic Resistance: Lessons for the Future? *Yale J Biol Med* 2017;90:135-145.
- [56] Zheng X, Sallum UW, Verma S, Athar H, Evans CL, Hasan T. Exploiting a bacterial drug-resistance mechanism: a light-activated construct for the destruction of MRSA. *Angew Chem Int Ed Engl* 2009;48:2148-2151.
- [57] Shah S, Barton G, Fischer A. Pharmacokinetic considerations and dosing strategies of antibiotics in the critically ill patient. *Journal of the Intensive Care Society* 2015;16:147-153.
- [58] Nation RL, Garonzik SM, Thamlikitkul V, Giamarellos-Bourboulis EJ, Forrest A, Paterson DL, *et al.* Dosing guidance for intravenous colistin in critically-ill patients. *Clin Infect Dis* 2017;64:565-571.
- [59] Nation RL, Garonzik SM, Li J, Thamlikitkul V, Giamarellos-Bourboulis EJ, Paterson DL, *et al.* Updated US and European Dose Recommendations for Intravenous Colistin: How Do They Perform? *Clin Infect Dis* 2016;62:552-558.

*Nanostructured lipid carriers (NLCs) for multiresistant infections*

[60] Garonzik SM, Li J, Thamlikitkul V, Paterson DL, Shoham S, Jacob J, *et al.* Population pharmacokinetics of colistin methanesulfonate and formed colistin in critically ill patients from a multicenter study provide dosing suggestions for various categories of patients. *Antimicrob Agents Chemother* 2011;55:3284-3294.

[61] Markou N, Markantonis SL, Dimitrakis E, Panidis D, Boutzouka E, Karatzas S, *et al.* Colistin serum concentrations after intravenous administration in critically ill patients with serious multidrug-resistant, gram-negative bacilli infections: a prospective, open-label, uncontrolled study. *Clin Ther* 2008;30:143-151.

[62] Imberti R, Cusato M, Villani P, Carnevale L, Iotti GA, Langer M, *et al.* Steady-state pharmacokinetics and BAL concentration of colistin in critically ill patients after IV colistin methanesulfonate administration. *Chest* 2010;138:1333-1339.

[63] Sadeghi K, Hamishehkar H, Najmeddin F, Ahmadi A, Hazrati E, Honarmand H, *et al.* High-dose amikacin for achieving serum target levels in critically ill elderly patients. *Infect Drug Resist* 2018;11:223-228.

[64] Galvez R, Luengo C, Cornejo R, Kosche J, Romero C, Tobar E, *et al.* Higher than recommended amikacin loading doses achieve pharmacokinetic targets without associated toxicity. *Int J Antimicrob Agents* 2011;38:146-151.

[65] Roberts JA, Kruger P, Paterson DL, Lipman J. Antibiotic resistance--what's dosing got to do with it? *Crit Care Med* 2008;36:2433-2440.

[66] Ehrentraut SF, Muenster S, Kreyer S, Theuerkauf NU, Bode C, Steinhagen F, *et al.* Extensive Therapeutic Drug Monitoring of Colistin in Critically Ill Patients Reveals Undetected Risks. *Microorganisms* 2020;8:415.

[67] Duszynska W, Taccone FS, Hurkacz M, Kowalska-Krochmal B, Wiela-Hojeńska A, Kübler A. Therapeutic drug monitoring of amikacin in septic patients. *Crit Care* 2013;17:R165.

[68] Kim EJ, Oh J, Lee K, Yu KS, Chung JY, Hwang JH, *et al.* Pharmacokinetic Characteristics and Limited Sampling Strategies for Therapeutic Drug Monitoring of Colistin in Patients With Multidrug-Resistant Gram-Negative Bacterial Infections. *Ther Drug Monit* 2019;41:102-106.

- [69] Kusowska J. Economic impact of standard antibiotic therapy combined with amikacin, in clinical unit, Lodz, Poland--part II. *Acta Pol Pharm* 2005;62:491-495.
- [70] Fulnecky EJ, Wright D, Scheld WM, Kanawati L, Shoham S. Amikacin and colistin for treatment of *Acinetobacter baumannii* meningitis. *J Infect* 2005;51:e249-51.
- [71] Kalhapure RS, Suleman N, Mocktar C, Seedat N, Govender T. Nanoengineered drug delivery systems for enhancing antibiotic therapy. *J Pharm Sci* 2015;104:872-905.
- [72] Muller RH, Shegokar R, Keck CM. 20 years of lipid nanoparticles (SLN and NLC): present state of development and industrial applications. *Curr Drug Discov Technol* 2011;8:207-227.
- [73] Wallace SJ, Li J, Nation RL, Prankerd RJ, Boyd BJ. Interaction of colistin and colistin methanesulfonate with liposomes: colloidal aspects and implications for formulation. *J Pharm Sci* 2012;101:3347-3359.
- [74] Li Y, Huang L, Tang C, Zhang E, Ding L, Yang L. Preparation and characterisation of the colistin-entrapped liposome driven by electrostatic interaction for intravenous administration. *J Microencapsul* 2016;33:427-437.
- [75] Li Y, Tang C, Zhang E, Yang L. Electrostatically entrapped colistin liposomes for the treatment of *Pseudomonas aeruginosa* infection. *Pharm Dev Technol* 2017;22:436-444.
- [76] Li Y, Tang C, Zhang E, Yang L. Colistin-entrapped liposomes driven by the electrostatic interaction: Mechanism of drug loading and *in vivo* characterization. *Int J Pharm* 2016;515:20-29.
- [77] Wallace SJ, Nation RL, Li J, Boyd BJ. Physicochemical aspects of the coformulation of colistin and azithromycin using liposomes for combination antibiotic therapies. *J Pharm Sci* 2013;102:1578-1587.
- [78] Wang S, Yu S, Lin Y, Zou P, Chai G, Yu HH, et al. Co-Delivery of Ciprofloxacin and Colistin in Liposomal Formulations with Enhanced *In Vitro* Antimicrobial

*Nanostructured lipid carriers (NLCs) for multiresistant infections*

Activities against Multidrug Resistant *Pseudomonas aeruginosa*. Pharm Res 2018;35:187-018-2464-8.

[79] Chai G, Park H, Yu S, Zhou F, Li J, Xu Q, *et al*. Evaluation of co-delivery of colistin and ciprofloxacin in liposomes using an *in vitro* human lung epithelial cell model. Int J Pharm 2019;569:118616.

[80] Yu S, Wang S, Zou P, Chai G, Lin YW, Velkov T, *et al*. Inhalable liposomal powder formulations for co-delivery of synergistic ciprofloxacin and colistin against multi-drug resistant gram-negative lung infections. Int J Pharm 2020;575:118915.

[81] Sans-Serramitjana E, Fuste E, Martinez-Garriga B, Merlos A, Pastor M, Pedraz JL, *et al*. Killing effect of nanoencapsulated colistin sulfate on *Pseudomonas aeruginosa* from cystic fibrosis patients. J Cyst Fibros 2016;15:611-618.

[82] Pastor M, Moreno-Sastre M, Esquisabel A, Sans E, Vinas M, Bachiller D, *et al*. Sodium colistimethate loaded lipid nanocarriers for the treatment of *Pseudomonas aeruginosa* infections associated with cystic fibrosis. Int J Pharm 2014;477:485-494.

[83] Moreno-Sastre M, Pastor M, Esquisabel A, Sans E, Vinas M, Bachiller D, *et al*. Stability study of sodium colistimethate-loaded lipid nanoparticles. J Microencapsul 2016;33:636-645.

[84] Sans-Serramitjana E, Jorba M, Pedraz JL, Vinuesa T, Vinas M. Determination of the spatiotemporal dependence of *Pseudomonas aeruginosa* biofilm viability after treatment with NLC-colistin. Int J Nanomedicine 2017;12:4409-4413.

[85] Vairo C, Basas J, Pastor M, Palau M, Gomis X, Almirante B, *et al*. *In vitro* and *in vivo* antimicrobial activity of sodium colistimethate and amikacin-loaded nanostructured lipid carriers (NLC). Nanomedicine. Accepted. <https://doi.org/10.1016/j.nano.2020.102259>

[86] Vairo C, Collantes M, Quincoces G, Villullas S, Penuelas I, Pastor M, *et al*. Preclinical safety of topically administered nanostructured lipid carriers (NLC) for wound healing application: biodistribution and toxicity studies. Int J Pharm 2019;569:118484.

- [87] Omri A, Ravaoarino M, Poisson M. Incorporation, release and *in vitro* antibacterial activity of liposomal aminoglycosides against *Pseudomonas aeruginosa*. *J Antimicrob Chemother* 1995;36:631-639.
- [88] Bricaire F. Liposomes: promising perspectives. *Presse Med* 1998; 27 Suppl 5:7-8.
- [89] Vestar's MiKasome (liposomal amikacin). 2020; Available at: <https://pink.pharmaintelligence.informa.com/PS022952/Vestars-MiKasome-liposomal-amikacin>, 1993.
- [90] NeXstar Begin Ph II MiKasome Trials. 2020; Available at: <https://www.thepharmaletter.com/article/nexstar-begin-ph-ii-mikasome-trials>, 1998.
- [91] Fielding RM, Lewis RO, Moon-McDermott L. Altered tissue distribution and elimination of amikacin encapsulated in unilamellar, low-clearance liposomes (MiKasome). *Pharm Res* 1998;15:1775-1781.
- [92] Fielding RM, Moon-McDermott L, Lewis RO. Bioavailability of a small unilamellar low-clearance liposomal amikacin formulation after extravascular administration. *J Drug Target* 1999;6:415-426.
- [93] Fielding RM, Moon-McDermott L, Lewis RO, Horner MJ. Pharmacokinetics and urinary excretion of amikacin in low-clearance unilamellar liposomes after a single or repeated intravenous administration in the rhesus monkey. *Antimicrob Agents Chemother* 1999;43:503-509.
- [94] Ehsan Z, Clancy JP. Management of *Pseudomonas aeruginosa* infection in cystic fibrosis patients using inhaled antibiotics with a focus on nebulized liposomal amikacin. *Future Microbiol* 2015;10:1901-1912.
- [95] Shah SP, Misra A. Liposomal amikacin dry powder inhaler: effect of fines on *in vitro* performance. *AAPS PharmSciTech* 2004;5:e65.
- [96] Li Z, Zhang Y, Wurtz W, Lee JK, Malinin VS, Durwas-Krishnan S, *et al.* Characterization of nebulized liposomal amikacin (Arikace) as a function of droplet size. *J Aerosol Med Pulm Drug Deliv* 2008;21:245-254.

*Nanostructured lipid carriers (NLCs) for multiresistant infections*

[97] Meers P, Neville M, Malinin V, Scotto AW, Sardaryan G, Kurumunda R, *et al.* Biofilm penetration, triggered release and *in vivo* activity of inhaled liposomal amikacin in chronic *Pseudomonas aeruginosa* lung infections. *J Antimicrob Chemother* 2008;61:859-868.

[98] Malinin V, Neville M, Eagle G, Gupta R, Perkins WR. Pulmonary Deposition and Elimination of Liposomal Amikacin for Inhalation and Effect on Macrophage Function after Administration in Rats. *Antimicrob Agents Chemother* 2016;60:6540-6549.

[99] Lee JH, Cheng KT, Malinin V, Li Z, Yao Z, Lee SJ, *et al.* (99m)Tc-labeled therapeutic inhaled amikacin loaded liposomes. *J Liposome Res* 2013;23:336-342.

[100] Weers J, Metzheiser B, Taylor G, Warren S, Meers P, Perkins WR. A gamma scintigraphy study to investigate lung deposition and clearance of inhaled amikacin-loaded liposomes in healthy male volunteers. *J Aerosol Med Pulm Drug Deliv* 2009;22:131-138.

[101] Okusanya OO, Bhavnani SM, Hammel J, Minic P, Dupont LJ, Forrest A, *et al.* Pharmacokinetic and pharmacodynamic evaluation of liposomal amikacin for inhalation in cystic fibrosis patients with chronic pseudomonal infection. *Antimicrob Agents Chemother* 2009;53:3847-3854.

[102] Clancy JP, Dupont L, Konstan MW, Billings J, Fustik S, Goss CH, *et al.* Phase II studies of nebulised Arikace in CF patients with *Pseudomonas aeruginosa* infection. *Thorax* 2013;68:818-825.

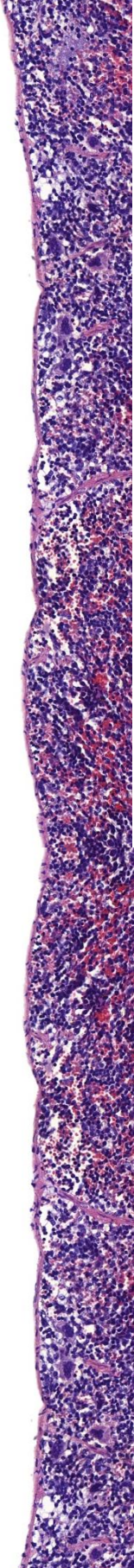
[103] Okusanya OO, Bhavnani SM, Hammel JP, Forrest A, Bulik CC, Ambrose PG, *et al.* Evaluation of the pharmacokinetics and pharmacodynamics of liposomal amikacin for inhalation in cystic fibrosis patients with chronic pseudomonal infections using data from two phase 2 clinical studies. *Antimicrob Agents Chemother* 2014;58:5005-5015.

[104] Bilton D, Pressler T, Fajac I, Clancy JP, Sands D, Minic P, *et al.* Amikacin liposome inhalation suspension for chronic *Pseudomonas aeruginosa* infection in cystic fibrosis. *J Cyst Fibros* 2020;19:284-291.

- [105] Varshosaz J, Ghaffari S, Khoshayand MR, Atyabi F, Azarmi S, Kobarfard F. Development and optimization of solid lipid nanoparticles of amikacin by central composite design. *J Liposome Res* 2010;20:97-104.
- [106] Varshosaz J, Ghaffari S, Khoshayand MR, Atyabi F, Dehkordi AJ, Kobarfard F. Optimization of freeze-drying condition of amikacin solid lipid nanoparticles using D-optimal experimental design. *Pharm Dev Technol* 2012;17:187-194.
- [107] Ghaffari S, Varshosaz J, Saadat A, Atyabi F. Stability and antimicrobial effect of amikacin-loaded solid lipid nanoparticles. *Int J Nanomedicine* 2010;6:35-43.
- [108] Varshosaz J, Ghaffari S, Mirshojaei SF, Jafarian A, Atyabi F, Kobarfard F, *et al.* Biodistribution of Amikacin Solid Lipid Nanoparticles after Pulmonary Delivery. *BioMed Research International* 2013:136859.
- [109] Trafny EA, Stepinska M, Antos M, Grzybowski J. Effects of free and liposome-encapsulated antibiotics on adherence of *Pseudomonas aeruginosa* to collagen type I. *Antimicrob Agents Chemother* 1995;39:2645-2649.
- [110] Trafny EA, Antos-Bielska M, Grzybowski J. Antibacterial activity of liposome-encapsulated antibiotics against *Pseudomonas aeruginosa* attached to the matrix of human dermis. *J Microencapsul* 1999;16:419-429.
- [111] Huh J, Chen JC, Furman GM, Malki C, King B, Kafie F, *et al.* Local treatment of prosthetic vascular graft infection with multivesicular liposome-encapsulated amikacin. *J Surg Res* 1998;74:54-58.
- [112] Howell SB. Clinical applications of a novel sustained-release injectable drug delivery system: DepoFoam technology. *Cancer J* 2001;7:219-227.



# Objectives





Antimicrobial resistance (AMR) is a major global threat and requires a drastic and immediate intervention. *Pseudomonas aeruginosa*, *Klebsiella pneumonia* and *Acinetobacter baumannii* are classified as principal responsible for multiresistant gram-negative bacterial infections, especially in skin and respiratory tract. Nowadays, few antibiotics have demonstrated certain effectiveness for such difficult-to-treat multiresistant infections. Among them, colistin (SCM) and amikacin (AMK) have recently gained importance as rescue therapy in clinical settings. However, their toxicity severely limits their use, especially after being applied systemically. Thus, new strategies should be investigated not only to enhance antibiotic safety, but also to preserve their effectiveness.

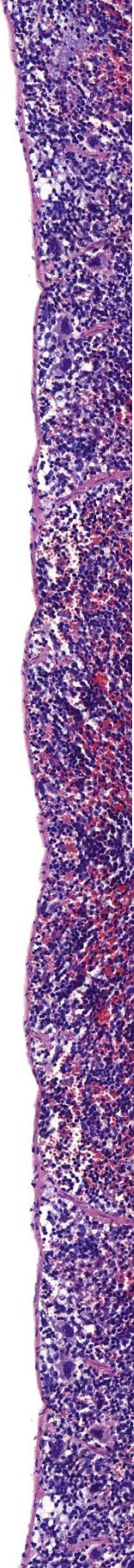
In view of these considerations, the main objective of the present work is the development of colistin- and amikacin-loaded nanostructured lipid carriers (NLCs), a novel drug delivery system capable of improving antibiotic safety and effectiveness against multiresistant respiratory tract and wound infections.

To accomplish this purpose, three specific objectives are considered:

1. To select the most suitable formulation among different AMK- and SCM-loaded NLCs and demonstrate their efficacy in a neutropenic murine acute pneumonia infection model caused by an extensively drug-resistant *A. baumannii* strain, following the intraperitoneal and intramuscular routes.
2. To evaluate SCM-NLC biodistribution, safety and efficacy in a murine acute pneumonia infection model caused by an extensively drug-resistant *P. aeruginosa* strain, following pulmonary and intramuscular administration.
3. To evaluate blank-NLC biodistribution and safety after topical administration on impaired and intact skin, respectively.



# Experimental work





## CHAPTER 1

### ***In vitro* and *in vivo* antimicrobial activity of sodium colistimethate and amikacin-loaded nanostructured lipid carriers (NLCs)**

C. Vairo<sup>a,b</sup>, J. Basas<sup>c</sup>, M. Pastor<sup>a</sup>, M. Palau<sup>c</sup>, X. Gomis<sup>c</sup>, B. Almirante<sup>c</sup>, E. Gainza<sup>a</sup>, R.M. Hernández<sup>b,d</sup>, M. Igartua<sup>b,d</sup>, J. Gavaldà<sup>c,\*</sup>, G. Gainza<sup>a,\*\*</sup>.

<sup>a</sup>BioKeralt Research Institute AIE, Albert Einstein 25 E/3, 01510 Miñano, Spain

<sup>b</sup>NanoBioCel Group, Laboratory of Pharmaceutics, University of the Basque Country (UPV/EHU), School of Pharmacy, Paseo de la Universidad 7, 01006 Vitoria-Gasteiz, Spain.

<sup>c</sup>Antimicrobial Resistance Laboratory, Vall d'Hebron Research Institute (VHIR). Infectious Diseases Department, Hospital Universitari Vall d'Hebron, Passeig de la Vall d'Hebron, 119-129, 08035 Barcelona.

<sup>d</sup>Biomedical Research Networking Center in Bioengineering, Biomaterials and Nanomedicine (CIBER-BBN). Vitoria-Gasteiz, Spain.

\*Corresponding author: Joan Gavaldà; \*\*Corresponding author: Garazi Gainza

---

### **ABSTRACT**

Sodium colistimethate (SCM) and amikacin (AMK) are among the few antibiotics effective against resistant *P. aeruginosa*, *K. pneumoniae* and *A. baumannii*; however, their toxicity severely limits their use. Enclosing antibiotics into nanostructured lipid carriers (NLC) might decrease drug toxicity and improve antibiotic disposition. In this work, SCM or AMK were loaded into different NLC formulations, through high pressure homogenization, and their *in vitro* and *in vivo* effectiveness was analyzed. The encapsulation process did not reduce drug effectiveness since *in vitro* SCM-NLC and AMK-NLC drug activity was equal to that of the free drugs. As cryoprotectant, trehalose showed better properties than dextran. Instead, positive chitosan coating was discarded due to its limited cost-efficiency. Finally, the *in vivo* study in acute pneumonia model revealed that intraperitoneal administration was superior to the intramuscular route and confirmed that (-) SCM-NLC with trehalose, was the most suitable formulation against an extensively drug-resistant *A. baumannii* strain.



## 1. Introduction

Antimicrobial resistance (AMR) is a global threat that has an enormous economic, social and public health impact worldwide. In 2016, the World Economic Forum risk report remarked that AMR was one of the major health hazards for society (1). In EU, 400,000 cases of infection due to resistant bacteria are diagnosed annually, leading to further 2,500,000 hospitalizations. Currently, 50,000 patients die every year in US and EU due to AMR, representing 1.5 billion € and US\$ 3.5 billion healthcare costs (2,3). In 2014, David Cameron, Prime Minister of UK, commissioned to Jim O'Neill an independent review on the economic issues related to AMR. This review revealed that AMR cost could rise to US\$ 100.2 trillion by 2050, positioning AMR as a serious challenge, just as climate change. A strong joint commitment to fight against AMR is needed to avoid 10 million deaths per year, an even higher death rate than cancer, which will exert an economic impact equal to an annual UK economic production (4).

AMR is basically caused by three superbugs, *P. aeruginosa*, *K. pneumoniae* and *A. baumannii*, which represent a critical global bacterial priority, as stated by WHO in 2016 (5,6).

According to the European Medicine Agency (EMA), the European Centre for Diseases Prevention and Control (ECDC) and the Infectious Disease Society of America (IDSA), there is a lack of new antimicrobials in a mature clinical development stage in the pipeline of pharmaceutical companies, especially against gram-negative resistant bacilli (7).

In many cases, colistin or its prodrug, *i.e.* sodium colistimethate (SCM), is the only active substance against certain pulmonary *K. pneumoniae* and *P. aeruginosa* infections and is used as the last resort due to the related dose-dependent toxicity (nephro- and neurotoxicity) (8).

Amikacin (AMK) is also indicated against severe pulmonary infections produced by *K. pneumoniae* and *P. aeruginosa*, and is the broadest spectrum aminoglycoside with the least resistance. However, the associated nephrotoxicity and ototoxicity risk limit its use, due to generation of free oxygen radicals as amikacin is not metabolized (9).

Nevertheless, it should be noted that both antibiotics are still used despite their serious side effects, because currently there is no available effective agent in the clinical practice.

In this regard, the use of nanotechnology could represent an interesting approach to reduce antibiotic toxicity. Especially, nanostructured lipid carriers (NLC), a disordered matrix composed of solid and liquid GRAS (Generally Recognized As Safe) lipids, have already demonstrated their effectiveness against multiresistant bacterial infections, providing a sustained, safe and advantageous drug release (10,11).

Altogether, the main goals of this research work were: (i) to produce effective SCM- and AMK-loaded NLC formulations (SCM-NLC and AMK-NLC) using different cryoprotectants (trehalose or dextran) and coatings (positive charged chitosan) through high pressure homogenization; (ii) to select the most cost-effective formulation by means of *in vitro* planktonic and biofilm susceptibility assays; and finally, (iii) to demonstrate effectiveness of NLC in an *in vivo* acute pneumonia animal model of neutropenic mice, following intramuscular or intraperitoneal route.

## **2. Materials and methods**

### **2.1. Bacterial strains and growth conditions**

(i) Cryoprotectant selection; for planktonic and biofilm susceptibility studies in *P. aeruginosa*, PAO1, FQSE06-403, Pa1m, Pa2m and Pa14 strains were used. PAO1 and Pa14 were two wild type biofilm-producing strains. The remaining three *P. aeruginosa* strains were obtained from cystic fibrosis patient sputum; FQSE06-403 was a moderately-drug resistant and non-mucoid strain (Sequence type (ST): ST274) and Pa1m and Pa2m were mucoid isolates harboring a hyperproduction of high level cephalosporinases and loss of porin OprD2, respectively.

(ii) Coating selection; for planktonic susceptibility studies in *P. aeruginosa*, *K. pneumoniae* and *A. baumannii*, forty-two strains were studied; 14 drug-resistant *P. aeruginosa* clinical isolates, 13 drug-resistant *K. pneumoniae* clinical isolates and 15 drug-resistant *A. baumannii* clinical isolates, from different hospitals.

All strains were stored in skim milk at -80 °C.

## 2.2. Preparation of nanoparticles

Sodium colistimethate- or amikacin-loaded nanostructured lipid carriers (SCM-NLC or AMK-NLC) were prepared using hot melt homogenization as previously reported by Pastor *et al.* (12), but including a high-pressure homogenization (HPH) step to better handle large batch volumes. Briefly, Precirol® ATO 5 (Gattefossé, Madrid, Spain) and Miglyol 182 N/F (Sasol, Hamburg, Germany) were melted together with the drug [SCM (Accord Healthcare, Barcelona, Spain) and AMK (VWR, Llinars del Vallès, Spain)] to achieve the oily phase (10:1:1). Simultaneously, the aqueous phase was prepared dissolving Tween® 80 (Panreac Química, Castellar del Vallès, Barcelona, Spain) at 2 % (w/v) and Poloxamer 188 (VWR, Llinars del Vallès, Spain) at 1 % (w/v) and then tempered. The two phases were mixed and sonicated (Branson Sonifier, Emerso, Saint Louis, MO, US) for 15 s at 20 W. The resulting emulsion was placed in a high pressure homogenizer (Panda Plus 2000, Gea Niro Soavi, Parma, Italy) and 10 homogenization cycles were applied at 500 Bar. Afterwards, the emulsion was gradually cooled down and kept under  $5 \pm 2$  °C for 2 h to allow lipid solidification. Subsequently, 15 % (w/w) of trehalose (Sigma-Aldrich, St. Louis, MO, US) or dextran, as cryopreserving agents, were added to the formulation prior to the freeze-drying step (45 h recipe, from -45 °C to 25 °C at 0.180 mBar). The total batch weight was 8.25 g.

The positive charged nanoparticles were prepared employing the chitosan concentration reported by Fonte *et al.* (13). In brief, after the cooling process, 0.5 % (w/v) chitosan [chitosan chloride, 50,000-150,000 g/mol molecular weight measured as chitosan acetate; degree of deacetylation 75-90 % (Protasan UP CL 113, FMC Biopolymers AS, Snadvika, Norway)] solution was added dropwise to the nanoparticle suspension (1:1 volume) and incubated for 30 min under magnetic stirring. In this case, the total batch weight was 8.75 g.

Eight different formulations of SCM-NLC and AMK-NLC were obtained starting from a single batch.

## 2.3. Nanoparticles characterization

## *Nanostructured lipid carriers (NLCs) for multiresistant infections*

Particle size along with PDI, and zeta potential were measured by means of the Zetasizer Nano ZS (Malvern Instruments, Worcestershire, UK) based on dynamic light scattering (DLS) and electrophoretic light scattering (ELS), respectively. Samples were analyzed in triplicates to obtain an accurate mean.

For nanoparticle morphology study, transmission electron microscopy (TEM) analysis was performed under negative staining.

Drug loading was estimated by means of the following formula:

$$\text{Drug loading} = \frac{\text{Initial Drug Amount (mg)}}{\text{Total Batch Weight (mg)}}$$

Encapsulation efficiency (EE) was calculated indirectly by quantifying the amount of drug present in the supernatant. Briefly, after cooling the suspension, 5 mL of the batch were centrifuged in an Amicon<sup>®</sup> centrifugal filtration unit (100 kDa molecular weight cut off membrane system, Millipore) for 15 min at 2,500 rpm in order to analyze the amount of non-encapsulated drug. SCM, a cyclic polypeptide, was determined by using the Micro BCA<sup>™</sup> Protein Assay Kit (Thermo Fisher Scientific, Madrid, Spain) following purchaser instructions. For AMK determination, the ultraviolet-visible (UV-VIS) spectrophotometric technique was used after fluorescamine derivatization (14,15).

Once quantified, encapsulation efficiency was estimated according to the following equation:

$$EE(\%) = \left( \frac{\text{Initial Drug Amount} - \text{Non Encapsulated Drug}}{\text{Initial Drug Amount}} \right) \times 100$$

Similarly, the drug release profile was also assessed. 25 mg of lyophilized NLC were weighed and re-suspended in phosphate buffered saline (PBS, Life Technology, Paisley, UK). Then, the suspension was stirred using rotary mixing at 37 °C. At pre-established time points, samples were filtrated using Amicon<sup>®</sup> centrifugal devices for 15 min and the drug content present in the supernatants analyzed as described above. Samples were studied in triplicates and results expressed as a percentage (%) of the drug released.

### 2.4. Antimicrobial activity against *P. aeruginosa* strains for cryoprotectant selection

The antimicrobial activity of the eight developed formulations was tested for planktonic and biofilm studies with the aim of selecting the most suitable cryoprotectant. *P. aeruginosa* was the strain of choice as our research group already demonstrated the capability of SCM-NLC to reduce pulmonary infection (12) and because it is one of the AMR superbugs (5,6).

#### *2.4.1. Planktonic susceptibility studies*

Bacterial susceptibility to the formulations was determined evaluating the minimum inhibitory concentration (MIC) through the microdilution technique according to the European Committee on Antimicrobial Susceptibility Testing (EUCAST) guidelines and breakpoints (16). Briefly, cells from a subculture were suspended in Müller Hinton Broth (MHB, Becton Dickinson, Le Pont de Clarx, France) to reach a turbidity of 0.5 in the McFarland scale [equivalent to  $1.5 \cdot 10^8$  colony-forming units (CFU)/mL] and subsequently the inoculum was adjusted to the desired concentration of  $1.6 \cdot 10^8$  CFU/mL. Different concentrations of the formulations (SCM-NLC and AMK-NLC) were prepared through serial dilutions with MHB (1:2 dilutions). Then, inocula were placed in a 96-well microtiter plate; except for the last two columns that corresponded to the sterility control, in which only culture medium was placed. Plates were then incubated at 37 °C for 24 h. MIC was defined as the lowest concentration of antibiotic which presented no bacterial culture turbidity. To compare the efficacy of the developed nanoparticles, the free drugs, *i.e.*, SCM and AMK, were also evaluated. Samples were analyzed in triplicates.

#### *2.4.2. Biofilm susceptibility studies*

Biofilm assays were carried out to study the minimum biofilm inhibitory concentration (MBIC) and the minimum biofilm eradication concentration (MBEC) by the Calgary assay as described by Moskowitz *et al.* (17) with few modifications. Isolates stored at -80 °C were first cultured on Tryptic Soy Agar (TSA) (BioMérieux® SA, Marcy l'Etoile, France) and then, grown overnight in Tryptic Soy Broth (TSB, Becton Dickinson, Le Pont de Clarx, France). After diluting culture to obtain a 0.5 McFarland pattern, the culture was transferred to a 96-well microtiter plate; except for the last two columns which corresponded to the growth and sterility controls, where inoculum and culture medium were placed, respectively. Bacterial biofilm was

formed immersing polystyrene microtiter pegs on the microtiter plate and incubating at 37 °C for 24 h under rocking stirring at 60 rpm. Then, pegs were rinsed three times in sterile distilled water and transferred to a standard 96-well plate where dilutions of the specified antibiotics/nanoparticles, prepared in MHB, were performed (range from 0.015 to 4,096 mg/L). Plates were incubated overnight at 37 °C without stirring. Finally, pegs were triple-washed with sterile water, in order to remove planktonic cells, and placed in a second TBS containing 96-well plate. The plate was then sonicated for 30 min at 43 kHz at room temperature to transfer the biofilms grown on pegs to the 96-well plate. The wells were seeded with TSA and incubated for further 16 h at 37 °C.

The MBIC was defined as the lowest concentration of antibiotic where no bacterial culture turbidity was appreciated. The MBEC was determined as the lowest antibiotic concentration required to eradicate the biofilm (17).

All samples were run in triplicates.

#### 2.5. Antimicrobial activity in *P. aeruginosa*, *K. pneumoniae* and *A. baumannii* strains for coating selection

Once the best cryoprotectant was selected from the previous *in vitro* activity assays, an in-depth activity study was performed using more strains with the aim of analyzing the chitosan coating cost-efficiency. Even though chitosan had shown to improve interactions with the bacterial surface (18), it appears noteworthy to study its effect in the developed SCM-NLC and AMK-NLC, as the more steps included within the production process, the more expensive and complicated could be to manufacture. Accordingly, three superbugs were used. Briefly, MIC was analyzed as previously described following the EUCAST guidelines and breakpoints (16). In this case, *P. aeruginosa* ATCC 27853, *E. coli* ATCC 25922 and *A. baumannii* ATCC 19606 were used as quality control strains for the susceptibility testing.

#### 2.6. *In vivo* efficacy study

##### 2.6.1. *Animals and ethics*

48 female RjOrl:SWISS mice weighing 22 to 24 g were acquired from Janvier (Janvier Labs, Le Genest-Saing-Isle, France). Upon arrival, animals were housed in regulation cages with HEPA filter, provided with water and food *ad libitum* throughout the experiments and housed under a reversed 12 h/12 h light/dark cycle.

Guide for the Care and Use of Laboratory Animals (19) and the Animal Research: Reporting of *in vivo* Experiments (ARRIVE) guidelines were followed. All the experimental procedures were performed in accordance with the Catalan (Decree 214/1997), Spanish (Royal Decree 53/2013) and European (European Directive 2010/63/EU) laws and regulations. The experimental protocol was approved by the Animal Experimentation Ethics Committee of Vall d'Hebron Research Institute (registration number 74/15 CEEA).

#### *2.6.2. Acute pneumonia A. baumannii infection model in neutropenic mice*

An extensively drug resistant (XDR) *A. baumannii* clinical strain was used for the *in vivo* model. *A. baumannii* Abl4; isolate harboring an OXA-51, was only susceptible to colistin, amikacin and tigecycline (ST2). In order to increase its virulence before being used in the experimental model, 0.5 mL of bacterial suspension of  $1.5 \cdot 10^8$  CFU/mL was injected both intravenously (IV) and intraperitoneally (IP) and 6 h later, the bacterial strain was recovered from blood and spleen.

The acute pneumonia model in neutropenic mice was developed at Vall d'Hebron Research Institute, based on previously published work (20). Firstly, mice were immunosuppressed with 0.1 mL cyclophosphamide (Baxter Oncology GmbH, Westfalen, Germany) 150 mg/kg at days -4, -3 and -1 before infection (day 0). Then, mice were anesthetized by an intramuscular (IM) injection of ketamine (Inresa Arzneimittel GmbH, Freigurb, Germany) 35 mg/kg and xylazine (Laboratorios Calier S.A., Barcelona, Spain) 5 mg/kg, and infected with orotracheal instillation through an Abbocath® of 24G x 19mm (3/4") with the aid of a laryngoscope (blade assembly small animal laryngoscope Model CS-2 for mouse. PennCentury, Inc. PA, USA). After inoculation of 30  $\mu$ L of Abl4 bacterial suspension in TSB at a final concentration of  $1 \cdot 10^6$  CFU/mL, mice remained in vertical position for 3 min and then in 30° position until awakening.

In order to test the efficacy of the antimicrobial agents, IM and IP administration routes were tested. Infected animals were randomly assigned to the following therapeutic groups: (i) growth control 0.9 % NaCl every 6 h (q6h) IM, (ii) free SCM 60 mg/kg q6h IM, (iii) SCM-NLC 12 mg/kg q12h IM, (iv) SCM-NLC 12 mg/kg q24h IM, (v) SCM-NLC 6 mg/kg q12h IP and (vi) SCM-NLC 6 mg/kg q24h IP. Therapy was initiated 2 h after infection and lasted 72 h. Four hours after the last treatment dose, animals were euthanized by cervical dislocation. Lungs were aseptically extracted and processed for quantitative culture. After homogenization (Ultra-Turrax® T25; IKA Works, Inc., Wilmington, USA) for 2 min in 4 mL of PBS (pH 7.2), lung samples were serially diluted and plated on TSA for 24 h at 37 °C. Results were expressed as log<sub>10</sub> CFU/g of lung.

### 2.7. Statistical analysis

Results of the *in vivo* assay were analyzed by two non-parametric tests: Mann Whitney and Wilcoxon tests using the SPSS (version 16.0) statistical package (SPSS Inc.). P values < 0.05 were considered statistically significant. Results were expressed as log<sub>10</sub> cfu/g lung median (IQR<sub>25-75</sub>).

## 3. Results

On the one hand, the effect of different cryoprotectant agents and chitosan coating was analyzed on terms of formulation characterization and antimicrobial activity.

In the case of SCM-NLC, size varied between 67 and 177 nm, while PDI fluctuated from 0.207 to 0.349 depending on the cryoprotectant and the charge. In addition, positive zeta potential of about 14 mV could be achieved by chitosan coated SCM-NLC, whereas uncoated SCM-NLC displayed negative zeta potential ranging from around -20 to -29 mV.

Encapsulation efficiency was set as 73 %. The final drug loading for negatively charged particles was 0.06 mg SCM/mg of formulation. In the case of positively charged nanoparticles, drug loading was 0.057 mg SCM/mg of formulation (Table 1).

Table 1. SCM-NLC characterization. Samples were run in triplicates and data are shown as  $\pm$  SD.

		SCM-NLC			
Pre-lyophilization		Post-lyophilization			
EE (%)		Size (nm)	PDI	Zeta (mV)	Drug Loading (mg SCM/mg NLC)
(-)	SCM-NLC Trehalose	67.33 $\pm$ 2.06	0.257 $\pm$ 0.01	-20.3 $\pm$ 0.75	0.06
	SCM-NLC Dextran	101.56 $\pm$ 0.41	0.207 $\pm$ 0.01	-29.03 $\pm$ 1.44	
73.14 $\pm$ 3.69					
(+) )	SCM-NLC Trehalose	177.63 $\pm$ 5.50	0.266 $\pm$ 0.03	14.77 $\pm$ 1.91	0.057
	SCM-NLC Dextran	146.46 $\pm$ 0.37	0.349 $\pm$ 0.09	14.16 $\pm$ 0.55	

SCM, sodium colistimethate; EE, encapsulation efficiency.

AMK-NLC displayed size values between 73 and 142 nm, while PDI varied from 0.139 to 0.280. In this case, the chitosan coating gave rise to a lower positive zeta potential value (about 1 mV) compared to SCM-NLC. AMK-NLC displayed higher encapsulation efficiency (92 %) and drug loading was the same as those for SCM-NLC (0.06 and 0.057 mg AMK/mg of formulation for negative particles and for positive particles, respectively) (Table 2).

Table 2. AMK-NLC characterization. Samples were run in triplicates and data are shown as  $\pm$  SD.

		AMK-NLC			
Pre-lyophilization		Post-lyophilization			
EE (%)		Size (nm)	PDI	Zeta (mV)	Drug Loading (mg AMK/mg NLC)
(-)	AMK-NLC Trehalose	89.71 $\pm$ 2.48	0.139 $\pm$ 0.00	-20.63 $\pm$ 2.12	0.06
	AMK-NLC Dextran	73.45 $\pm$ 0.28	0.264 $\pm$ 0.03	-15.63 $\pm$ 0.55	
92.8 $\pm$ 4.18					
(+) )	AMK-NLC Trehalose	114.1 $\pm$ 1.19	0.234 $\pm$ 0.03	0.11 $\pm$ 0.14	0.057
	AMK-NLC Dextran	142.4 $\pm$ 2.54	0.280 $\pm$ 0.02	1.81 $\pm$ 0.08	

AMK, amikacin; EE, encapsulation efficiency.

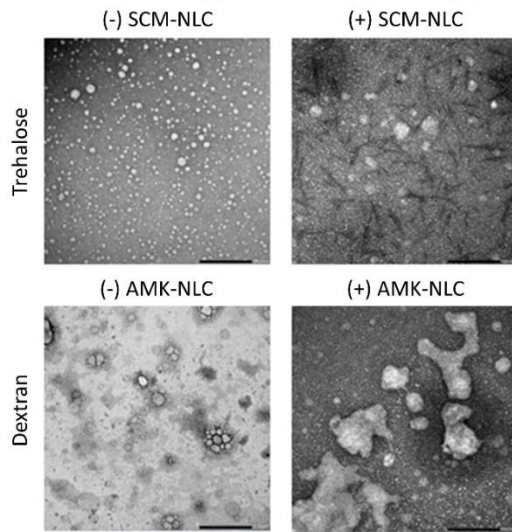


Fig. 1. TEM images of antibiotic-loaded NLC. SCM-NLC, sodium colistimethate-loaded nanostructured lipid carriers; AMK-NLC, amikacin-loaded nanostructured lipid carriers; (-), negatively charged NLC without chitosan; (+), positively charged NLC with chitosan. Scale bar 450 nm.

As Fig. 1. displays, TEM images showed spherical small particles, regardless the cryoprotectant agent. In the positively charged NLC, excess of chitosan could be observed. This excess could be detected as small crystals in the SCM-NLC samples, whereas AMK-NLC looked amorphous. As TEM images revealed, AMK-NLC tended to form small aggregates of 2-10 particles.

Fig. 2 and Fig. 3 show the release profiles of SCM-NLC and AMK-NLC formulations, respectively. In general, SCM-NLC were able to release almost all the drug in 7 days and a minimum of about 75 % of drug in 24 h.

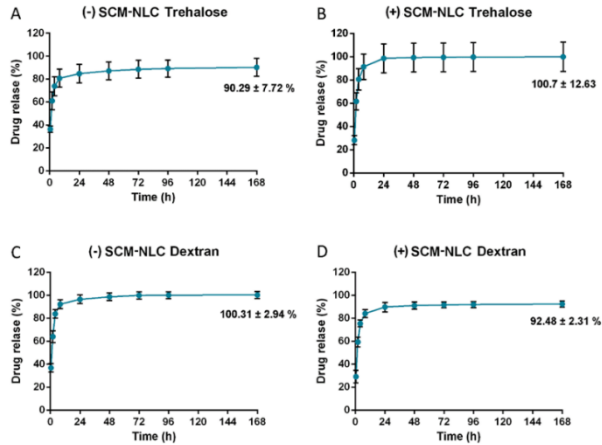
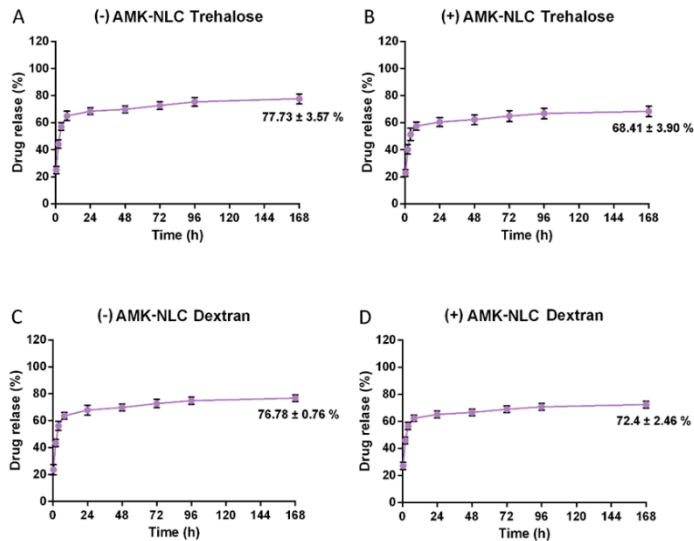


Fig. 2. Release profile of SCM-NLC. SCM-NLC, sodium colistimethate-loaded nanostructured lipid carriers; (-), negatively charged NLC without chitosan; (+), positively charged NLC with chitosan.

On the contrary, AMK-NLC reached a 75 % of drug release in 7 days (Fig. 3). All AMK-NLC formulations displayed a slower release profile, about 65 % of the loaded drug was released during the 24 h incubation period.



## Nanostructured lipid carriers (NLCs) for multiresistant infections

Fig. 3. Release profile of AMK-NLC. AMK-NLC, amikacin-loaded nanostructured lipid carriers; (-), negatively charged NLC without chitosan; (+), positively charged NLC with chitosan.

A preliminary antimicrobial activity was carried out in five *P. aeruginosa* strains, selected for a fast planktonic and biofilm antimicrobial activity screening. Overall, all strains were susceptible to SCM and AMK.

As observed in Table 3, strains displayed different susceptibilities to SCM-NLC formulations (*i.e.*, 0.06-1 mg/L MIC, 0.125-128 mg/L MBIC and 1-512 mg/L MBEC). Both (-) SCM-NLC and (+) SCM-NLC, regardless of the cryoprotectant, presented a decrease of at least 2-fold in MIC, MBIC or MBEC in most of the strains compared to free SCM (Table 3). Concretely, (-) SCM-NLC were able to exert a maximum of 2-fold enhanced results compared to free SCM, in terms of MIC, MBIC and MBEC. In contrast, (+) SCM-NLC were able to improve the antimicrobial activity even more, at least 2-fold for FQSE06-0403 and Pa2m strains and more than 4-fold for Pa1m strain. It should be noted that (+) SCM-NLC trehalose displayed the highest activity for all tested strains for the three parameters studied. It is remarkable that (+) SCM-NLC dextran also exerted excellent results, but displayed slightly higher MIC, MBIC and MBEC values (therefore lower activity) in some cases. There were no differences between MBIC or MBEC of (-) SCM-NLC compared to free SCM (Table 3).

Table 3. Planktonic and biofilm susceptibility studies. MIC, MBIC and MBEC values for SCM-NLC formulations against *P. aeruginosa* strains. All the results are expressed in mg/L.

Strain	(-) SCM-NLC Trehalose			(+) SCM-NLC Trehalose		
	MIC	MBIC	MBEC	MIC	MBIC	MBEC
PAO1	0.5	64	128-256	0.25	16-32	64-128
FQSE06-0403	1	128	256-512	0.25	8-16	64-128
Pa1m	1	0.5	1	0.06	0.125	1
Pa2m	0.5	32	256-512	0.25-0.5	8-16	8-16
Pa14	0.5	16-32	64	0.125	16	16
Strain	(-) SCM-NLC Dextran			(+) SCM-NLC Dextran		
	MIC	MBIC	MBEC	MIC	MBIC	MBEC
PAO1	0.5	64	128-256	0.25	32	64-128
FQSE06-0403	1	128	256	0.25	8-16	128
Pa1m	1	0.5	1	0.06-0.125	0.125-0.25	1
Pa2m	0.5	32	256	0.25-0.5	16	32-64
Pa14	0.25	16-32	64	0.25	16	32-64
Free SCM						
Strain	MIC	MBIC	MBEC			

PAO1	1-2	32-64	128-256
FQSE06-0403	0.5	32-64	256-512
Pa1m	0.06-	1	2
Pa2m	0.125	32-64	64
Pa14	0.5	32-64	32-64
	0.25-0.5		

Pa, *Pseudomonas aeruginosa*; SCM-NLC, sodium colistimethate loaded-nanostructured lipid carriers; MIC, minimum inhibitory concentration; MBIC, minimum biofilm inhibitory concentration; MBEC, minimum biofilm eradication concentration; (-), negatively charged NLC without chitosan; (+), positively charged NLC with chitosan.

Table 4. Planktonic and biofilm susceptibility studies. MIC, MBIC and MBEC values for AMK-NLC formulations against *P. aeruginosa* strains. All the results are expressed in mg/L.

Strain	(-) AMK-NLC Trehalose			(+) AMK-NLC Trehalose		
	MIC	MBIC	MBEC	MIC	MBIC	MBEC
PAO1	0.25	0.25	256-512	0.5-1	0.5-1	128-256
FQSE06-0403	0.25	0.25	64	0.25-0.5	1-2	256
Pa1m	1	1	1	1	1	1
Pa2m	2	8	256	2	2	1024
Pa14	0.5	1	64-128	0.5-1	0.5-1	32-64
Strain	(-) AMK-NLC Dextran			(+) AMK-NLC Dextran		
	MIC	MBIC	MBEC	MIC	MBIC	MBEC
PAO1	0.25	0.25	1024	0.25-0.5	0.5-1	256-512
FQSE06-0403	0.25	0.25	64-128	0.25-0.5	0.5-1	128-256
Pa1m	1	1	1	1	1	1
Pa2m	2	8	256-512	1	2	512-1024
Pa14	0.5	1	32-64	0.5	0.5	32-64
Strain	Free AMK					
	MIC	MBIC	MBEC			
PAO1	0.25-0.5	0.5-1	128-256			
FQSE06-0403	0.25	0.5-1	256-512			
Pa1m	1	1	1			
Pa2m	2	32	512			
Pa14	0.5-1	0.5	32-64			

Pa, *Pseudomonas aeruginosa*; AMK-NLC, amikacin loaded-nanostructured lipid carriers; MIC, minimum inhibitory concentration; MBIC, minimum biofilm inhibitory concentration; MBEC, minimum biofilm eradication concentration; (-), negatively charged NLC without chitosan; (+), positively charged NLC with chitosan.

As observed in Table 4, strains displayed different susceptibilities to AMK-NLC formulations (*i.e.*, 0.25-2 mg/L MIC, 0.25-32 mg/L MBIC and 1-1024 mg/L MBEC).

Regardless of the cryoprotectant, both (-) AMK-NLC and (+) AMK-NLC presented the same MIC value in almost all of the strains (Table 4) compared to free AMK. In

addition, these formulations showed a decrease of a minimum 4-fold in MBIC in some strains (e.g., Pa2m); however, this activity enhancement was not transferred to improve MBEC. Concretely, the activity against PAO1 and Pa14 was very similar among AMK-NLC and free AMK. For FQSE06-0403 strain, nanoencapsulation led to a mild improvement of the activity, whereas Pa1m displayed the same results for all the formulations and the free drug control. To summarize, all AMK-NLC showed effectiveness close to that of free AMK. However, (-) AMK-NLC trehalose seemed to present a little better result in comparison to the other AMK-NLC formulations since it displayed a slight improvement in MBIC and MBEC values.

As (+) SCM-NLC and (-) AMK-NLC, both with trehalose, were the formulations presenting the best activity against *P. aeruginosa*, this cryoprotectant was selected to proceed an in-depth screening using *P. aeruginosa*, *K. pneumoniae* and *A. baumannii* strains. On the one hand, results of the MIC susceptibility studies for (-) SCM-NLC and (+) SCM-NLC against these three superbugs are shown in Table 5. Regarding particle charge, no differences were observed among the tested strains. In fact, for *P. aeruginosa* strains, both formulations showed a slight better activity since MICs were reduced 2-fold compared to free SCM. Certainly, Pa10, an XDR strain resistant to SCM, showed much better activity (MIC reduction of 16-fold relative to free SCM); however, definitively, positive and negative SCM-NLC showed better results against *K. pneumoniae* and, especially, against *A. baumannii* strains (MIC reductions of 4/10-fold relative to SCM, respectively).

Table 5. MIC values of SCM-NLC and free SCM against *P. aeruginosa* (A), *K. pneumoniae* (B) and *A. baumannii* (C); (-), negatively charged NLC without chitosan; (+), positively charged NLC with chitosan. *Pa*, *Pseudomonas aeruginosa*; *Kp*, *Klebsiella pneumoniae*; *Ab*, *Acinetobacter baumannii*; details about all strains can be found in supplementary material.

A	<i>P. aeruginosa</i>			MIC (mg/L)
	Strain	(-) SCM-NLC Trehalose	(+) SCM-NLC Trehalose	Free SCM
	ATCC Pa 27853	0.5	0.5	1
	Pa1016	0.25	0.25	0.5
	Pa3	0.25	0.25	0.5
	Pa4	0.25	0.25	0.5
	Pa46	0.5	0.5	0.5
	Pa54	0.5	0.5	0.5
	Pa116	0.125	0.125	0.25
	Pa166	0.5	0.5	0.5
	Pa167	0.25	0.25	0.5

Pa179	0.25	0.25	0.5
Pa17	0.25	0.125	0.5
Pa10	8	8	128
Pa11	0.25	0.25	1
Pa13	0.25	0.25	1
Pa15	0.03	0.03	0.03
<b>B</b>	<b><i>K. pneumoniae</i></b>		<b>MIC (mg/L)</b>
<b>Strain</b>	<b>(-) SCM-NLC</b>	<b>(+) SCM-NLC</b>	<b>Free SCM</b>
	<b>Trehalose</b>	<b>Trehalose</b>	
ATCC <i>E. coli</i> 25922	0.25	0.25	1
Kp1	0.25	0.25	1
Kp2	0.25	0.25	1
Kp3	0.25	0.25	1
Kp4	0.5	0.5	2
Kp5	0.5	0.5	2
Kp6	1	1	4
Kp7	0.25	0.25	2
Kp8	0.5	0.5	1
Kp9	0.25	0.25	2
Kp10	0.5	0.25	2
Kp11	32	32	32
Kp12	0.5	0.5	2
Kp13	0.5	0.5	1
<b>C</b>	<b><i>A. baumannii</i></b>		<b>MIC (mg/L)</b>
<b>Strain</b>	<b>(-) SCM-NLC</b>	<b>(+) SCM-NLC</b>	<b>Free SCM</b>
	<b>Trehalose</b>	<b>Trehalose</b>	
ATCC Ab 19606	0.25	0.25	1
Ab360	0.5	0.5	2
Ab3581	0.5	0.5	2
Ab4249	0.25	0.25	1
Ab4275	0.5	0.25	2
Ab60	0.25	0.25	1
Ab3343	0.5	0.5	1
Ab4256	0.25	0.25	2
Ab3202	0.25	0.125	1
Ab771	0.5	0.25	2
Ab769	0.5	0.5	2
Ab181	0.25	0.25	1
Ab1959	0.25	0.25	2
Ab11	0.25	0.25	2
Ab14	0.5	0.25	1
Ab308	0.25	0.25	1

On the other hand, results of the MIC susceptibility studies for (-) AMK-NLC and (+) AMK-NLC are shown in Table 6. No differences were observed in their activities against all the tested strains. For *P. aeruginosa* and some *A. baumannii* strains, both formulations showed a slight better activity (MIC reductions of 2-fold compared to the activity of free AMK). Nevertheless, for *K. pneumoniae* strains, no differences were observed in the activity of AMK-NLC formulations and free AMK.

*Nanostructured lipid carriers (NLCs) for multiresistant infections*

Table 6. MIC values of AMK-NLC and free AMK against *P. aeruginosa* (A), *K. pneumoniae* (B) and *A. baumannii* (C); (-), negatively charged NLC without chitosan; (+), positively charged NLC with chitosan. *Pa*, *Pseudomonas aeruginosa*; *Kp*, *Klebsiella pneumoniae*; *Ab*, *Acinetobacter baumannii*; details about all strains can be found in supplementary material.

<b>A</b> <i>P. aeruginosa</i>		<b>MIC (mg/L)</b>		
<b>Strain</b>	<b>(-) AMK-NLC Trehalose</b>	<b>(+) AMK-NLC Trehalose</b>	<b>Free AMK</b>	
ATCC Pa 27853	0.5	0.5	1	
Pa1016	0.5	0.5	1	
Pa3	8	8	32	
Pa4	0.5	0.5	1	
Pa46	8	8	16	
Pa54	8	8	16	
Pa116	1	1	1	
Pa166	1	1	2	
Pa167	2	2	4	
Pa179	1	1	1	
Pa17	0.5	0.5	1	
Pa10	4	4	4	
Pa11	1	1	1	
Pa13	0.5	0.5	1	
Pa15	8	8	8	
<b>B</b> <i>K. pneumoniae</i>		<b>MIC (mg/L)</b>		
<b>Strain</b>	<b>(-) AMK-NLC Trehalose</b>	<b>(+) AMK-NLC Trehalose</b>	<b>Free AMK</b>	
ATCC <i>E. coli</i> 25922	2	2	2	
Kp1	2	2	2	
Kp2	>64	>64	>64	
Kp3	16	16	16	
Kp4	2	2	2	
Kp5	2	2	2	
Kp6	2	4	2	
Kp7	2	2	2	
Kp8	2	2	4	
Kp9	0.5	0.5	0.5	
Kp10	1	2	2	
Kp11	2	2	2	
Kp12	0.5	0.5	0.5	
Kp13	0.5	0.5	0.5	
<b>C</b> <i>A. baumannii</i>		<b>MIC (mg/L)</b>		
<b>Strain</b>	<b>(-) AMK-NLC Trehalose</b>	<b>(+) AMK-NLC Trehalose</b>	<b>Free AMK</b>	
ATCC Ab 19606	1	1	1	
Ab360	4	4	2	
Ab3581	2	2	4	
Ab4249	8	8	8	
Ab4275	4	2	4	
Ab60	2	2	2	
Ab3343	8	8	16	
Ab4256	1	1	1	
Ab3202	2	2	2	
Ab771	4	4	8	
Ab769	8	8	8	
Ab181	>256	>256	128	

Ab1959	8	8	16
Ab11	>256	>256	64
Ab14	4	4	4
Ab308	16	16	32

All in all, it can be concluded that it is not worthwhile using chitosan with the aim of improving antibiotic-NLC activity since no significant differences were found between particles and free drug, despite analyzing a high number of strains in planktonic conditions, also considering the associated higher production costs compared to negative formulations. However, it is important to note that the negatively charged formulation that gave the best activity results was (-) SCM-NLC, concretely against *A. baumannii*. For these reasons, an *in vivo* neutropenic murine pneumonia model infected with *A. baumannii* was developed to test (-) SCM-NLC efficacy.

Results from the efficacy *in vivo* study are shown in Table 7. It can be observed that IM free SCM 60 mg/kg q6h, IP (-) SCM-NLC q12h and IP (-) SCM-NLC q24h treatments were significantly more effective than the saline control group, showing a reduction of 2.75, 2.98 and 3.31 log<sub>10</sub> CFU/g lung median, respectively (p < 0.05). However, no significant effect was observed among IM free SCM 60 mg/kg q6h and the two IP (-) SCM-NLC treatment groups. (-) SCM-NLC 12 mg/kg q12h and q24h IM presented the same effect as the saline control group.

Table 7. Results from the *in vivo* studies

Route	Treatment	N	Log <sub>10</sub> cfu/g lung median (IQR <sub>25-75</sub> )
IM	Control 0.9 % NaCl q6h	10	6.33 (4.94-7.07)
	SCM 60 mg/kg q6h	8	3.58 (3.15-4.01) <sup>a</sup>
	(-) SCM-NLC 12 mg/kg q12h	8	5.91 (4.57-6.41)
	(-) SCM-NLC 12 mg/kg q24h	7	6.56 (5.37-7.09)
IP	(-) SCM-NLC 6 mg/kg q 12h	7	3.35 (2.87-4.67) <sup>a</sup>
	(-) SCM-NLC 6 mg/kg q24h	8	3.02 (2.19-4.40) <sup>a</sup>

N; number of animals IQR; interquartile range, NaCl; sodium chloride, CFU; colony-forming units, SCM; sodium colistimethate, IM; intramuscular, IP; intraperitoneal; <sup>a</sup>p value < 0.05 vs control

#### **4. Discussion**

Nanoencapsulation provides a sustained release of the active ingredient that can lead to lower plasmatic concentration of the drug, contributing to a safer toxicological profile. In addition, it has been described in the literature that nanoencapsulation of antibiotics could improve antibiotic disposition leading to an enhanced activity of the drug. Based on these hypotheses, in this work, SCM and AMK were selected to be encapsulated into lipid nanoparticles, concretely into NLC, to obtain SCM- or AMK-loaded NLC (SCM-NLC or AMK-NLC) with the aim of testing their efficacy against a range of different resistant strains. Previous works reported that freeze-dried SCM-NLC, including trehalose as cryoprotectant (SCM-NLC trehalose), displayed higher antimicrobial activity than nanoparticles using mannitol (9). In the present work, cryoprotectant effectiveness of trehalose was compared to that of dextran. Dextran was selected because it has been found to provide protection and improved stability of drugs in amorphous matrices during storage (21), as it is the case of NLC. On the other hand, negative and positive surface charges were also assessed. It has been widely reported in the literature that positively charged nanoparticles might increase antimicrobial activity due to surface/membrane stronger interaction (18). In addition, it is well known that, specifically, chitosan has considerable antibacterial properties (22), which possibly could have a synergistic effect with the loaded antibiotic. Finally, a HPH step was included to the production process in order to handle higher working volumes during industrial batch preparation. Most industries have already adopted HPH for various applications. The main advantages of our preparation method coupled to HPH are i) good reproducibility, ii) suitability of the homogenization technology for large scale productions, and iii) organic solvent free method (23).

Regarding to the particle size, HPH step inclusion led to a smaller size compared to the previous data reported on SCM-NLC trehalose ( $412.5 \pm 13.9$  nm vs  $67.33 \pm 2.06$  nm). This size reduction could play an important role in terms of penetration across different layers. It has been widely described that in the case of liposomes, a significant penetration is detected in the size range of hundreds of nanometers (24). In addition, for instance, in cystic fibrosis the mesh spacing of the sputum is reported to present an average size of  $\sim 140 \pm 50$  nm (range: 60–300 nm) and hence, this smaller particle size could improve mucus penetration (25). As it could be expected, the

coating process led to bigger particle size. Such increase could be attributed to the chitosan coating around the NLC or a possible aggregation of the particles caused by the sticky nature of the polymer (13). However, no particle aggregation was expected since PDI values were acceptable for such lipid-based carriers (26), as verified by the ease of resuspending after lyophilization.

Turning to zeta potential, all SCM-NLC resulted to be stable just as (-) AMK-NLC, while (+) AMK-NLC showed lower values, close to 0 mV, providing a less stable colloidal system.

On the other hand, AMK-NLC achieved the highest EE, very likely due to a lower drug water solubility and a higher affinity for the lipid phase. Also, AMK-NLC showed a slower drug release profile compared to SCM-NLC, mainly due to amikacin hydrophobicity, and partly because of the lower amount of non-encapsulated drug that led to a milder initial release. The release profile, as well as EE, can vary from one drug to another depending on the affinity of the drug to the lipid matrix and to the aqueous media (27). In addition, it is noteworthy to mention that administration of free and nanoencapsulated drug might present a synergic effect by rapidly making available a small drug amount and slowly releasing the encapsulated drug, as already reported by Pulmaquin<sup>®</sup> (Aradigm Corporation, Hayward, CA, US) (28).

TEM images showed that 0.5 % chitosan concentration (13) turned out to be excessive and therefore, the coating process should be optimized either by adding less coating agent or by incorporating a washing step. In addition, in the case of both (-) AMK-NLC and (+) AMK-NLC, a stronger mixing conditions should have been used, as it seems that aggregation was higher for AMK-NLC than for SCM-NLC. Only (-) SCM-NLC showed a homogeneous and spherical shape, in accordance to TEM images of other NLC (11).

Also, one of the aims of this work was to study the antimicrobial activity of SCM-NLC and AMK-NLC pointing out the effectiveness in planktonic and biofilm cells. The first preliminary screening in *P. aeruginosa* strains revealed that trehalose seemed to be the most suitable cryoprotectant, capable of better preserving antibiotic efficacy. This result is in accordance with the investigation of Crowe *et al.*, who demonstrated

that trehalose might be superior to other sugars for preserving freeze-dried lipid carriers (29).

Besides, it is postulated that as bacteria present negative net charge, they can interact with positively charged particles, easing penetration through biofilm and even inducing cell wall disruption, as occur with ammonium quaternary salts (18,30). As a matter of fact, (+) SCM-NLC led to lower MIC, MBIC and MBEC, especially in *P. aeruginosa*, in accordance with other authors reporting that positively charged small particles diffuse more efficiently through the biofilm formed by this bug (18,31,32). On the contrary, (+) AMK-NLC displayed similar effectiveness to free AMK, probably because the positive coating did not achieve high zeta potential and thus could hinder charge interaction. When an in-depth screening was carried out in a higher amount of strains, no significant differences were found between positive and negative antibiotic-loaded nanoparticles; thus, chitosan coating was discarded, taking into account the inconvenient manufacturing process cost-efficiency, from both an economical and production time point of view.

For those reasons, (-) SCM-NLC were the selected formulation to perform an efficacy *in vivo* study. It is noteworthy to mention that, on the one hand, IP (-) SCM-NLC 6 mg/kg q12h and IP (-) SCM-NLC 6 mg/kg q24h achieved the same efficacy as that for free SCM with a ten times lower dose and; on the other hand, a dose interval of q24h for IP (-) SCM-NLC 6 mg/kg achieved the same activity as free SCM 60 mg/kg, with a q6h dose interval, potentially reducing treatment cost. So, it can be speculated that encapsulation process enhanced the antimicrobial activity of SCM, probably because NLC are capable of avoiding early drug degradation; hence, improving its stability and enhancing *in vivo* drug disposition. Those findings are in line with Puglia *et al.* who reported that curcumin availability was considerably improved when embedded into NLC (33). In addition, it is worth noting that the fewer administrations the better patient quality of life. Therefore, (-) SCM-NLC 6mg/kg q24h seems a promising innovative formulation that could become a very useful weapon to fight against resistant pulmonary bacterial infections, above all when administered following IP route. Achieving a considerable antibiotic dose reduction paves the way to the possibility of greatly enhancing SCM safety and perhaps of obtaining better efficacy with a future dose escalation.

## 5. Conclusion

In conclusion, in an attempt to improve the disposition and, consequently, the antimicrobial activity of SCM and AMK, these drugs were nano-encapsulated into nanostructured lipid carriers or NLC. The addition of a high-pressure homogenization step allowed to work with bigger size batches and both negatively and positively charged NLC were correctly produced. It was shown that encapsulation did not reduce drug efficacy but positive chitosan coating was discarded due to its low cost-efficiency. Negatively charged SCM-NLC, with trehalose as cryoprotectant, were selected for their better efficacy in several bacteria strains, especially in *A. baumannii*. Finally, the *in vivo* efficacy study revealed that (-) SCM-NLC could be administered with a dose interval of q24h (in spite of q6h for free SCM) and with a 10-fold lower dose (6 mg/kg) to achieve the same effect of the current SCM treatment dose (60 mg/kg). IP (-) SCM-NLC 6mg/kg q24h could represent a promising option to fight against resistant pulmonary infections due to *A. baumannii* and successfully tackle the alarming AMR problem.

## 6. Acknowledgment

This work was carried out under the Nanogrow project, with file number ZE-2017/00014, supported by the Department of Economic Development and Infrastructure of the Basque Government budget, through the Hazitek business I+D support program and co-financed by the European Regional Development Fund (ERDF). Also, under NanoGSkin project, which has received founding from the 8<sup>th</sup> Joint Transnational Call for Proposals for "European Innovative Research & Technological Development Projects in Nanomedicine" within the framework of the ERA-NET EuroNanoMed-III.

## **7. References**

- (1) World Health Organization. Antimicrobial resistance [article online], 2018. Available from <http://www.who.int/en/news-room/fact-sheets/detail/antimicrobial-resistance>
- (2) The bacterial challenge: time to react [article online], 2009. Available from [https://www.ecdc.europa.eu/sites/portal/files/media/en/publications/Publications/0909\\_TER\\_The\\_Bacterial\\_Challenge\\_Time\\_to\\_React.pdf](https://www.ecdc.europa.eu/sites/portal/files/media/en/publications/Publications/0909_TER_The_Bacterial_Challenge_Time_to_React.pdf)
- (3) Antibiotic Resistance Threats in the United States, 2013 [article online], 2018. Available from <https://www.cdc.gov/drugresistance/pdf/ar-threats-2013-508.pdf>
- (4) Antimicrobial Resistance: Tackling a crisis for the health and wealth of nations [article online], 2014. Available from [https://amr-review.org/sites/default/files/AMR%20Review%20Paper%20-%20Tackling%20a%20crisis%20for%20the%20health%20and%20wealth%20of%20nations\\_1.pdf](https://amr-review.org/sites/default/files/AMR%20Review%20Paper%20-%20Tackling%20a%20crisis%20for%20the%20health%20and%20wealth%20of%20nations_1.pdf)
- (5) Tacconelli E, Carrara E, Savoldi A, Harbarth S, Mendelson M, Monnet DL, Pulcini C, Kahlmeter G, Kluytmans J, Carmeli Y, Ouellette M, Outterson K, Patel J, Cavalieri M, Cox EM, Houchens CR, Grayson ML, Hansen P, Singh N, Theuretzbacher U, Magrini N. WHO Pathogens Priority List Working Group. Discovery, research, and development of new antibiotics: the WHO priority list of antibiotic-resistant bacteria and tuberculosis. *Lancet Infect Dis* 2018;18(3):318-327
- (6) Global priority list of antibiotic-resistant bacteria to guide research, discovery, and development of new antibiotics [article online], 2017. Available from [https://www.who.int/medicines/publications/WHO-PPL-Short\\_Summary\\_25FebET\\_NM\\_WHO.pdf?ua=1](https://www.who.int/medicines/publications/WHO-PPL-Short_Summary_25FebET_NM_WHO.pdf?ua=1)
- (7) Alliance for the Prudent Use of Antibiotics (APUA). The cost of antibiotic resistance to US families and the health care system [article online], 2010. Available from [http://emerald.tufts.edu/med/apua/consumers/personal\\_home\\_5\\_1451036133.pdf](http://emerald.tufts.edu/med/apua/consumers/personal_home_5_1451036133.pdf)

- (8) Beringer P. The clinical use of colistin in patients with cystic fibrosis. *Curr Opin Pulm Med* 2001;7(6):434-40
- (9) Kent A, Turner MA, Sharland M, Heath PT. Aminoglycoside toxicity in neonates: Something to worry about? *Expert Rev Anti Infect Ther* 2014;12(3):319-31
- (10) Pastor M, Basas J, Vairo C, Gainza G, Moreno-Sastre M, Gomis X, Fleischer A, Palomino E, Bachiller D, Gutiérrez FB, Aguirre JJ, Esquisabel A, Igartua M, Gainza E, Hernandez RM, Gavaldà J, Pedraz JL. Safety and effectiveness of sodium colistimethate-loaded nanostructured lipid carriers (SCM-NLC) against *P. aeruginosa*: *in vitro* and *in vivo* studies following pulmonary and intramuscular administration. *Nanomedicine* 2019;18:101-111
- (11) Vairo C, Collantes M, Quincoces G, Villullas S, Peñuelas I, Pastor M, Gil AG, Gainza E, Hernandez RM, Igartua M, Gainza G. Preclinical safety of topically administered nanostructure lipid carriers (NLC) for wound healing application: biodistribution and toxicity studies. *Int J Pharm* 2019;569:118484
- (12) Pastor M, Moreno-Sastre M, Esquisabel A, Sans E, Viñas M, Bachiller D, Asensio VJ, Pozo AD, Gainza E, Pedraz JL. Sodium colistimethate loaded lipid nanocarriers for the treatment of *Pseudomonas aeruginosa* infections associated with cystic fibrosis. *Int J Pharm* 2014;477(1):485-494
- (13) Fonte P, Nogueira T, Gehm C, Ferreira D, Sarmiento B. Chitosan-coated solid lipid nanoparticles enhance the oral absorption of insulin. *Drug Deliv and Transl Res* 2011;1(4):299-308
- (14) Sampath SS, Robinson DH. Comparison of new and existing spectrophotometric methods of analysis of tobramycin and other aminoglycosides. *J Pharm Sci* 1990; 79(5):428-31
- (15) Ungaro F, d'Angelo I, Coletta C, d'Emmanuele di Villa Bianca R, Sorrentino R, Perfetto B, Tufano MA, Miro A, La Rotonda MI, Quaglia F. Dry powders based on PLGA nanoparticles for pulmonary delivery of antibiotics: Modulation of encapsulation efficiency, release rate and lung deposition pattern by hydrophilic polymers. *J Control Release* 2012;157(1):149-159

(16) Media preparation for EUCAST disk diffusion testing and for determination of MIC values by the broth microdilution method [article online], 2020. Available from [http://www.eucast.org/fileadmin/src/media/PDFs/EUCAST\\_files/Disk\\_test\\_documents/2020\\_manuals/Media\\_preparation\\_v\\_6.0\\_EUCAST\\_AST.pdf](http://www.eucast.org/fileadmin/src/media/PDFs/EUCAST_files/Disk_test_documents/2020_manuals/Media_preparation_v_6.0_EUCAST_AST.pdf)

(17) Moskowitz SM, Foster JM, Emerson J, Burns JL. Clinically Feasible Biofilm Susceptibility Assay for Isolates of *Pseudomonas aeruginosa* from Patients with Cystic Fibrosis. *J Clin Microbiol* 2004;42(5):1915-1922

(18) Gottenbos B, Grijpma DW, van der Mei HC, Feijen J, Busscher H. Antimicrobial effects of positively charged surface on adhering Gram-positive and Gram-negative bacteria. *J Antimicrob Chemother* 2001;48(1):7-13

(19) National Research Council. Guide for the Care and Use of Laboratory Animals: Eighth Edition. Washington, DC: The National Academies Press, 2011

(20) Rodriguez-Hernandez MJ, Pachon J, Pichardo C, Cuberos L, Ibanez-Martinez J, Garcia-Curiel A, Caballero FJ, Moreno I, Jiménez-Mejías ME. Imipenem, doxycycline and amikacin in monotherapy and in combination in *Acinetobacter baumannii* experimental pneumonia. *J Antimicrob Chemother* 2000;45(4):493-501

(21) Sun WQ, Davidson P. Effect of dextran molecular weight on protein stabilization during freeze-drying and storage. *Cryo Letters* 2001;22(5):285-92

(22) Kong M, Chen XG, Xing K, Park HJ. Antimicrobial properties of chitosan and mode of action: A state of the art review. *Int J Food Microbiol* 2010;144(1):51-63

(23) Cui B, Feng L, Wang C, Yang D, Yu M, Zeng Z, Wang Y, Sun C, Zhao X, Cui H. Stability and Biological Activity Evaluation of Chlorantraniliprole Solid Nanodispersions Prepared by High Pressure Homogenization. *PLoS ONE* 2016;11(8):e0160877

(24) Meers P, Neville M, Malinin V, Scotto AW, Sardaryan G, Kurumunda R, Mackinson C, James G, Fisher S, Perkins WR. Biofilm penetration, triggered release and *in vivo* activity of inhaled liposomal amikacin in chronic *Pseudomonas aeruginosa* lung infections. *J Antimicrob Chemother* 2008;61(4):859-68 2008

- (25) Suk JS, Lai SK, Wang Y, Ensign LM, Zeitlin PL, Boyle MP, Hanes J. The penetration of fresh undiluted sputum expectorated by cystic fibrosis patients by non-adhesive polymer nanoparticles. *Biomaterials* 2009;30(13):2591-2597
- (26) Danaei M, Dehghankhold M, Ataei S, Hasanzadeh Davarani F, Javanmard R, Dokhani A, Khorasani S, Mozafari MR. Impact of Particle Size and Polydispersity Index on the Clinical Applications of Lipidic Nanocarrier Systems. *Pharmaceutics* 2018 18;10(2):57
- (27) zur Mühlen A, Schwarz C, Mehnert W. Solid lipid nanoparticles (SLN) for controlled drug delivery – Drug release and release mechanism. *Eur J Pharm Biopharm* 1998;45(2):149-55
- (28) Cipolla D, Blanchard J, Gonda I. Development of Liposomal Ciprofloxacin to Treat Lung Infections. *Pharmaceutics* 2016;8(6)
- (29) Crowe LM, Reid DS, Crowe JH. Is trehalose special for preserving dry biomaterials? *Biophys J* 1996;71(4):2087-2093
- (30) Lawrence AC. Quaternary ammonium surface-active disinfectants. In *Disinfection, Sterilization and Preservation*. 1<sup>st</sup> ed. Lawrence AC, Block SS, Eds. Philadelphia, Lea & Febiger, 1968, p. 430-452
- (31) Chronopoulou L, Di Domenico EG, Ascenzioni F, Palocci C. Positively charged biopolymeric nanoparticles for the inhibition of *Pseudomonas aeruginosa* biofilms. *J Nanopart Res* 2016;18(10):308
- (32) Peulen T, Wilkinson K. Diffusion of Nanoparticles in a Biofilm. *Environ Sci Technol* 2011;45(8):3367-73
- (33) Puglia C, Frasca G, Musumeci T, Rizza L, Puglisi G, Bonina F, Chiechio S. Curcumin loaded NLC induces histone hypoacetylation in the CNS after intraperitoneal administration in mice. *Eur J Pharm Biopharm* 2012;81(2):288-93



## CHAPTER 2

### Safety and effectiveness of sodium colistimethate-loaded nanostructured lipid carriers (SCM-NLC) against *P. aeruginosa*: *in vitro* and *in vivo* studies following pulmonary and intramuscular administration

Marta Pastor<sup>1</sup>, Jana Basas<sup>b,1</sup>, Claudia Vairo<sup>c,1</sup>, Garazi Gainza<sup>a</sup>, María Moreno-Sastre<sup>c,d</sup>, Xavier Gomis<sup>b</sup>, Aarne Fleischer<sup>e</sup>, Esther Palomino<sup>e</sup>, Daniel Bachiller<sup>e</sup>, Francisco Borja Gutiérrez<sup>f</sup>, Jose Javier Aguirre<sup>a,f</sup>, Amaia Esquisabel<sup>c,d</sup>, Manoli Igartua<sup>c,d</sup>, Eusebio Gainza<sup>a</sup>, Rosa Maria Hernandez<sup>c,d</sup>, Joan Gavaldà<sup>b,\*</sup>, José Luis Pedraz<sup>c,d,\*\*</sup>

<sup>a</sup>BioPraxis Research AIE, R&D Department, Miñano (Araba), Spain; <sup>b</sup>Antimicrobial Resistance Laboratory, Vall d'Hebron Research Institute (VHIR), Infectious Diseases Department, Hospital Universitari Vall d'Hebron, Passeig Vall d'Hebron, Barcelona, Spain; <sup>c</sup>NanoBioCel Group, Laboratory of Pharmaceutics, University of the Basque Country (UPV/EHU), School of Pharmacy, Vitoria-Gasteiz, Spain; <sup>d</sup>Biomedical Research Networking Center in Bioengineering, Biomaterials and Nanomedicine (CIBER-BBN), Vitoria-Gasteiz, Spain; <sup>e</sup>Consejo Superior de Investigaciones Científicas (CSIC/IMEDEA), Esporles, Spain; <sup>f</sup>Department of Pathological Anatomy, Hospital Universitario de Álava (HUA), Vitoria-Gasteiz, Spain

\*Corresponding author: Joan Gavaldà; \*\*Corresponding author: José Luis Pedraz

---

#### ABSTRACT

The usefulness of nanotechnology to increase the bioavailability of drugs and decrease their toxicity may be a tool to deal with multiresistant *P. aeruginosa* respiratory infections. We describe the preparation and the *in vivo* efficacy and safety of sodium colistimethate-loaded nanostructured lipid carriers (SCM-NLC) by the pulmonary and intramuscular routes. Nanoparticles showed 1-2 mg/L minimum inhibitory concentration against eight extensively drug-resistant *P. aeruginosa* strains. *In vivo*, SCM-NLC displayed significantly lower CFU/g lung than the saline and similar to that of the free SCM, even the dose in SCM-NLC group was lower than free SCM. There was no tissue damage related to the treatments. Biodistribution assessments showed a mild systemic absorption after nebulization and a notorious absorption after IM route. Altogether, it could be concluded that SCM-NLC were effective *in vivo* against *P. aeruginosa*, not toxic and distribute efficiently to the lung and liver after pulmonary or intramuscular administrations.



## 1. Introduction

Antimicrobial resistance has emerged as a result of the use and misuse of antibiotics, leading to the beginning of a post-antibiotic era where minor injuries and previously treatable illnesses will be fatal again. Indeed, antibiotic resistance is a serious threat for global public health, jeopardizing the latest improvements in control of diseases, such as organ transplants, cancer chemotherapy or major surgery [1]. It is estimated that 51,000 health care-associated *P. aeruginosa* infections occur in the United States every year. More than 6000 (or 13 %) of these are multidrug-resistant, with roughly 400 deaths per year attributed to these infections. Alarmingly, some of these strains were not susceptible to any antipseudomonal compound [2]. In this framework, colistin, and its pro-drug, sodium colistimethate, were proposed as rescue therapy in late 1990s and 2000s. Colistin is an antimicrobial peptide that is used for handling multidrug-resistant gram-negative bacteria, but cases of colistin-resistance are becoming widely reported and there are even cases of resistance to colistin in patients that have never previously used this antibiotic [3]. Moreover, the difficulty of using colistin, mainly in severely ill patients, and its high nephro- and neurotoxicity should be highlighted [4].

In this regard, the use of nanotechnology has arisen as an alternative against multidrug-resistant bacteria. Depending on the nature of the polymer, nanoparticles can be biodegradable, be biocompatible and release drugs in a controlled manner preventing drug deactivation or fostering mucoadhesion. Nanoparticles can be tailored depending on the drug, the route of administration or the target disease. Among different drug delivery systems, nanostructured lipid carriers (NLC) have gained the attention of many research groups as promising second-generation of lipid nanoparticles. These nanoparticles present a lipid core made of liquid and solid lipids leading to disordered matrix and providing more space for drug loading. Our research group has already encapsulated different compounds showing the versatility of these drug delivery systems [5–8]. NLC offers high drug loading and stability as well as good tolerability as the lipids selected for the preparation are under GRAS (Generally Refer As Safe) FDA-denomination [9].

Overall, the aims of this study are the following; first, to prepare sodium colistimethate-loaded nanostructured lipid carriers (SCM-NLC) and prove their *in vitro* antimicrobial activity against different multiresistant *P. aeruginosa* (Mr-Pa) clinical isolates; second, to evaluate the toxicity, the biodistribution and the effectiveness of the pulmonary administration of nebulized SCM-NLC and intramuscular (IM) administration of SCM-NLC against an extensively drug-resistant (XDR)-Pa strain in an acute pneumonia model in mice.

## **2. Materials and methods**

### **2.1. Materials**

Precirol® ATO 5 and Miglyol 182 N/F were kindly provided by Gattefossé (Madrid, Spain) and Sasol (Hamburg, Germany), respectively. Poloxamer 188, Lutrol® LF68 was a kind gift by BASF (Ludwigshafen, Germany). Polysorbate, Tween® 80 was purchased by Panreac Química (Castellar del Vallès, Barcelona, Spain). Sodium colistimethate was provided by LGC and trehalose and IR-783 dye were purchased from Sigma-Aldrich (St. Louis, MO, US). Amicon® centrifuge filters presenting a molecular weight cut-off of 100 kDa were purchased from Merck Millipore (Darmstadt, Germany). Tryptic Soy Agar (TSA) and McFarland pattern, DensiCHEK™ Plus, were purchased from BioMérieux® SA (Marcy l'Etoile, France) and Tryptic Soy Broth (TSB) and Müller Hinton Broth (MHB) were purchased from Becton Dickinson (Le Pont de Clarx, France). Other chemicals were all analytical grade.

### **2.2. Methods**

#### **2.2.1. NLC preparation**

Sodium colistimethate loaded-nanostructured lipid carriers (SCM-NLC) were prepared using hot melt homogenization following the protocol previously reported by our research group with a slight variation in sonication potency, as a scale-up process implementation [7]. Briefly, Precirol® ATO 5 and Miglyol 182 N/F were melted with the drug to achieve the oily phase (10:1:1). Simultaneously, the aqueous phase was prepared dissolving Tween® 80 at 1.3% (w/v) and Poloxamer 188 at 0.6% (w/v) and then the solution was tempered above the melting temperature of the solid

lipid. Both phases were mixed and emulsified under sonication for 15 s at 50 W. Afterwards, the resulting emulsion was gradually cooled down and kept under  $5 \pm 2$  °C overnight. Subsequently, particles were washed three times by ultrafiltration using Amicon® filters provided with molecular weight cut-off membrane. 15% (w/w) of trehalose was added to the formulation as cryo-preserving agent prior to the freeze-drying step.

For biodistribution assays, infrared labeled NLC (IR-NLC) were prepared as mentioned before but using IR-783 dye at 3.8 % (w/w) instead of the antibiotic.

Henceforth, bear in mind that any dose (mostly expressed as mg/kg) of SCM-NLC refers to the drug and not to the total nanoparticles weight.

### *2.2.2. NLC characterization*

First, nanoparticles were defined for size, polydispersity index and zeta potential determination by means of Zetasizer Nano ZS (Malvern Instruments, Worcestershire, UK).

For microscopy analysis, the cryo-technique was selected. Samples were processed directly in liquid ethane (without staining) to observe the nanoparticles in the hydrated and almost-native state [10].

Fourier transform infrared (FTIR) spectra of free SCM, SCM-NLC and blank-NLC (NLC with no loaded drug) were carried out on a Nicolet Nexus FTIR spectrometer using ATR Golden Gate (Thermo Scientific, Madrid, Spain) with a crystal ZnSe. The sample was placed directly onto the ATR crystal and spectrum was obtained in transmittance mode. Each spectrum was the result of the average of 32 scans at  $4 \text{ cm}^{-1}$  resolution. Measurements were recorded in the wavelength range of  $4000\text{-}750 \text{ cm}^{-1}$ .

Encapsulation efficiency was calculated indirectly by HPLC, quantifying the amount of the drug in the supernatant [7]. Briefly, the chromatographic conditions were set as follows: a Novapak C18×150 mm column with a  $4 \mu\text{m}$  pore size, the mobile phase consisting of 77% of an aqueous solution and 23 % of acetonitrile, and detection wavelength of 206 nm. Once quantified, the encapsulation efficiency (EE) was estimated according to this equation:

$$EE \% = \frac{[(\text{initial amount of drug}) - (\text{non - encapsulated drug})]}{\text{initial amount of drug}} \times 100$$

Similarly, the drug release profile was also assessed by HPLC. 25 mg of NLC was weighed and re-suspended in 5 ml of PBS (pH 7.4). Then, the suspension was stirred using rotary mixing at 37 °C. At pre-established time points, samples were ultrafiltrated by Amicon® centrifugal devices for 15 min and the drug content in the supernatants was analyzed by HPLC as described above. Samples were studied in triplicate and results are expressed as the percentage of the drug released.

### 2.2.3. Microbiological test

Antimicrobial activity of SCM-NLC was tested against eight clinical isolates of *Pseudomonas aeruginosa*, more precisely against three extensively drug-resistant (XDR) strains (Pa1016, Pa46, Pa54), four multidrug-resistant (MDR) strains (Pa116, Pa166, Pa167, Pa179) and one moderate drug-resistant (modR) strain (Pa17). Strains were originally isolated of patients from different hospitals in Spain. Molecular multilocus sequence typing (MLST), according to protocols and databases available ([pubmlst.org/paeruginosa](http://pubmlst.org/paeruginosa)), revealed that modR isolate belonged to clone ST162, and 3 XDR and 4 MDR strains belonged to ST175 or ST111, both recognized as international high-risk clones circulating in Spain [11,12]. Regarding to resistance mechanisms of these strains: one ST175 (Pa1016) included specific chromosomal-mutational mechanism like inactivation of the porin OprD, hyperproduction of AmpC and overexpression of efflux pumps, where another ST175 (Pa167) and two ST111 (Pa46, Pa54) included an acquired resistance mechanism, mediated by the production of the VIM-2  $\beta$ -lactamase. ModR strain (Pa17) presented an inactivation of the porin OprD. PCR of genes encoding blaKPC, blaOXA, blaNDM, blaOXA-48, blaVIM and blaIMP was negative for the other strains.

The minimum inhibitory concentration (MIC) values of SCM-NLC and free SCM were determined by broth microdilution method according to Clinical and Laboratory Standards Institute (CLSI) guidelines and breakpoints [13]. *P. aeruginosa* ATCC 27853 was used as a control strain for the susceptibility testing. Briefly, SCM-NLC or free SCM was resuspended in MHB and placed in the first row of 96-well plates. Next, decreasing concentrations were obtained by serial dilutions (1:2), starting from 32

mg/L. A concentration of  $5 \cdot 10^5$  colony-forming units (CFU)/mL bacterial suspension was added to each well. Finally, the plates were incubated for 24 h at 37 °C. Negative controls and positive control were also assessed. The MIC was defined as the lowest antibiotic concentration that can prevent visible bacterial growth. The assay was run in triplicate.

#### *2.2.4. In vivo experiments*

148 Balb/c female mice, weighing 20 to 22 g, were purchased from Charles River (Spain) and all of them were treated following the Spanish legislation and the European Community Council Directive on “Protection of Animals used in Experimental and Other Scientific purpose” from July the 22<sup>nd</sup> 2003 (2033/65/CE). The experimental protocols were approved by the Animal Experimentation Ethics Committee of Vall d’Hebron Research Institute (registration number 79/12 CEEA) and the Ministry of Environment of the Catalan Government (registration number 8077). The mice were housed under controlled conditions: 12 h dark/light cycles, food and water *ad libitum* and hyperoxia (95% O<sub>2</sub>, measured by Beckman oxygen analyzer).

Two different administration routes were selected in these experiments: (i) the pulmonary administration of nebulized SCM-NLC in order to develop a drug delivery system with local action for lung infections; (ii) the intramuscular (IM) route as an alternative route that could be used in severe infections or in combination with the pulmonary route.

Three different experiments were designed for the evaluation of the *in vivo* behavior of the SCM-NLC. The efficacy and safety of the SCM-NLC were assessed against free SCM and blank-NLC.

#### *2.2.5. In vivo efficacy study in acute pneumonia model*

The acute pneumonia model and the assay procedure were developed at Vall d’Hebron Research Institute, based on previously published work [14]. Briefly, Balb/c female mice (n=40) were infected with  $1 \cdot 10^8$  CFU/mL of XDR *P. aeruginosa* 1016R strain by nasal instillation of 30 µL. Therapy was initiated 1.5 h after infection. The mice were treated for 3 days with: nebulized saline q12h (every 12 h); nebulized free SCM

*Nanostructured lipid carriers (NLCs) for multiresistant infections*

15 mg/kg q12h; nebulized SCM-NLC 2.8 mg/kg q12h or q24h (every 24 h); IM free SCM 80 mg/kg q12h; IM SCM-NLC 2.8 mg/kg q12h or q24h. The groups receiving the free drug were administered 324 µg of antibiotic (15 mg/kg) and 1700 µg of antibiotic (80 mg/kg) q12h, whereas the SCM-NLC groups received 70 µg of antibiotic (2.8 mg/kg) per dose. All treatments were resuspended in saline. Table 1 details the route, dose and schedule of administration of the studied groups. To administer free or encapsulated antibiotic by pulmonary route, the mice were anaesthetized with isoflurane (O<sub>2</sub> at 1 L/min) and placed on a suitable platform for the use of the nebulization device, MicroSprayer<sup>®</sup> aerosolizer (Model IA-1C, PennCentury, Inc. PA, USA) through a high pressure syringe FMJ-250 (PennCentury, Inc. PA, USA) with the aid of a laryngoscope (PennCentury, Inc. PA, USA). For IM route, animals were anesthetized and free SCM or SCM-NLC were administered in the thigh muscles of the hind limb. During the study, animals were kept under hyperoxia (O<sub>2</sub> 95%) to better simulate the mechanical ventilation conditions associated with the clinical context. Mice were euthanized 4 h after the last dose by cervical dislocation. The lungs were processed for quantitative culture, after being homogenized (UltraTurrax<sup>®</sup> T25; IKA Works, Inc., Wilmington, USA) for 2 min in 5 mL of sterile PBS pH 7.2. Samples were plated on agar for 24 h at 37 °C and lung bacterial density (log<sub>10</sub> CFU/g lung) among groups was compared.

Table 1. Mouse group distribution in the efficacy study.

Route	Description	Amount of SCM per dose ( $\mu\text{g}$ )	Daily dose ( $\mu\text{g}$ )	Total dose ( $\mu\text{g}$ )
Pulmonary	Control NaCl q12h	0	0	0
	Free SCM 15 mg/kg q12h	324	648	1944
	SCM-NLC 2.8 mg/kg q12h	70	140	420
	SCM-NLC 2.8 mg/kg q24h	70	70	210
IM	Free SCM 80 mg/kg q12h	1700	3400	10,200
	SCM-NLC 2.8 mg/kg q12h	70	140	420
	SCM-NLC 2.8 mg/kg q24h	70	70	210

Table 2. Experimental groups in the toxicity study.

Route	Group	Description	Amount of SCM per dose ( $\mu\text{g}$ )	Total dose ( $\mu\text{g}$ )
Pulmonary	T1.1	SCM-NLC 2.8 mg/kg q12h (hyperoxia)	70	420
	T1.2	SCM-NLC 2.8 mg/kg q24h (hyperoxia)	70	210
	T1.3	Control NaCl q12h (hyperoxia)	0	0
IM	T2.1	SCM-NLC 2.8 mg/kg q12h	70	560
	T2.2	SCM-NLC 2.8 mg/kg q24h	70	280
	T2.3	Blank-NLC q24h (equiv. to 2.8 mg/kg)	0	0
	T2.4	Free SCM 2.8 mg/kg q12h	70	560
	T2.5	Free SCM 2.8 mg/kg q24h	70	280
	T2.6	Control NaCl q12h	0	0
IM	T3.1	SCM-NLC 5.6 mg/kg q24h	140	560

*Nanostructured lipid carriers (NLCs) for multiresistant infections*

T3.2	SCM-NLC 11.2 mg/kg q24h	280	1,120
T3.3	Blank-NLC q24h (equiv. to 5.6 mg/kg)	0	0
T3.4	Blank-NLC q24h (equiv. to 11.2 mg/kg)	0	0
T3.5	Free SCM 8 mg/kg q24h	200	800
T3.6	Control NaCl q12h	0	0

---

### *2.2.6. In vivo toxicity studies in healthy mice*

To evaluate the potential toxicity of the SCM-NLC, three different studies were carried out in healthy mice (Table 2). On the one hand, three groups (T1.1. to T1.3.) of mice were maintained under hyperoxia conditions and received SCM-NLC 2.8 mg/kg either q12h or q24h pulmonary administered (n=10). At the end of the study at the third day, the lungs were dissected and fixed in paraformaldehyde 4%. On the other hand, six groups (T2.1. to T2.6.) received SCM-NLC 2.8 mg/kg, free SCM 2.8 mg/kg or the equivalent amount of blank-NLC by the IM route (n=40). All treatments were resuspended in saline. However, this time, the mice were kept in a normal oxygen environment, so that the damage in any tissue could be attributed to NLC and not to the hyperoxia. When the study ended, after four days of treatment, the spleen, brain, heart, liver, lung and kidneys were removed.

In both cases, to analyze the potential tissue damage, hematoxylin and eosin (Sigma-Aldrich, St Louis, US) dying was performed after samples had been dehydrated, paraffin embedded and cut into 4  $\mu\text{m}$  sections. In order to describe the inflammatory stage, a scoring system (0-4) was used, based on the leukocyte infiltration degree into the connective tissue. The score was set as, 0 no leukocytes, 1 a few leukocytes, 2 a ring of single-cell layer leukocytes, 3 a ring of 2-4 leukocytes layer deep and 4 a ring of leukocytes deeper than 4 cell layers [15].

Finally, six additional experimental groups (T3.1. to T3.6.) were tested to evaluate whether higher doses could exert toxic effects (n=30). In this regard, the toxicity of SCM-NLC 5.6 mg/kg and 11.2 mg/kg, blank-NLC, free SCM 8 mg/kg and saline solution was assessed by administering them daily by the IM route. At the end of the study, after four days of treatment, lungs, spleen, liver and kidneys were dissected and fixed, dehydrated and paraffin embedded to obtain 4  $\mu\text{m}$  slide cuts.

### *2.2.7. In vivo biodistribution studies in healthy mice*

Finally, biodistribution of NLC was studied in healthy mice, after pulmonary and IM administration (n=28). For this purpose, infrared-labeled NLC were prepared as reported in section 2.2.1. by loading IR-783 dye. Mice were administered IR-NLC 2.8 mg/kg by the pulmonary or IM route using a Microsprayer® aerosolizer. All

treatments were resuspended in saline. At pre-established time points (5 min, 30 min, 24 h and 48 h, see Figure 1), the mice were sacrificed and observed under LI-COR Pearl® impulse small animal imaging system (LI-COR Corporate). In Groups 6-7, additional doses of IR-NLC (at 24 and 48 h) were administered to study the cumulative effect that NLC might present; mice were sacrificed 2 h after the repeated dose administration.

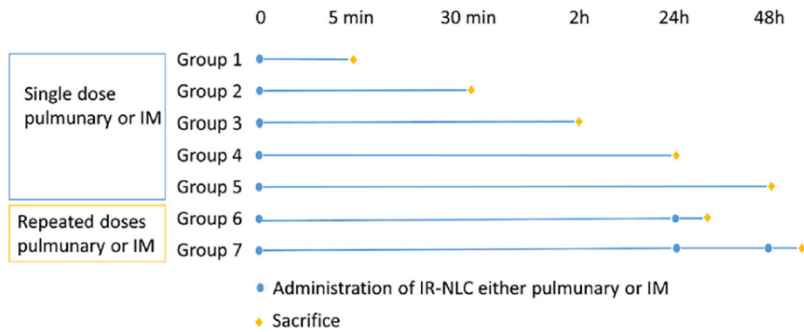


Figure 1. Schematic representation of the experimental groups in the biodistribution test.

### 2.2.8. Statistical analysis

Statistical Package for Social Sciences (SPSS) version 16.0 was used for statistical analysis. Concretely, Mann-Whitney U test were performed, and differences were considered statistically significant at  $P < 0.05$ .

## 3. Results

### 3.1. *In vitro* characterization

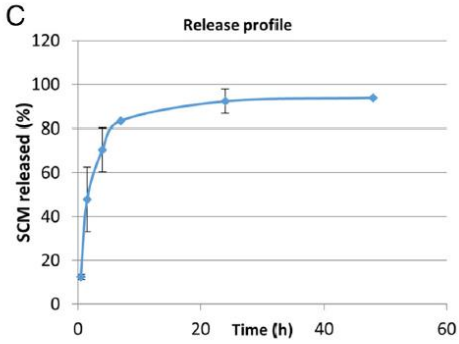
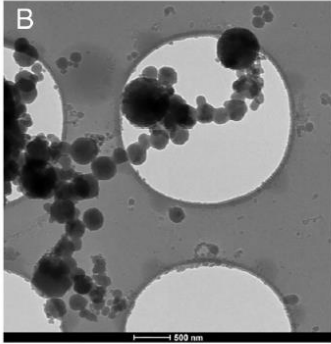
Figure 2 summarizes the main characteristics of SCM-NLC. Nanoparticles displayed a particle size around ~350 nm with 0.29 polydispersity index (PDI), negative zeta potential and high encapsulation efficiency of ~95 %, giving 70 µg of SCM per formulation mg (Figure 2, A). In addition, cryo-TEM images revealed that the NLC consisted of spherical particles and the size observed in TEM was in accordance with the results obtained by dynamic light scattering technique (Figure 2, B). FTIR spectroscopy was used to determine any possible interaction between SCM and lipid carrier components (*i.e.* blank-NLC) at the level of functional groups. The FTIR spectrum of SCM exhibited a number of characteristic protein transmission bands ( $\text{cm}^{-1}$ ) representing C=O (1645, amide I) and CN stretching (1525, amide II). Blank-

NLC showed typical peaks of lipid components such as O–H stretching (3382), aliphatic C–H (2914, CH<sub>3</sub> and CH<sub>2</sub>) asymmetrical stretching, aliphatic C–H (2849, CH<sub>3</sub> and CH<sub>2</sub>) symmetrical stretching, C=O (1735, carboxylic group) stretching, in addition to the vibrations associated with C–O and C–C (from 1150 to 800) bonds. SCM-NLC spectrum showed to be the combination of SCM and blank-NLC spectra since all peaks, described above, appeared. On the one hand, transmission value corresponding to SCM was slightly reduced, which indicated that SCM was successfully incorporated inside the lipid carrier. On the other hand, all the characteristic peaks of the blank-NLC were observed in the SCM-NLC spectrum and no predominate shifting of existing peaks or creation of new peaks occurred, suggesting that no chemical interaction took place among SCM and lipid components. Spectra of the three formulations can be found in Figure S1 (Supplementary Material). As to the release profile, it could be observed that SCM was released in a sustained manner, releasing 92 % of the content over 24 h (Figure 2, C). Using the CLSI interpretative standards, microbiological tests revealed that MIC values of SCM-NLC and free SCM were between 0.125 and 2 mg/L for all *P. aeruginosa* MDR/XDR/modR strains (Figure 2, D).

*Nanostructured lipid carriers (NLCs) for multiresistant infections*

A

Formulation	Size (nm)	PDI	Zeta Potential	EE (%)	Drug loading
SCM-NLC	354.1±2.85	0.291±0.014	-20.35±0.05	94.94 ± 0.04	70 µg/mg of NLC



D

ID <sup>a</sup>	ST <sup>b</sup>	Profile	β-lactam resistant mechanism	MIC (mg/L)	
				SCM-NLC	Free SCM
Pa1016	175	XDR	Hiperproduction AmpC, OprD, inactivation (Q142X)	2	1
Pa46	111	XDR	VIM-2	2	0.5
Pa54	111	XDR	VIM-2	2	0.5
Pa116	175	MDR	*	1	0.25
Pa166	111	MDR	*	2	0.25
Pa167	175	MDR	VIM-2	1	0.25
Pa179	175	MDR	*	2	0.25
Pa17	162	modR	OprD	2	0.125

Figure 2. (A) Main properties of the SCM-NLC, where PDI means polydispersity index and EE represents encapsulation efficiency. (B) CryoTEM images. (C) The SCM-NLC release profile. (D) Sequence type, profile, resistance mechanism and MIC values of SCM-NLC and free SCM against 8 *P. aeruginosa* strains. <sup>a</sup>ID, strain identification number; <sup>b</sup>ST, sequence type; \*PCR of genes encoding blaKPC, blaOXA, blaNDM, blaOXA-48, blaVIM, blaIMP was negative for these strains.

### 3.2. *In vivo* efficacy study

Table 3 summarizes the results of CFU per gram of lung obtained in this study. It should be pointed out that the groups nebulized with free SCM 15 mg/kg and SCM-NLC 2.8 mg/kg, either q12h or q24h, presented significantly ( $P < 0.05$ ) lower bacterial density in the lungs than the NaCl control group. SCM-NLC 2.8 mg/kg q24h achieved the highest reduction of more than 1 log<sub>10</sub> CFU/g lung ( $P < 0.05$ ). Regarding the IM route, free SCM 80 mg/kg and SCM-NLC 2.8 mg/kg q24h showed a significantly ( $P < 0.05$ ) lower bacterial count in the lungs than the control group (Table 3). In other words, by the pulmonary route, 70 or 140 µg of SCM encapsulated in the nanoparticles achieved the same results as 648 µg of free SCM. Moreover, 140 µg of SCM encapsulated in NLC by the IM route presented a similar bacterial count to 3,400 µg of free SCM.

Table 3. Lung bacterial density after the treatment with free SCM and SCM-NLC of an experimental acute pneumonia animal model caused by *Pseudomonas aeruginosa* 1016R.

Route	Treatment	Pa 1016R (XDR)	
		Total dose (µg)	log <sub>10</sub> cfu/g lung median (IQ <sub>25-75</sub> )
Pulmonary	Control NaCl q12h	0	6.66 (6.50-7.61)
	Free SCM 15mg/kg q12h	1944	5.70 (5.03-6.61)*
	SCM-NLC 2.8mg/kg q12h	420	6.21 (4.97-6.74)*
	SCM-NLC 2.8mg/kg q24h	210	5.64 (5.24-6.14)*
IM	Free SCM 80mg/kg q12h	10,200	6.03 (4.90-6.44)*
	SCM-NLC 2.8mg/kg q12h	420	6.37 (5.85-7.43)
	SCM-NLC 2.8mg/kg q24h	210	5.85 (4.97-6.45)*

\*  $P < 0.05$  comparing with Control group

### 3.3. *In vivo* toxicity studies

When toxicity was studied under the pulmonary route, animals from control groups (T1.1. to T1.3.) were fixed under hyperoxia conditions (section 2.2.4.). Those animals survived until the end of the study and their behavior and aspect were almost the same as a healthy laboratory Balb/c mouse. However, histological analysis revealed that lung inflammation had already started in all the studied groups, probably because of hyperoxia condition. As shown in Figure 3, the results for all groups were quite similar, and the dosing schedule (SCM-NLC q12h or q24h) did not affect the

histological output significantly. For SCM-NLC administered q24h, the score of all the samples was defined as 4, whereas SCM-NLC q12h presented a lower mean score (2.6) but sample score distribution ranged from 1 to 4 points, leading to no significant differences ( $P > 0.05$ ). When toxicity was studied under the IM route, in this case under environmental oxygen concentration (T2.1. to T2.6.), the animals grew healthily and, as shown in Figure 4, A, without significant differences ( $P > 0.05$ ) between animal weights prior to the treatment and at the end of the study.

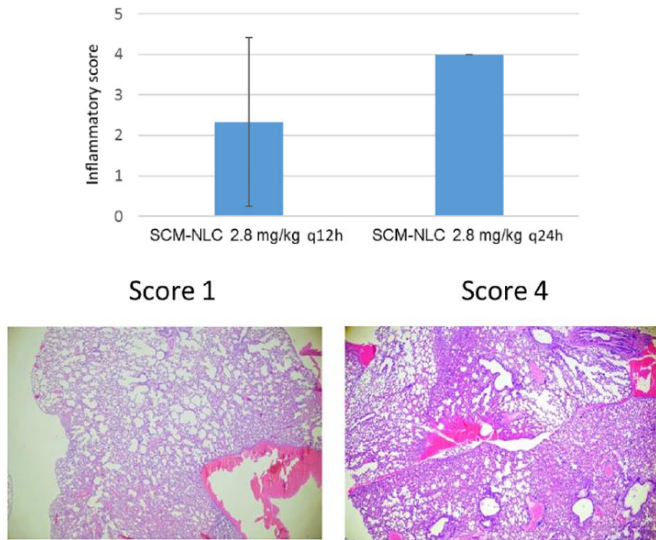


Figure 3. Above, lung inflammatory scores for SCM-NLC given q12h or q24h when maintained under hyperoxia. Below, histological slides of two samples scored as 1 and 4.

Also, free SCM 2.8 mg/kg (T2.4. and T2.5.) was administered by the IM route in order to ensure that low free SCM doses were innocuous. The histological analysis revealed no toxicity in tissues. The most remarkable events were splenic hematopoiesis (white arrows, Figure 4, B) and the effect called “dark neuron” in the brain (black arrows, Figure 4, B). However, both phenomena were detected in all groups (*i.e.* SCM-NLC, blank-NLC, free SCM and Control), suggesting that NLC were not responsible of that. Finally, no damage was found in the kidneys and brain in any case, reasserting the lack of toxicity of SCM-NLC.

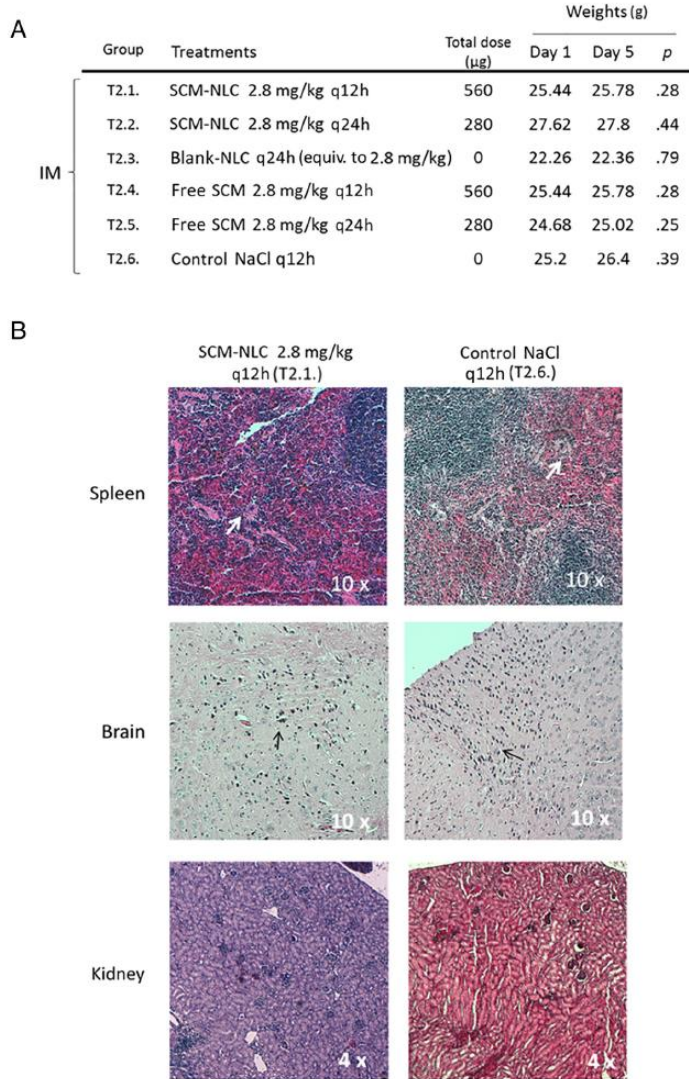


Figure 4. (A) Weight evolution during toxicity study. (B) Histological slides of the spleen, brain and kidney at the end of the study; the slides were H&E stained. White arrows pointing to the splenic hematopoiesis and black arrows indicating the dark neurons phenomenon (both events were also found in Control groups).

As Figure 5 shows, when the dose was increased in the IM route (groups T3.1. to T3.6.), no significant toxicity ( $P > 0.05$ ) effect was detected. Weights increased slightly as the study went on. In the lungs, alveolar walls were congested and extravasation of red blood cells was detected. The examination of the histological slides of the spleens revealed the presence of hematopoietic precursor cells related to an extramedullary hematopoietic process; however, this finding was observed in all the groups (including controls). All the liver samples displayed deposits of glycogen with granular degeneration changes that are especially clear in one mouse belonging to the T3.3. group (blank-NLC equivalent to 5.6 mg/kg of SCM-NLC). In this animal, the deposits were also observed macroscopically when removing the liver. On the contrary, the deposits detected in the T3.2, T3.4, and T3.5 groups were minimum.

#### 3.4. *In vivo* biodistribution study

After nebulization (Figure 6, A), IR-NLC were mainly biodistributed in the lungs and to a lesser extent in liver. After 48 h, the signal of the liver decreased sharply, whereas the signal in the lung was still high. In addition, lungs displayed broad, homogeneous signal, meaning that IR-NLC were able to spread all over the lungs. IR-NLC were also detected in the kidneys and spleen, although at significantly lower concentrations. When extra doses were administered at 24 and 48 h, it could be observed that the signal in the lung had increased. Likewise, the signal from the liver, kidneys and gallbladder was also incremented but to a lesser extent.

When IR-NLC were administered by the IM route, firstly the main signal was located at the injection site. However, within the 0.5-2 h period, the signal was transferred to other organs, such as the liver and gallbladder. After 24 h, the signal spread to other organs such as the lungs, kidneys and heart. When no additional doses were administered, this signal was detectable for 48 h, while when repeated doses were administered the signal stayed the same and increased over the study. Spleen displayed very low intensity.

A	Group	Treatments	Total dose ( $\mu\text{g}$ )	Weights (g)		
				Day 1	Day 5	p.
IM	T3.1.	SCM-NLC 5.6 mg/kg q24h	560	19.76	20	.235
	T3.2.	SCM-NLC 11.2 mg/kg q24h	1,120	20.9	21.3	.183
	T3.3.	Blank-NLC q24h (equiv. to 5.6 mg/kg)	0	21.28	21.8	.011
	T3.4.	Blank-NLC q24h (equiv. to 11.2 mg/kg)	0	21.52	21.62	.866
	T3.5.	Free SCM 8 mg/kg q24h	800	21	21.24	.509
	T3.6.	Control NaCl q12h	0	20.48	20.74	.065

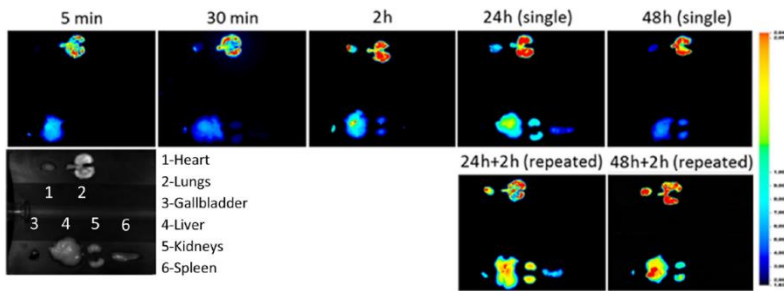
  

B	Treatments	Lungs	Spleen	Liver	Kidneys
		T3.1. SCM-NLC 5.6 mg/kg q24h			
T3.2. SCM-NLC 11.2 mg/kg q24h					
T3.3. Blank-NLC q24h (equiv. to 5.6 mg/kg)					
T3.4. Blank-NLC q24h (equiv. to 11.2 mg/kg)					
T3.5. Free SCM 8 mg/kg q24h					
T3.6. Control NaCl q12h					

Figure 5. Results of the toxicological study of the higher doses of SCM-NLC, free SCM and saline control administered by IM route. (A) Weight evolution during the study. (B) Histological slides of the lungs, spleen, liver and kidney at the end of the study; the slides were H&E stained.

*Nanostructured lipid carriers (NLCs) for multiresistant infections*

**A** IR-NLC, Pulmonary



**B** IR-NLC, IM

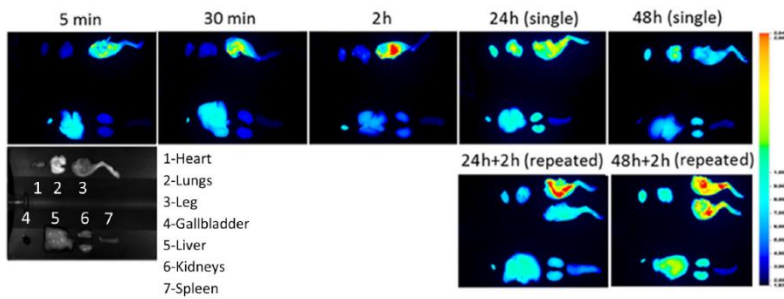


Figure 6. Biodistribution study. (A) IR-NLC distribution after nebulization by Microsprayer<sup>®</sup> aerosolizer. (B) IR-NLC biodistribution after IM administration.

#### 4. Discussion

Our research group has already demonstrated the capability of SCM-NLC as a promising drug delivery system suitable for the treatment of *Pseudomonas aeruginosa* (IJP1) [7]. However, the effectiveness of the SCM-NLC *in vivo* and its toxicological profile remained unknown. Thus, this work was designed and carried out in order to shed light in these two issues: on the one hand, *in vivo* efficacy of SCM-NLC was tested against an extensively drug-resistant (XDR)-Pa strain in an acute pneumonia model in mice; on the other hand, safety aspects of SCM-NLC were investigated through *in vivo* toxicity and biodistribution studies. The size, encapsulation efficiency and zeta potential of the SCM-NLC were appropriate to dosage SCM efficiently and administrate the SCM-NLC using both administration routes; pulmonary and intramuscular route. Also, as FTIR assay showed, SCM was successfully incorporated inside nanoparticles and it appeared to be compatible with lipid carriers since no chemical interaction was found among them. This finding suggested that NLC could be suitable carriers for improving SCM efficiency since they might be capable of increasing SCM stability, preserving its structure and avoiding its rapid degradation. MIC values of SCM-NLC were similar to the free SCM value used as reference data obtained in a previous study by Aoki and colleagues [14]. These data demonstrate that nanoencapsulation did not affect the antimicrobial activity of SCM.

The first issue aimed to address in this study was to test whether the SCM-NLC were able to exert antibiotic effect under acute pneumonia animal model. The effect showed by SCM-NLC during the efficacy study was similar to that of the free SCM group, either at pulmonary or at IM route. In this sense, it is important to highlight that the drug dose of SCM-NLC groups was significantly lower than the groups receiving free drug; *i.e.* maximum daily dose for SCM-NLC was 2.8-5.6 mg/kg, whereas free SCM 15-30 mg/kg was administered by daily nebulization or free SCM 80-160 mg/kg by daily intramuscular administrations. These striking results demonstrate the SCM-NLC *in vivo* are more active than the free SCM because the same effect was observed using at least five times lower dose in SCM-NLC than free SCM. All these data demonstrate that the encapsulation process enhances the pharmacological effect of SCM. These results are in line with Wang *et al.* who reported that florfenicol encapsulated into lipid nanoparticle was more effective than free florfenicol [16]. In

addition, it is important to highlight that it has been widely reported that NLC are capable of improving the stability of different type of drugs, preserving their structure and avoiding its rapid degradation; also it has been proven that their composition allows the control of drug release, thereby drug concentration remains appropriate over time [17].

In a next attempt, the toxicity of SCM-NLC was studied after pulmonary or IM administration. First, the toxicity of SCM-NLC under hyperoxia conditions was tested and although inflammatory state was established, this phenomenon was related to the increased presence of oxygen and not to SCM-NLC, since control groups also showed this phenomenon and it has already been proven that prolonged exposure to hyperoxia leads to lung inflammation and acute lung injury [17].

Under atmospheric pressure, IM administration of SCM-NLC, blank-NLC or low doses of free SCM (T2.1. to T2.6.) led to absence of histological damage. Therefore, the non-toxic effect of SCM-NLC might be related to the low dosage of the drug. Splenic hematopoiesis was found in all groups so it seems not to be directly related to drug administration (*i.e.*, free SCM and SCM-NLC). Also, the dark neuron phenomenon was detected for all groups and it has been previously reported to be associated with the biochemical processes related to the peri-mortem period, which induced tissue depolarization followed by peri- and intraneuronal attachment breakage during fixation, rather than to the treatments [18].

When the higher doses were assessed (T3.1. to T3.6), almost no toxicologically important events that could be attributed to the treatments were detected. In lungs, just alveolar walls were congested and extravasation of red blood cells was detected while in spleens an extramedullary hematopoietic process was showed. This finding was observed in all the groups (including controls), suggesting it might be recognized as physiological events related to the *in vivo* manipulation of mice. Only one mouse of the T2.3. group (blank-NLC 5.6 mg/kg) presented granular deposits in liver. Deposits detected in the T3.2, T3.4 and T3.5 groups were minimum and they could be considered secondary physiologic glycogen accumulation.

Thus, overall, it might be stated that the toxicity effect of SCM-NLC at different doses and the toxicity of NLC itself were negligible. Accordingly, the research work

published by Jamshidzadeh and colleagues reported that nanoencapsulated gentamycin displayed no nephrotoxicity at 100 mg/kg dose, whereas the free form of gentamycin presented severe degeneration of kidney proximal tubule cells, an increase in serum creatinine and blood urea nitrogen increase. Thus, in that study, nanoencapsulation resulted in a satisfactory approach for toxicity decrease [19].

In the next study, the fate of the NLC was explored in a biodistribution study using NLC labeled with IR. Nebulization gave rise to a predominant lung disposition of NLC but also IR signal was slightly detected in other organs, suggesting a mild systemic absorption. In our previous work, where 1.6 mg of IR-NLC was administered by means of an inhalation tower, no systemic absorption was detected [7]. This change could be explained by the dose difference in the lungs of the mice, since when the inhalation tower was used a substantial part of the dose ended up in the gastrointestinal track lowering the dose that reached the lungs. In addition, the microsyringe used in this study allowed the whole dose to reach the lung (IJP1). As lungs display high vascularization, it is clear that part of the dose reaches systemic circulation. However, it is noteworthy to mention that, for pulmonary route, the signal detected in the kidneys was low. This fact could play a major role also decreasing nephrotoxicity. Contrary, the biodistribution images obtained after IM administration revealed that NLC remain mainly in the injection site, but also, in other organs such as, liver, gallbladder, lungs, kidneys and heart; suggesting a notorious systemic absorption of the NLC after IM route. Taking into account the results mentioned above, it could be speculated that pulmonary route might be selected in case of maintenance therapy for its main effect in lungs and its low nephrotoxicity, whereas, IM route may be more useful in an emergency situation as it showed a faster absorption.

## 5. Conclusion

In conclusion, the nanoparticles described in this work represent a promising approach for fighting against MDR/XDR *Pseudomonas aeruginosa* infections. Firstly, these nanoparticles displayed suitable size, zeta potential, MIC and sustained drug release. Moreover, it was confirmed that SCM-NLC were active against XDR *Pseudomonas aeruginosa* in an acute pneumonia model in mice and in addition presented no toxic effect. Finally, it is particularly noteworthy to mention that both administration routes

can be exploited, depending on specific needs: (i) in case of maintenance therapy, pulmonary route is recommended; (ii) for an emergency circumstance, IM route is advisable. Further studies are required for the preclinical development of the lipid nanoparticle, but this work provides an early proof of the effectiveness and non-toxicity of SCM-NLC, under pulmonary and IM administration routes.

## **6. Acknowledgements**

The production and characterization of nanoparticles have been performed at the ICTS “NANBIOSIS”, more specifically by the Drug Formulation Unit (U10) of the CIBER in Bioengineering, Biomaterials & Nanomedicine (CIBER-BBN) at the University of the Basque Country (UPV/EHU). This work was supported by the TERFIQEC Project, IPT-2011-1402-900000 (funded by the Ministry of Economy and Competitiveness MINECO, Spain). The authors gratefully acknowledge the support of the University of the Basque Country UPV/EHU (UFI11/32), HUA, VHIR, UIB and CSIC-FISIB Caubet-Cimera. M. Moreno-Sastre thanks UPV/EHU for the ZabaldUz fellowship grant. J. Basas thanks ESCMID for the research grant- Protneb-Par PI13/02551. Technical and human support provided by Mariano Barrado and SGIker (UPV/EHU) is gratefully acknowledged. The help of Dr. Fernández-Vega for brain histological analysis is also deeply appreciated.

## 7. Supplementary data

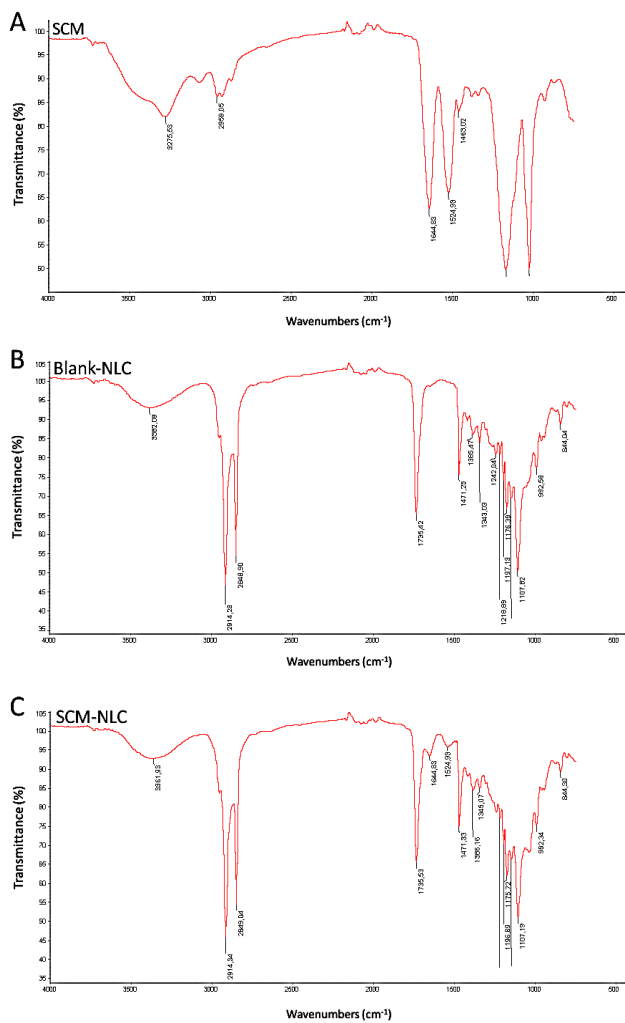


Figure S1. FTIR spectra of SCM (A), blank-NLC (B) and SCM-NLC (C)

## **8. References**

- [1] World Health Organization. Antimicrobial resistance. Available at: <http://www.who.int/en/news-room/fact-sheets/detail/antimicrobialresistance> 2018.
- [2] Centers for Disease Control and Prevention. Antibiotic resistance threats in the United States, 2013. Available at: <https://www.cdc.gov/drugresistance/threat-report-2013/> 2018.
- [3] Olaitan AO, Morand S, Rolain J. Emergence of colistin-resistant bacteria in humans without colistin usage: a new worry and cause for vigilance. *Int J Antimicrob Agents* 2016;47:1-3.
- [4] Wolinsky E, Hines JD. Neurotoxic and nephrotoxic effects of colistin in patients with renal disease. *N Engl J Med* 1962;266:759-62.
- [5] Gainza G, Pastor M, Aguirre JJ, Villullas S, Pedraz JL, Hernandez RM, et al. A novel strategy for the treatment of chronic wounds based on the topical administration of rhEGF-loaded lipid nanoparticles: in vitro bioactivity and in vivo effectiveness in healing-impaired db/db mice. *J Control Release* 2014;185:51-61.
- [6] Gartzandia O, Herran E, Pedraz JL, Carro E, Igartua M, Hernandez RM. Chitosan coated nanostructured lipid carriers for brain delivery of proteins by intranasal administration. *Colloids Surf B: Biointerfaces* 2015;134:304-13.
- [7] Pastor M, Moreno-Sastre M, Esquisabel A, Sans E, Viñas M, Bachiller D, et al. Sodium colistimethate loaded lipid nanocarriers for the treatment of *Pseudomonas aeruginosa* infections associated with cystic fibrosis. *Int J Pharm* 2014;477:485-94.
- [8] Moreno-Sastre M, Pastor M, Esquisabel A, Sans E, Viñas M, Fleischer A, et al. Pulmonary delivery of tobramycin-loaded nanostructured lipid carriers for *Pseudomonas aeruginosa* infections associated with cystic fibrosis. *Int J Pharm* 2016;498:263-73.
- [9] Das S, Ng WK, Tan RBH. Are nanostructured lipid carriers (NLCs) better than solid lipid nanoparticles (SLNs): development, characterizations and comparative

evaluations of clotrimazole-loaded SLNs and NLCs? *Eur J Pharm Sci* 2012;47:139-51.

[10] McKenzie BE, Holder SJ, Sommerdijk NAJM. Assessing internal structure of polymer assemblies from 2D to 3D CryoTEM: Bicontinuous micelles. *Curr Opin Colloid Interface Sci* 2012;17:343-9.

[11] Cabot G, Ocampo-Sosa A, Domínguez MA, Gago JF, Juan C, Tubau F, et al. Genetic markers of widespread extensively drug-resistant *Pseudomonas aeruginosa* high-risk clones. *Antimicrob Agents Chemother* 2012;56:6349-57.

[12] Viedma E, Juan C, Villa J, Barrado L, Orellana MÁ, Sanz F, et al. VIM- 2-producing multidrug-resistant *Pseudomonas aeruginosa* ST175 clone, Spain. *Emerg Infect Dis* 2012;18:1235-41.

[13] Wayne P. Methods for dilution antimicrobial susceptibility tests for bacteria that grow aerobically; approved standard—ninth edition. Available at: <https://www.researchgate.net/file.PostFileLoader.html>

[14] Aoki N, Tateda K, Kikuchi Y, Kimura S, Miyazaki C, Ishii Y, et al.

Efficacy of colistin combination therapy in a mouse model of pneumonia caused by multidrug-resistant *Pseudomonas aeruginosa*. *J Antimicrob Chemother* 2009;63:534-42.

[15] Bae H, Kim R, Kim Y, Lee E, Jang Y, Jung S, et al. Effects of *Schisandra chinensis* Baillon (Schizandraceae) on lipopolysaccharide induced lung inflammation in mice. *J Ethnopharmacol* 2012;142(1):41-7.

[16] Wang T, Chen X, Lu M, Li X, Zhou W. Preparation, characterisation and antibacterial activity of a florfenicol-loaded solid lipid nanoparticle suspension. *IET Nanobiotechnol* 2015;9(6):355-61.

[17] Lv R, Zheng J, Ye Z, Sun XJ, Tao Y, Liu K, et al. Advances in the therapy of hyperoxia-induced lung injury: Findings from animal models, 41(3); 2014:183-202.

[18] Wohlsein P, Deschl U, Baumgärtner W. Nonlesions, unusual cell types, and postmortem artifacts in the central nervous system of domestic animals. *Vet Pathol* 2013;50:122-43.

[19] Jamshidzadeh A, Heidari R, Mohammadi Samani S, Azarpira N, Najibi A, Jahani P, et al. A comparison between the nephrotoxic profile of gentamicin and gentamicin nanoparticles in mice. *J Biochem Mol Toxicol* 2015;29(2):57-62.





## CHAPTER 3

### **Preclinical safety of topically administered nanostructured lipid carriers (NLC) for wound healing application: biodistribution and toxicity studies**

Claudia Vairo<sup>a,b</sup>, María Collantes<sup>c</sup>, Gemma Quincoces<sup>c</sup>, Silvia Villullas<sup>a</sup>, Iván Penuelas<sup>c,d</sup>, Marta Pastor<sup>a</sup>, Ana Gloria Gil<sup>e,f</sup>, Eusebio Gainza<sup>a</sup>, Rosa María Hernandez<sup>b,g</sup>, Manoli Igartua<sup>b,g</sup>, Garazi Gainza<sup>a,\*</sup>

<sup>a</sup>BioKeralt Research Institute AIE, Albert Einstein, 25-E3, 01510 Miñano, Araba, Spain;

<sup>b</sup>NanoBioCel Group, Laboratory of Pharmaceutics, University of the Basque Country (UPV/EHU), School of Pharmacy, Paseo de la Universidad 7, 01006 Vitoria-Gasteiz, Spain;

<sup>c</sup>Nuclear Medicine Department, Clínica Universidad de Navarra, Pamplona, Spain; <sup>d</sup>Small Animal Imaging Research Unit, Center for Applied Medical Research (CIMA) and Clínica Universidad de Navarra, Pamplona, Spain;

<sup>e</sup>Department of Pharmacology and Toxicology, University of Navarra, 31008 Pamplona, Spain;

<sup>f</sup>Toxicology Unit, Drug Development Unit University of Navarra (DDUNAV), 31008 Pamplona, Spain;

<sup>g</sup>Biomedical Research Networking Center in Bioengineering, Biomaterials and Nanomedicine (CIBER-BBN), Vitoria-Gasteiz, Spain

\*Corresponding author: Garazi Gainza

---

### **ABSTRACT**

Re-activation of the healing process is a major challenge in the field of chronic wound treatment. For that purpose, lipid-nanoparticles, especially nanostructured lipid carriers (NLC), possess extremely useful characteristics such as biodegradability, biocompatibility and long-term stability, besides being suitable for drug delivery. Moreover, they maintain wound moisture due to their occlusive properties, which have been associated with increased healing rates. In the light of above, NLC have been extensively used topically for wound healing; but to date, there are no safety-preclinical studies concerning such type of application. Thus, in this work, biodistribution studies were performed in rats with the NLC previously developed by our research group, using technetium-99m (<sup>99m</sup>Tc-NLC) as radiomarker, topically administered on a wound. <sup>99m</sup>Tc-NLC remained on the wound for 24 h and systemic absorption was not observed after administration. In addition, toxicological studies were performed to assess NLC safety after topical administration. The results obtained demonstrated that NLC were non-cytotoxic, non-sensitizing and non-irritant/corrosive. Overall, it might be concluded that developed NLC remained at the

administration area, potentially exerting a local effect, and were safe after topical administration on wounds.

---

**Published in:** International Journal of Pharmaceutics  
569 (2019) 118484, doi: <https://doi.org/10.1016/j.ijpharm.2019.118484>

## 1. Introduction

In recent years, lipid-nanoparticles, *i.e.* solid lipid nanoparticles (SLN) and nanostructured lipid carriers (NLC), have attracted much attention as effective, biodegradable, biocompatible and non-toxic carriers, exhibiting many adequate features for dermal application of cosmetics and pharmaceuticals [1]. Consequently, SLN and NLC have been broadly considered as suitable and efficient systems for improving wound healing because of their occlusive properties that increase skin hydration and enhance drug penetration [2,3]. Therefore, the use of these lipid nanoparticles is an interesting strategy for chronic wound treatment as they promote an appropriate wound bed that could re-activate the healing process.

Wound healing is an indispensable and complex physiological process required to regenerate and repair any damaged area in the shortest time. This process starts with an inflammatory phase, followed by proliferative and remodeling ones [4]. Chronic wounds tend to stall in the inflammatory phase, hampering progression into the proliferative step and delaying or stopping the wound healing process; thus, affecting the patient quality of life [5]. In view of the foregoing, development of effective and safe therapeutic alternatives able to re-activate healing is a major breakthrough.

To date, NLC have shown greater stability and loading capacity compared to SLN due to their composition, as NLC are composed of a blend of solid and liquid lipids that leads to a less ordered inner structure compared to the crystalline matrix of SLN [1]. Moreover, several research groups have demonstrated the efficacy of NLC as drug delivery systems to improve wound healing. Previous studies published by our research group have shown that epidermal growth factor (EGF) loaded NLC enhanced wound healing both *in vitro* and *in vivo* [6-8] and LL37 (a human antimicrobial peptide) loaded NLC improved wound closure [9]. In addition, Motawea *et al.* (2017) found phenytoin loaded NLC a promising strategy for promoting wound healing [10] and Saporito *et al.* proved the capability of NLC loaded with eucalyptus or rosemary essential oils to improve healing *in vivo* [11].

So far, there is no information available regarding biodistribution and toxicity studies of topically administered nanoparticles, which will be very helpful to further evaluate their suitability in the treatment of non-healing wounds.

On the one hand, *in vivo* and *ex vivo* biodistribution studies are considered important evaluation tools during development of nanosized drug delivery systems, because they provide information about location, magnitude and kinetics of the drug biodistribution in an individual over time [12]. This type of studies can be performed labeling the nanoparticles with a radioisotope, which allows their detection by a scanner. Technetium-99m ( $^{99m}\text{Tc}$ ), obtained as pertechnetate ( $^{99m}\text{TcO}_4^-$ ), is widely used as radiomarker due to its easy availability, high  $\gamma$  emission (140 keV) and adequate half-life (approximately 6 h). These characteristics allow carrying out *in vivo* biodistribution studies for about 24 h by single photon emission tomography (SPECT). Moreover,  $^{99m}\text{Tc}$  allows direct radiolabeling with minimal or without changes in the structure and surface of the carrier [13,14].

On the other hand, it is known that nanoparticles, ranged between 2 and 1000 nm, are susceptible to be internalized by macrophages as foreign body, which might cause undesired side effects such as an overstimulation of the immune system. In addition, nanoparticles smaller than 100 nm can also be uptaken in a non-specific manner through endocytosis [15]. For these reasons, they could show a high toxicity potential that should be evaluated. Therefore, *in vitro* cytotoxicity assays as well as dermal parameters, such as *in vivo* skin sensitization and irritation/corrosion, were evaluated with the developed NLC, following ISO 10,993 standard (Biological evaluation of medical devices).

Summarizing, in the present work, biodistribution and toxicology studies were performed with the NLC developed by our research group in order to determine the safety profile of topically administered lipid nanoparticles on wounds.

## **2. Materials and methods**

### **2.1. Preparation of NLC**

NLC were prepared slightly modifying the procedure previously reported by Gainza *et al.* (2014). Briefly, Precirol<sup>®</sup> ATO 5 (Gattefosse, Madrid, Spain) and Miglyol 182 N/F (Sasol, Hamburg, Germany) were melted to achieve the oily phase (10:1). Simultaneously, the aqueous phase was prepared dissolving Tween<sup>®</sup> 80 (Panreac Quimica, Castellar del Valles, Barcelona, Spain) at 2 % (w/v) and Poloxamer 188

(Panreac Quimica, Castellar del Valles, Barcelona, Spain) at 1 % (w/v) followed by solution tempering. The two phases were mixed and sonicated (Branson Sonifier, Emerson, Saint Louis, MO, US) for 1 min at 50 W. Afterwards, the emulsion was cooled down and kept under  $5 \pm 3$  °C for 2 h to allow lipid solidification. Subsequently, trehalose was added as cryo-preserving agent prior to the freeze-drying step in a final concentration of 100 % (w/w) of the weighed lipid. The total weight of the batch was 12 g.

## 2.2. Characterization of NLC

The mean particle size (Z-average diameter), polydispersity index (PDI) and zeta potential were analyzed by means of Zetasizer Nano ZS (Model Zen 3600; Malvern Instruments Ltd, Worcestershire, UK); which is based on dynamic light scattering (DLS) technology. The measurement medium was water (pH 5.6). Samples were analyzed in triplicate to obtain an accurate mean.

Transmission electron microscopy (TEM, Philips EM208S) analysis was held under negative staining in order to study nanoparticle morphology. Images were acquired with an Olympus Fluoview FV500 confocal microscope using sequential acquisition to avoid overlapping of fluorescent emission spectra.

NLC capability of resuspension was also assessed. Only those suspensions without visible aggregates were considered acceptable. For this purpose, 2 mg of NLC were added to 1 mL of Milli-Q water and vortexed for 1 min (n=3).

## 2.3. Radiolabeling of NLC with $^{99m}\text{Tc}$

Radiolabeling of NLC was performed by a direct method using stannous chloride ( $\text{SnCl}_2$ ) as reducing agent and following the procedure previously developed by Areses *et al.* (2010). Briefly, 0.03 mL of a 5 mg/mL  $\text{SnCl}_2$  solution (pH=4 adjusted with 0.1 N HCl) was added to 5 mg of NLC. Subsequently, 14.8 GBq (MBq) of freshly eluted  $^{99m}\text{TcO}_4^-$  in 1 mL of NaCl 0.9 % were added. The mixture was vortexed for 30 s and incubated at room temperature for 10 min. The overall procedure was carried out in helium-purged vials to minimize oxygen content and avoid oxidation of pre-reduced tin. For biodistribution studies, 20 mg of NLC were added at the end of the

## *Nanostructured lipid carriers (NLCs) for multiresistant infections*

radiolabeling procedure to obtain a suitable NLC concentration for *in vivo* administration.

$^{99m}\text{Tc}$ -NLC labeling efficiency was assessed by ascending instant thin layer chromatography (ITLC) using Whatman 3 MM strips and NaCl 0.9 % as mobile phase. Radiochromatograms were obtained with a scanner MiniGita (Raytest GmbH, Dortmund, Germany) equipped with a  $2 \times 2$  NaI (Tl) detector. Percentage of free  $^{99m}\text{TcO}_4^-$  was calculated from the regions of interest (solvent front for the free  $^{99m}\text{TcO}_4^-$  and bottom of the strip for the  $^{99m}\text{Tc}$ -NLC) with Nina software (Raytest GmbH, Dortmund, Germany).

### 2.4. Biodistribution studies

#### 2.4.1. *Animals and experimental design*

For the biodistribution studies, all the procedures involving animals were performed in accordance with the guidelines of the European Communities Council Directive (2010/63/UE) and the Spanish Government (Real Decreto 53/2013) and were approved by the Ethics Committee for Animal Experimentation of the University of Navarra (protocol 035-16) and the Government of Navarra. The studies were carried out in sixteen female Wistar rats weighting  $212 \pm 9$  g. Firstly, buprenorphine (Buprex 0.05 mg/Kg) was administered subcutaneously 30 min prior to create the lesions on the back of the animals. Then, rats were anesthetized (isoflurane 2 % in 100 %  $\text{O}_2$ ) and their dorsum shaved using an electric clipper. One full-thickness excisional wound was made by punch biopsy using a dermatome of 10 mm in diameter. After wound creation,  $^{99m}\text{Tc}$ -NLC (5 mg/3 MBq per animal, n=8) or free  $^{99m}\text{Tc}$ , used as negative control (free  $^{99m}\text{Tc}$  5.5 MBq, n=8), were topically administered on the wound. Finally, wounds were covered with one layer of petrolatum gauze (Tegaderm®, 3M GmbH) secured with an auto adhesive tape (Hypafix, BSN medical). Half-life of technetium-99m and the initial administered dose (AD) were taken into account for data analysis.

#### 2.4.2. *In vivo biodistribution studies by SPECT/CT*

*In vivo* biodistribution studies were performed by single photon emission computed tomography/computed tomography (SPECT/CT) (Symbia T2 Truepoint, Siemens) at

1, 2, 4, 8, 10 and 24 h post-administration. For imaging studies, animals were anesthetized just before each study (isoflurane 2 % in 100 % O<sub>2</sub>) and placed in prone position. A high resolution low-energy parallel-hole collimator was used for this study and images acquired using a 128×128 matrix, 7 images/s. CT was set to 110 mAs, 130 kV and 130 images of 3 mm on thick. In order to quantitatively compare the images to each other avoiding the effect of physical disintegration of <sup>99m</sup>Tc, image acquisition time was increased over the temporal points. Images were reconstructed applying attenuation and dispersion corrections. Image fusion was performed using Syngo MI Applications TrueD software and all the images were then exported to PMOD v3.2 software (PMOD Technologies, Switzerland). After visual inspection of the images, a quantitative analysis was performed by drawing volumes of interest (VOIs) of the total body, wound area, stomach and intestine over anatomical CT images that were transferred to SPECT. Percentage of activity in the organs was calculated considering the activity measured in the VOI of the total body from the image acquired 1 h post-administration as the total administered dose.

#### 2.4.3. *Ex vivo* biodistribution studies: gamma counter

*Ex vivo* biodistribution studies were carried out at the end of the study (24 h). The following organs were then dissected in their entirety: ovaries, spleen, kidneys, small intestine, large intestine, stomach, lungs, thyroid, brain, eyes and gastrocnemius muscle. Samples of liver, skin (abdominal area), blood and urine were also taken. To analyze the wound area in more detail, skin adjacent to the wound, the fatty layer of the subcutaneous tissue (*panniculus adiposus*) and the muscle tissue (*panniculus carnosus*) were dissected separately. All tissue and organ samples together with the dressing were measured in a gamma-counter (Compugamma CS, RIA; LKB Pharmacia). Likewise, two separate equal doses administered to the animals were also counted, in order to consider the mean value as total activity to calculate the percentage of administered dose (% AD/organ). To calculate the activity in blood and in whole-liver, a total blood volume of 60 mL/kg and a standard liver weight of 13.31 g were considered.

## 2.5. Toxicity studies

### 2.5.1. *In vitro* cytotoxicity study

### *Nanostructured lipid carriers (NLCs) for multiresistant infections*

For the cytotoxicity study, mouse embryo fibroblasts (Balb/3T3) were maintained in DMEM Glutamax culture medium supplemented with 10 % Fetal Bovine Serum (FBS) and 1 % Penicillin-Streptomycin. Cells were incubated (at 37 °C, 5% CO<sub>2</sub> and humidity on saturation) in 75 cm<sup>3</sup> cell culture flasks until reaching sub-confluence. Seeding was carried out in a 96-well plate, dispensing 10<sup>4</sup> cells per well into 100 µL of complete culture medium.

On each treated well, 100 µL of NLC at 3, 1, 0.3 and 0.1 mg/mL were added. Sodium dodecyl sulfate (SDS) was used as positive control and 0.5 % FBS and complete culture medium were used as negative and growth control, respectively. One hour after treatment, 50 µL of 3-(4,5- dimethylthiazol-2-yl)-2,5-diphenyltetrazolium bromide (MTT) solution (1 mg/mL in culture medium) were added to each well and cells were further incubated for 2 h. MTT solution was then decanted and 100 µL of isopropanol added and shook for approximately 1 h. Cell viability was measured by reading the optical density of the suspension at 570 (± 30) nm on a microplate spectrophotometer (Spectra MRTM Dynex Technologies, Chantilly, VA. USA).

To guarantee the validity of the results, the experiment was carried out following the criteria of ISO 10993-5:1999: (i) confluence of the growth control wells must be ≥ 80 % and the absolute value of the mean of their optical densities must be ≥ 0.2 prior subtracting the blank; (ii) mean value of the absorbance of the growth control in the left and right column of the plates could not differ by more than 15 % from their mean value; and (iii) coefficient of variation between replicas of each condition must be ≤ 20 %. Lastly, viability of positive control and negative control must be ≤ 40 % and ≥ 80 %, respectively.

Once fulfilment of all the acceptance criteria was confirmed, cell viability [expressed in percent survival (%)] was calculated by means of the optical density (OD) and applying the following formula:

$$\text{Cell viability (\%)} = \frac{OD \text{ Mean (treatment)} - OD \text{ Mean (blank)}}{OD \text{ Mean (negative control)} - OD \text{ Mean (blank)}} \times 100$$

NLC were considered non-cytotoxic if cell viability was higher than 70 % compared to the negative control.

### 2.5.2. *In vivo* sensitization study

For the *in vivo* sensitization study, all the procedures involving animals were approved by the Ethics Committee for Animal Experimentation of the University of Navarra (protocol 142-15) and the Government of Navarra. This study was carried out using the Skin Sensitization Local Lymph Node Assay (LLNA:DA), which is a test that quantifies the adenosine triphosphate (ATP) content via bio-luminescence as an indicator of lymphocyte proliferation. Such proliferation can be given by the exposure to a sensitizer and the indicator used to classify the skin sensitization potency of a compound as extreme, strong, moderate or weak sensitizers is called Stimulation Index (SI). For this purpose, twenty-four female CBA/CaOlaHsd mice of approximately 8 weeks weighting 16-19 g were used (ENVIGO, Spain). Animals were housed in six groups of four with 12 h light/dark cycles, a relative humidity of  $50 \pm 20\%$  and an air temperature of  $22 \pm 2$  °C. Animals had free access to standard rodent maintenance diet and water, provided *ad libitum*.

In order to ensure reliability of the test, 2-Mercaptobenzothiazole (2-MBT) was used as positive control and a solution of carboxymethylcellulose (CMC) in saline as negative control. According to OECD criteria (2010): Skin Sensitization Local Lymph Node Assay: DA, Test Guideline no. 442A, the positive control response at an exposure level, must produce an increase in the SI superior or equal to 1.8 over the negative control.

On days 1, 2, 3 and 7, animals received a pre-treatment with aqueous solution of 1% Sodium Lauril Sulfate (SLS) using a swab. Then, the atrial back of each ear was covered completely. One hour later, treatments were administered on the back of each ear. The studied groups were the following: 25  $\mu$ L of NLC at 340 mg/mL, 170 mg/mL and 85 mg/mL; positive and negative control and DMSO (vehicle control of the positive control). On day 8, animals were sacrificed and, immediately after, the auricular ganglia excised. Both ganglia were processed as a single sample. Ganglia placed in 2 glass slides were crashed and disintegrated until formation of a thin layer of tissue. The lymph node cell suspension was then rinsed with 1 mL of phosphate buffered saline (PBS) using a cell scraper. 20  $\mu$ L of this suspension was mixed with 1.98 mL of PBS to obtain 1 mL of 1% lymph node cell suspension.

### *Nanostructured lipid carriers (NLCs) for multiresistant infections*

Quantification of the ATP content by the luciferin-luciferase method was carried out using the ATP measurement kit (Vialight® Plus Kit; Lonza Rockland, Inc., ME, USA) following manufacturer's instructions. This kit measures bioluminescence in Relative Luminescence Units (RLU). RLU calculation allows determining the SI, which was calculated using the following formula:

$$\text{Cell viability (\%)} = \frac{RLUmice}{RLU(\text{MeanNegativeControl})}$$

According to the OECD Guidelines, a result is considered positive when  $SI \geq 1.8$ . However, if a borderline positive response of SI between 1.8 and 2.5 occur, the study should be subjected to additional considerations.

#### *2.5.3. In vivo irritation/corrosion study*

The *in vivo* irritation/corrosion study was carried out in accordance with OECD (2002), Test No. 404: Acute Dermal Irritation/Corrosion and all the procedures involving animals were approved by the Ethics Committee for Animal Experimentation of the University of Navarra (protocol 092-16) and the Government of Navarra. Three male New Zealand rabbits weighting between 2.5 kg and 3 kg were obtained from Granja San Bernardo (Spain). Animals were housed in 12 h light/dark cycles, a relative humidity of  $30 \pm 70\%$  and an air temperature of 15-21 °C. Animals had free access to standard non-rodent maintenance diet and water, provided *ad libitum*.

The experiment was performed in two steps: an initial test followed by a confirmation test if required. The initial test was carried out in a single animal and its main objective was to detect possible corrosive effects of the developed NLC. If no corrosive effects were detected, the confirmation test would be executed. As that was the case, this second test was carried out in two further animals. Thus, three animals were used to evaluate the irritant potential of the developed NLC. On each animal, four areas covering a body surface of 2.5 cm<sup>2</sup> were marked. Two areas were treated with NLC in 0.5 % CMC saline solution in an exposure time of 4 h; and the other two received no treatment and served as normality control.

The Primary Irritation Index (PII) was calculated following the Draize test, which is based on the erythema/edema evaluation [16]. The evaluation was done at 24 ( $\pm 2$ ), 48 ( $\pm 2$ ) and 72 ( $\pm 2$ ) hours. PII was obtained for each animal, dividing the total score of the treated areas by 6 (2 test-observation sites and 3 observation times) and correcting the result with the score obtained from the control areas. The category of the irritation/corrosion was estimated following the ISO 10993-10: 2010 criteria (Table 1).

Table 1. Description of the PII scores based on ISO 10993-10:2010.

Score	Category response
0-0.4	Negligible
0.5-1.9	Mild
2-4.9	Moderate
5-8	Severe

## 2.6. Statistical analysis and evaluation of the results

Results from characterization and *in vivo* and *ex vivo* biodistribution studies are expressed as mean  $\pm$  standard deviation (SD). The analysis of differences between the experimental groups of *in vivo* biodistribution studies was performed by two-way ANOVA (group per time) followed by Fisher's Least Significant Difference (LSD) *post-hoc* tests when an interaction was found. *Ex vivo* data were analyzed by *t*-test. Calculations were performed using StataIC 12 software (StataCorp, Texas, USA). A p-value lower than 0.05 was considered statistically significant.

## 3. Results and discussion

Our research group have already demonstrated the effectiveness of drug loaded-NLC for wound healing applications [6-9]; however, so far, preclinical safety data of blank-NLC, such as *in vitro* biodistribution and cytotoxicity studies, are lacking. Certainly, taken into account that all the components of nanoparticles are certified as GRAS (Generally Recognize As Safe) by the FDA [17], NCL final formulation should be considered as well tolerated when applied on a wound. Nonetheless, nanotoxicity is a relatively new concept to science as nanoparticles with certain size, shape and chemistry could reach many tissues and organs causing abnormal function or cell

death [18]. For this reason, in order to shed light on NLC safety, the main objectives of this research were (i) to achieve a suitable radiolabeling for the detection of NLC through a living organism, (ii) to clarify the biodistribution of NLC after their administration on an open wound and (iii) to analyze any bio-incompatibility in terms of toxicity, both *in vitro* and *in vivo*.

In view of this, nanoparticles developed by our laboratory, with  $133.48 \pm 4.40$  nm in size (Fig. 1A), were designed to exert a local effect on a wound as it is well known that particles above 20 nm do not penetrate into damaged skin [19]; therefore, no penetration of the formulation was expected. PDI and zeta potential values also confirmed the homogeneity and stability of the NLC suspension, respectively; fundamental parameters when a uniform NLC distribution on the wound is desired. A PDI of  $0.22 \pm 0.05$  indicated lack of aggregates and an excellent dispersion and the zeta potential values revealed that NLC presented a negatively charged surface of approximately  $17.43 \pm 3.15$  mV, conferring good stability in liquid phase. TEM images showed nanoparticles with a uniform size distribution and spherical shape (Fig. 1B), along with excellent resuspension properties, as all samples were easily resuspended (Fig. 1C).

Once physicochemical NLC properties were confirmed to be suitable for topical application on wounds, an optimization of the radiolabeling method for nanoparticles was carried out.  $^{99m}\text{Tc}$  has been previously used as radiotracer to study NLC biodistribution in living organisms since its incorporation into NLC does not affect neither the morphology nor the size of nanoparticles [20, 21]. Thus,  $^{99m}\text{Tc}$  was the radiomarker of choice. Our results showed that the direct radiolabeling led to a high yield process (> 98%), avoiding further purification methods. Regarding the amount of  $\text{SnCl}_2$  required to obtain a high labeling efficiency, we found that 5, 10 and 20 mg/mL achieved adequate radiolabeling; but in order to use the lowest amount of  $\text{SnCl}_2$  showing the greatest efficiency, the selected  $\text{SnCl}_2$  concentration was 5 mg/mL (Table 2).

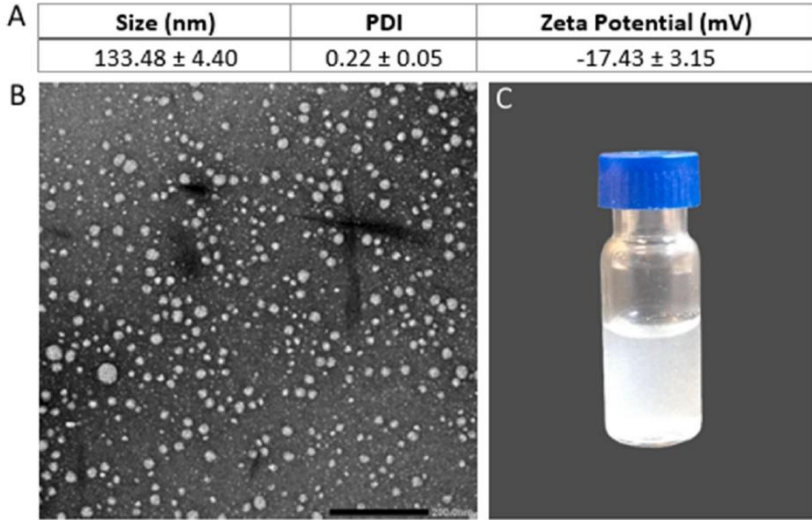


Figure 1. Characterization of NLC. (A) Mean Size, PDI and Zeta Potential. Data are shown as mean ± SD. (B) TEM image of NLC (scale bar 200 nm). (C) NLC suspension in 1 mL of Mili-Q water after 1 min of mixing by vortex.

Table 2. Influence of the amount of SnCl<sub>2</sub> on the radiolabeling efficiency of NLC. Data are shown as mean ± SD (n=3).

SnCl <sub>2</sub> mg/ml	% efficiency
0.005	41.3 ± 4.7
0.05	60.6 ± 5.5
0.5	83.2 ± 2.3
5	98.4 ± 0.7
10	99.6 ± 0.6
20	98.4 ± 1.2

Consequently, after obtaining <sup>99m</sup>Tc-NLC, *in vivo* biodistribution studies by SPECT/CT could be performed. As shown in Fig. 2, the qualitative analysis of the images demonstrated that the signal at the wound area in those animals treated with <sup>99m</sup>Tc-NLC was stable over time, indicating that NLC remained at the wound area and were not absorbed for at least 24 h (Fig. 2A, B and S1). In control animals, free <sup>99m</sup>Tc was quickly absorbed, producing a signal in the stomach in the earliest images (Fig. 2A) that decreased over time, accompanied by a slight increase in the signal shown in the large intestine (Fig. 2B). This signal shown at the level of the gastrointestinal

### *Nanostructured lipid carriers (NLCs) for multiresistant infections*

system is compatible with the natural metabolism of  $^{99m}\text{Tc}$  [22]. Also, Fig. 3 shows the quantitative analysis of SPECT/CT images that was consistent with the visual results. Almost 100 % of the signal remained at the wound site for 24 h after administration of  $^{99m}\text{Tc}$ -NLC. In control animals, free  $^{99m}\text{Tc}$  was absorbed, as only 7.3% was retained at the wound area after 24 h. Since free  $^{99m}\text{Tc}$  is accumulated and actively secreted in the gastric mucosa, signal from the control animals was concentrated in the stomach (51.8 % at 1 h to 38.3 % at 24 h) and gradually detected in the intestine area (12.3 % at 1 h to 46.6 % at 24 h) as the digestion process went on. Differences between groups were statistically significant ( $p < 0.001$ ) for all regions and all times. As mentioned, this data verified that the developed NLC remained at the wound site for at least 24 h, confirming their potential local effect and the absence of systemic absorption. Besides, data obtained *in vivo* were confirmed by *ex vivo* biodistribution studies. The high sensitivity of the gamma counters allows detection of compounds at a tissue level in those organs where the distribution is very low and which signal is not high enough to be detected by *in vivo* imaging techniques. As observed in Table 3, in  $^{99m}\text{Tc}$ -NLC treated animals, the wound dressing retained 41.1 % of the AD, 57.4 % was found in the skin, 1.1 % in subcutaneous tissue and 0.0 % in the *panniculus carnosus*. These data confirmed that the developed NLC were not absorbed after topical administration on wounds, potentially exerting a local effect; which are in line with the results obtained in the *in vivo* biodistribution study. In contrast, free  $^{99m}\text{Tc}$  control showed AD values significantly lower than the  $^{99m}\text{Tc}$ -NLC treated groups at the wound area. After free  $^{99m}\text{Tc}$  administration, most of the activity was found in the stomach (20.5 %) and intestines (small intestine: 11.2 %; large intestine: 21.8 %; caecum: 20 %), showing that free  $^{99m}\text{Tc}$  was absorbed after administration on the wound. The other organs collected showed negligible and undetectable signals. It should be noted that this represents an extremely original finding, which cannot be compared with other studies, as no biodistribution studies are available.

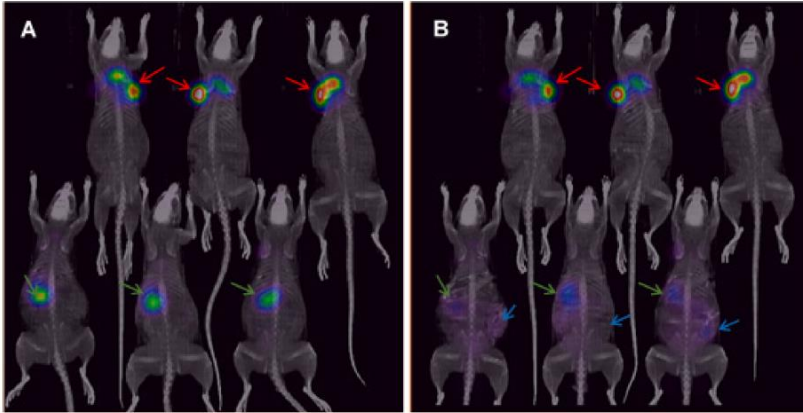


Figure 2. 3D images of the SPECT/CT studies at 1 h (A) and 24 h (B). The three rats in the upper part of the image were treated with  $^{99m}\text{Tc}$ -NLC on the wound area (red arrow), producing a stable signal over time. The three rats at the bottom of the image were control animals receiving free  $^{99m}\text{Tc}$  on the wound. The green arrows indicate the stomach area, more evident at early times, and the blue arrows point to the large intestine.

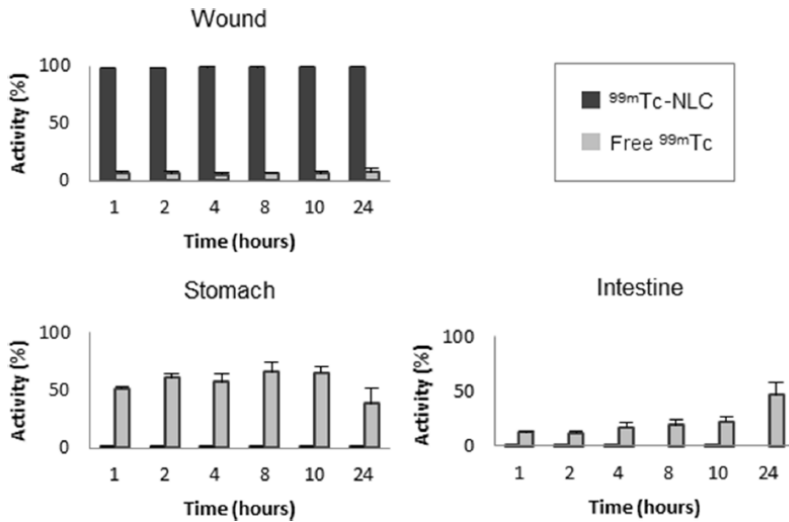


Figure 3. Graphs showing the average activity for NLC treated and control experimental groups detected in *in vivo* SPECT/CT images over time.

### Nanostructured lipid carriers (NLCs) for multiresistant infections

Table 3. *Ex vivo* biodistribution data at 24 h post-administration (% AD). Data are expressed as mean  $\pm$  SD. Values were calculated for whole organ (except for urine and skin samples). The different elements of the wound area were analyzed separately. \* $p < 0,001$ , statistical significance referred to free  $^{99m}\text{Tc}$  control group.

	$^{99m}\text{Tc}$ -NLC	Free $^{99m}\text{Tc}$
<i>TOTAL ORGANS</i>		
Total blood	0.0 $\pm$ 0.0	1.1 $\pm$ 0.6
Skin	0.0 $\pm$ 0.0	0.0 $\pm$ 0.0
Muscle (gastrocnemius)	0.0 $\pm$ 0.0	0.0 $\pm$ 0.0
Urine	0.0 $\pm$ 0.0*	1.5 $\pm$ 0.3
Ovaries	0.0 $\pm$ 0.0	0.0 $\pm$ 0.0
Spleen	0.0 $\pm$ 0.0	0.0 $\pm$ 0.0
Kidneys	0.3 $\pm$ 0.1*	4.4 $\pm$ 1.8
Stomach	0.1 $\pm$ 0.2*	20.5 $\pm$ 13.0
Small intestine	0.0 $\pm$ 0.0*	11.2 $\pm$ 3.3
Large intestine	0.0 $\pm$ 0.0*	21.8 $\pm$ 4.3
Caecum	0.0 $\pm$ 0.0*	20.0 $\pm$ 7.6
Liver	0.0 $\pm$ 0.0*	3.6 $\pm$ 1.6
Lungs	0.0 $\pm$ 0.0	0.0 $\pm$ 0.0
Thyroid	0.0 $\pm$ 0.0	0.0 $\pm$ 0.0
Brain	0.0 $\pm$ 0.0	0.0 $\pm$ 0.0
Eye	0.0 $\pm$ 0.0	0.0 $\pm$ 0.0
<i>WOUND AREA</i>		
Dressing	41.1 $\pm$ 15.1*	6.0 $\pm$ 3.8
Wound' s skin	57.4 $\pm$ 14.7*	13.1 $\pm$ 9.5
Subcutaneous tissue	1.1 $\pm$ 1.2*	0.2 $\pm$ 0.2
<i>Panniculus carnosus</i> muscle	0.0 $\pm$ 0.0	0.0 $\pm$ 0.0

Regarding the toxicity assays, *in vitro* cytotoxicity showed that at 0.1, 0.3 and 1 mg/mL, no cytotoxicity was observed since cell viability were 102  $\pm$  3, 113  $\pm$  9 and 77  $\pm$  4 %, respectively. Thus, the acceptance criteria were met, as the viability of those three concentrations was higher than 70 % compared to the negative control. Instead, at 3 mg/mL, viability was 55  $\pm$  10 % probably because cells were exposed to higher levels of nanoparticles, which might prevent cell proliferation, as previously described by Rocha *et al.* [23]. Cell viability data are represented in Fig. 4. In conclusion, the developed NLC at a concentration equal to or lower than 1 mg/mL were considered non-cytotoxic *in vitro*. This result was reasonably expected since the excipients used

for the NLC formulation are considered biodegradable, biocompatible and non-toxic carriers for human use by FDA and EMA [4].

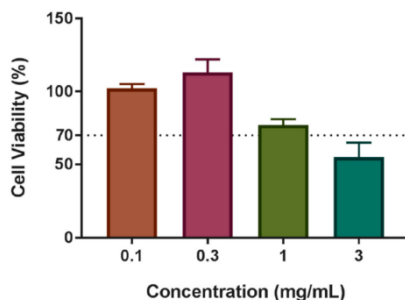


Figure 4. Percentages of cell viability in the Balb/3T3 cell line after being in contact with NLC at 3, 1, 0.3 and 0.1 mg/mL. Cell viability is expressed as percentage of survival (%) compared to the negative control.

In the LLNA:DA study, quantification of the ATP content via bioluminescence was used as an indicator of lymphocyte proliferation, and thus, as the skin sensitization potential of the developed NLC. The ATP content and SI values of 2-MBT, used as positive control, were  $2299 \pm 1087$  and 2.9, respectively. Since the SI value of the positive control was 2.9 ( $\geq 2.5$ ), it could be considered as a positive sensitizer, confirming its suitability to detect the sensitization capability of the test compounds. Table 4 shows the ATP content and SI values of animals treated with the developed NLC at 340 mg/mL, 170 mg/mL and 85 mg/ mL concentrations. SI rates were 1.4, 1.9 and 1.5 respectively. Since one of the results was found in the range of 1.8-2.5, evaluation of the dose-response relationship, erythema, edema or any other visual reaction in the application area were also required, as stated in the OECD guidelines. In this regard, none of the studied animals showed any skin sensitization reaction, or any dose-response relationship. Thus, it was concluded that the developed NLC were not sensitizing [4].

## Nanostructured lipid carriers (NLCs) for multiresistant infections

Table 4. Results obtained for the developed NLC in the LLNA:DA test (n=4). Values are expressed as the mean  $\pm$  SD (n=4). RLU, relative light units.

NLC	Test concentration (%)	ATP content (RLU)	
		Mean $\pm$ SD	SI
340 mg/ml	100	1007 $\pm$ 112	1.4 $\pm$ 0.2
170 mg/ml	50	1306 $\pm$ 197	1.9 $\pm$ 0.3
85 mg/ml	25	1048 $\pm$ 308	1.5 $\pm$ 0.4

The *in vivo* irritation/corrosion study was then carried out in order to evaluate if the developed NLC were able to provoke any damage on the animal skin after dermal application. The PII scores obtained are presented in Table 5.

Table 5. Skin reaction scores in rabbit: PII obtained for each animal in the *in vivo* irritation/corrosion study. PII=mean score at 24 ( $\pm$  2), 48 ( $\pm$  2) and 72 ( $\pm$  2) hours/6.

Rabbit No.	Erythema and eschar	Edema
1	0	0
2	0	0
3	0	0

The initial test did not show any ulcers, hemorrhages or scabs on the areas where NLC were applied; thus, a confirmation test was required. In this second study, no erythema, edema or any other reactions were observed in the NLC treated areas. All the control areas (not treated) presented 0 values for erythema and edema. At the histological level, special attention was paid to the thickness of the epidermis and the *stratum corneum*, not finding alterations or differences between NLC treated and control areas (Fig. 5). Observation of the dermis and the hypodermis revealed no inflammatory infiltration in any of the NLC treated or untreated sites. Regarding the glands, hair follicles and adipose and muscle tissue, no alteration was found. These data confirmed the results obtained in the visual examination. From this particular study, it can be concluded that the developed NLC were not irritant/corrosive *in vivo*, according to ISO 10993-10:2010, which evaluates the *in vivo* irritation response [4].

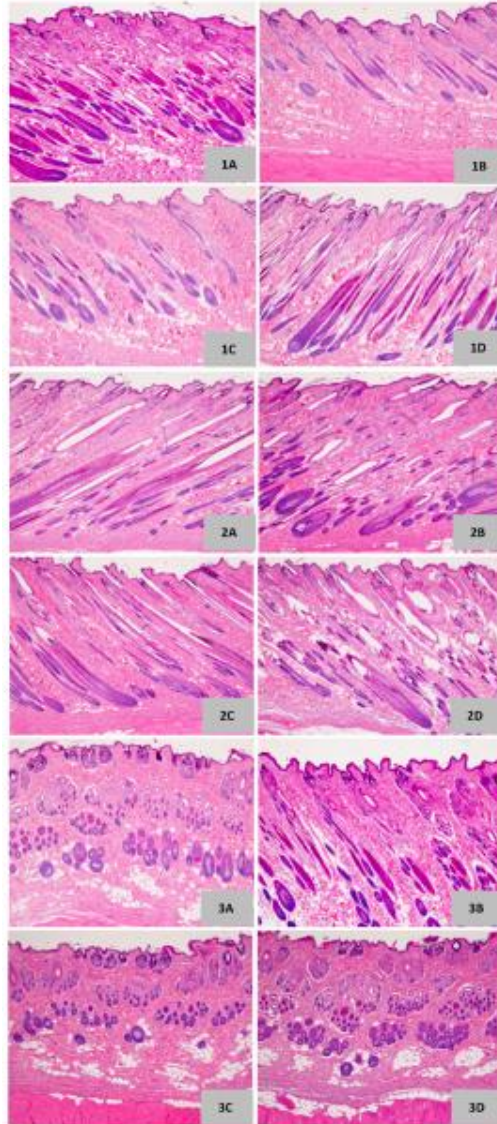


Figure 5. Histopathology of rabbit skin obtained in the *in vivo* irritation/corrosion study. No histopathology changes were observed in the NLC treated areas (1A, 1B, 2A, 2B, 3A, 3B) and in untreated areas (1C, 1D, 2C, 2D, 3C, 3D). Hematoxylin & eosin.  $\times 40$  magnification.

#### 4. Conclusion

The results from the current study suggest that the lipid-nanoparticles described in this work are safe and may potentially exert a local effect after topical administration on wounds. *In vivo* and *ex vivo* biodistribution studies showed that NLC remained on the

wound and were not absorbed for at least 24 h, probably due to their particle size, which does not allow nanoparticle penetration. *In vitro* cytotoxicity and *in vivo* sensitization and irritation/corrosion studies, based on ISO 10,993 standard (Biological evaluation of medical devices), demonstrated that the developed NLC were safe. Overall, results indicate that our NLC might present an alternative tool for local treatment of skin wounds.

## **5. Acknowledgments**

This work was carried out under the NANOPLATFORM Project (ELKARTEK 2015, KK-2015/0000036) funded by the Basque Government. Also, under the NANOGROW projects, with file number ZE-2017/00014, supported by the Department of Economic Development and Infrastructure of the Basque Government budget, through the Hazitek business I+D support program and co-financed by the European Regional Development Fund (ERDF). Technical and human support provided by SGIker (UPV/EHU, MICINN, GV/EJ, ERDF and ESF) is gratefully acknowledged. Authors also wish to thank the intellectual and technical assistance from the University of Navarra (UNAV) and the Basque Government (Consolidated Groups, IT907-16).

## 6. Supplementary data

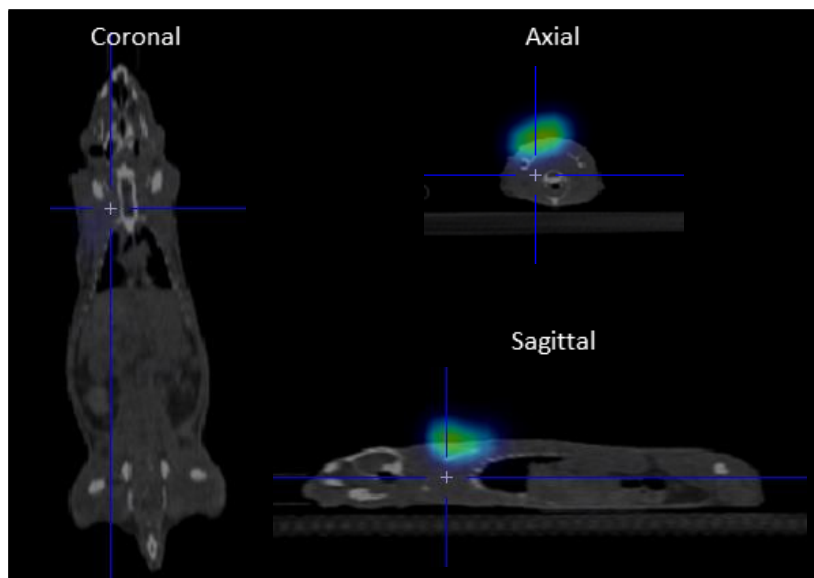


Figure S1. SPECT-CT slices of an animal treated with  $^{99m}\text{Tc}$ -NLC. The signal is observed on the surface of the body, although the spillover effect caused by the limited resolution of the tomography makes part of the signal seem to be included in the interior of the body.

## **7. References**

- [1] Müller RH, Radtke M, Wissing SA. Solid lipid nanoparticles (SLN) and nanostructured lipid carriers (NLC) in cosmetic and dermatological preparations. *Advanced Drug Delivery Reviews* 2002;54:S131-S155.
- [2] Naderi N, Karponis D, Mosahebi A, Seifalian AM. Nanoparticles in wound healing; from hope to promise, from promise to routine. *Frontiers in bioscience (Landmark edition)*.
- [3] Pardeike J, Hommoss A, Müller RH. Lipid nanoparticles (SLN, NLC) in cosmetic and pharmaceutical dermal products. *International Journal of Pharmaceutics* 2009;366(1):170-184.
- [4] Reinke JM, Sorg H. Wound repair and regeneration. *European surgical research. Europäische chirurgische Forschung. Recherches chirurgicales europeennes* 2012
- [5] Landén NX, Li D, Stähle M. Transition from inflammation to proliferation: a critical step during wound healing. *Cellular and Molecular Life Sciences* 2016;73(20):3861-3885.
- [6] Gainza G, Pastor M, Aguirre JJ, Villullas S, Pedraz JL, Hernandez RM, et al. A novel strategy for the treatment of chronic wounds based on the topical administration of rhEGF-loaded lipid nanoparticles: In vitro bioactivity and in vivo effectiveness in healing-impaired db/db mice. *Journal of Controlled Release* 2014;185:51-61.
- [7] Gainza G, Celdran Bonafonte D, Moreno B, Aguirre Anda JJ, Gutierrez FB, Villullas S, et al. The topical administration of rhEGF-loaded nanostructured lipid carriers (rhEGF-NLC) improves healing in a porcine full-thickness excisional wound model 2014.
- [8] Gainza G, Chu WS, Guy RH, Pedraz JL, Hernandez RM, Delgado-Charro B, et al. Development and in vitro evaluation of lipid nanoparticle-based dressings for topical treatment of chronic wounds. *International Journal of Pharmaceutics* 2015;490(1):404-411.
- [9] Garcia-Orue I, Gainza G, Girbau C, Alonso R, Aguirre JJ, Pedraz JL, et al. LL37 loaded nanostructured lipid carriers (NLC): A new strategy for the topical treatment

of chronic wounds. *European Journal of Pharmaceutics and Biopharmaceutics* 2016;108:310-316.

[10] Motawea A, Borg T, El-Gawad HAE. Topical Phenytoin Nanostructured Lipid Carriers: Design and Development. *Drug development and industrial pharmacy* 2017.

[11] Saporito F, Sandri G, Bonferoni MC, Rossi S, Boselli C, Icaro Cornaglia A, et al. Essential oil-loaded lipid nanoparticles for wound healing. *International Journal of Nanomedicine* 2017.

[12] Areses P, Agüeros MT, Quincoces G, Collantes M, Richter JÁ, López-Sánchez LM, et al. Molecular Imaging Techniques to Study the Biodistribution of Orally Administered <sup>99m</sup>Tc-Labelled Naive and Ligand-Tagged Nanoparticles. *Molecular imaging and biology* 2010.

[13] Psimadas D, Baldi G, Ravagli C, Bouziotis P, Xanthopoulos S, Comes-Franchini M, et al. Preliminary Evaluation of a <sup>99m</sup>Tc Labeled Hybrid Nanoparticle Bearing a Cobalt Ferrite Core: In Vivo Biodistribution. *Journal of biomedical nanotechnology* 2012.

[14] Zhao L, Zhu M, Li Y, Xing Y, Zhao J. Radiolabeled Dendrimers for Nuclear Medicine Applications. *Molecules* 2017.

[15] Müller R H, Shegokar R, Keck C. 20 Years of Lipid Nanoparticles (SLN & NLC): Present State of Development & Industrial Applications. *Current drug discovery* 2011.

[16] González-Mira E, Nikolić S, García ML, Egea MA, Souto EB, Calpena AC. Potential Use of Nanostructured Lipid Carriers for Topical Delivery of Flurbiprofen. *Journal of Pharmaceutical Sciences* 2011;100(1):242-251.

[17] Pastor M, Basas J, Vairo C, Gainza G, Moreno-Sastre M, Gomis X, et al. Safety and effectiveness of sodium colistimethate-loaded nanostructured lipid carriers (SCM-NLC) against *P. aeruginosa*: in vitro and in vivo studies following pulmonary and intramuscular administration. *Nanomedicine: Nanotechnology, Biology and Medicine* 2019;18:101-111.

*Nanostructured lipid carriers (NLCs) for multiresistant infections*

[18] Buzea C, Pacheco II, Robbie K. Nanomaterials and nanoparticles: sources and toxicity. *Biointerphases* 2007;2(4):MR17-71.

[19] Campbell CSJ, Contreras-Rojas LR, Delgado-Charro MB, Guy RH. Objective assessment of nanoparticle disposition in mammalian skin after topical exposure. *Journal of Controlled Release* 2012;162(1):201-207.

[20] Esposito E, Boschi A, Ravani L, Cortesi R, Drechsler M, Mariani P, et al. Biodistribution of nanostructured lipid carriers: a tomographic study. *European Journal of Pharmaceutics and Biopharmaceutics* 2015;89:145-156.

[21] Ucar E, Teksoz S, Ichedef C, Kilcar AY, Medine EI, Ari K, et al. Synthesis, characterization and radiolabeling of folic acid modified nanostructured lipid carriers as a contrast agent and drug delivery system. *Applied Radiation and Isotopes* 2017;119:72-79.

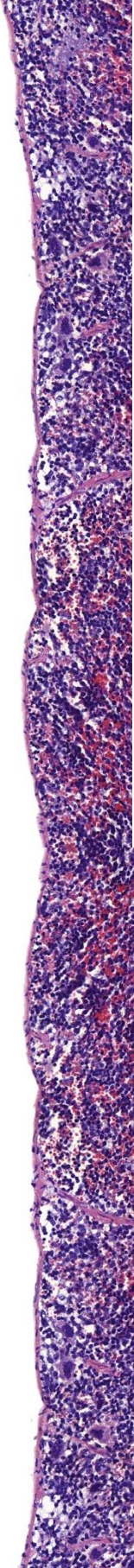
[22] Emamian SA, Shalaby-Rana EF, Majd M. The spectrum of heterotopic gastric mucosa in children detected by Tc-99m pertechnetate scintigraphy. *Clinical nuclear medicine* 2001.

[23] Rocha V, Marques C, Figueiredo JL, Gaio AR, Costa PC, Sousa Lobo JM, et al. In vitro cytotoxicity evaluation of resveratrol-loaded nanoparticles: Focus on the challenges of in vitro methodologies. *Food and Chemical Toxicology* 2017;103:214-222.





# Discussion





As previously stated, antimicrobial resistance (AMR) is a serious issue facing global public health, and requires a drastic and immediate intervention of governments and society. AMR causes life-threatening wound and lung infections, requiring long hospital stays and expensive drug therapies. In the United States alone, an estimated two million people were annually affected by AMR, leading to 23,000 deaths (1). In addition, 25,000 patients died in the European Union because of nosocomial resistant bacterial infections (2). Therefore, if no action is taken, AMR is highly likely to become a massive killer reaching 10 million deaths worldwide by 2050 (surpassing cancer deaths) and costing up to \$ 100 trillion (3).

It is worth mentioning that *P. aeruginosa*, *K. pneumoniae* and *A. baumannii* gram-negative bacteria have developed numerous strategies to avoid antibiotic effects and cause two-thirds of AMR related deaths in Europe (4-6). Colistin and amikacin have been used for decades due to their excellent activity to treat multidrug resistant gram-negative infections. However, both are neuro- and nephrotoxic, being severe renal impairment their worst reported side effect.

Nanotechnology-based formulations could represent an excellent choice for overcoming antibiotic limitations associated to toxicity (7). In this regard, lipid-based drug delivery systems, such as liposomes, solid lipid nanoparticles (SLNs) and nanostructured lipid carriers (NLCs), are considered the most promising approaches due to their biocompatibility and capability to improve drug disposition. Particularly, NLCs represent the most recent and improved lipid-based delivery system due to their high stability and greater drug loading capacity. NLCs also represent an interesting controlled release strategy, enabling dose reduction and, consequently, drug toxicity (8).

Bearing these considerations in mind, in the current doctoral thesis, we have focused on the development and preclinical testing of antibiotic-loaded NLCs to enhance safety and effectiveness of current treatments for wound and pulmonary multiresistant infections. *P. aeruginosa*, *K. pneumoniae* and *A. baumannii* are the bacteria of choice for both *in vitro* and *in vivo* evaluation, being considered as the worst AMR scenario. In addition, the animal models used have been carefully designed in order to better simulate the clinical conditions.

The unfolding of the previous objectives is described hereafter.

- 1. To select the most suitable formulation among different AMK- and SCM-loaded NLCs and to demonstrate their efficacy in a neutropenic murine acute pneumonia infection model caused by an extensively drug-resistant *A. baumannii* strain, following intraperitoneal and intramuscular routes.**

To achieve this end, four SCM-loaded NLCs (SCM-NLCs) and four AMK-loaded NLCs (AMK-NLCs) were developed. *In vitro* activity against a wide range of clinical multiresistant isolates was then evaluated and the efficacy of the most efficient formulation was finally assessed *in vivo* in a neutropenic murine acute pneumonia infection model.

NLCs were prepared through the hot melt homogenization method (sonication at 20 W for 15 s) followed by a high-pressure homogenization (HPH) step, which allowed handling higher working volumes during batch preparation. Most industries have already adopted HPH for various applications. The main advantages of this combined preparation method are: i) high reproducibility, ii) suitability for large scale productions and iii) absence of organic solvents (9). In order to improve NLC stability, especially during the freeze-drying process, two different cryoprotectants, trehalose and dextran (15 % w/w), were investigated. Both compounds were chosen because they have shown to improve drug stability in lipid-amorphous-matrices during storage (10,11). In addition, considering that positively charged nanoparticles have been reported to increase antimicrobial activity due to stronger surface/membrane interactions, NLCs were also coated with chitosan. Chitosan was also selected due to its intrinsic antibacterial properties, which could have a synergistic effect with the loaded antibiotic (12,13). A total of eight formulations, with (+) or without (-) chitosan, were produced and named as follows: (-) SCM-NLC trehalose, (+) SCM-NLC trehalose, (-) SCM-NLC dextran, (+) SCM-NLC dextran; (-) AMK-NLC trehalose, (+) AMK-NLC trehalose, (-) AMK-NLC dextran and (+) AMK-NLC dextran.

NLCs were characterized for their size, polydispersity index (PDI), zeta potential, release profile and encapsulation efficacy (EE). Results are shown in Table 1. Also,

macroscopic morphology was studied by transmission electron microscopy (TEM) analysis under negative staining.

Table 1. Size, PDI, zeta potential, release profile and EE characterization.

		Size (nm)	PDI	Zeta Potential (mV)	Release profile (%)	EE (%)
(-)	SCM-NLC Trehalose	67.33 ± 2.06	0.257 ± 0.01	-20.3 ± 0.75	90.29 ± 7.72	73.14 ± 3.69
	SCM-NLC Dextran	101.56 ± 0.41	0.207 ± 0.01	-29.03 ± 1.44	100.31 ± 2.94	
(+) )	SCM-NLC Trehalose	177.63 ± 5.50	0.266 ± 0.03	14.77 ± 1.91	100.7 ± 12.63	
	SCM-NLC Dextran	146.46 ± 0.37	0.349 ± 0.09	14.16 ± 0.55	92.48 ± 2.31	
(-)	AMK-NLC Trehalose	89.71 ± 2.48	0.139 ± 0.00	-20.63 ± 2.12	77.73 ± 3.57	92.8 ± 4.18
	AMK-NLC Dextran	73.45 ± 0.28	0.264 ± 0.03	-15.63 ± 0.55	76.78 ± 0.76	
(+) )	AMK-NLC Trehalose	114.1 ± 1.19	0.234 ± 0.03	0.11 ± 0.14	68.41 ± 3.90	
	AMK-NLC Dextran	142.4 ± 2.54	0.280 ± 0.02	1.81 ± 0.08	72.4 ± 2.46	

As expected, positively charged particles presented a bigger size compared to negative nanoparticles due to chitosan addition. Even so, PDI values were acceptable for all lipid-based carriers, as verified by the ease of resuspension after lyophilization (14). Turning to zeta potential, only (+) AMK-NLCs showed values close to 0 mV, providing a less stable colloidal system. On the other hand, the main differences between colistin and amikacin-loaded NLCs concerned antibiotic EE and drug release. In fact, AMK-NLCs achieved higher EE, probably due to AMK lower water solubility and higher affinity to the lipid phase. AMK-NLCs also showed a slower drug release profile compared to SCM-NLCs, again due to amikacin hydrophobicity, but also because of the lower amount of surface associated non-encapsulated drug that led to a milder initial release. These data are in line with zur Mühlen *et. al*, since they proved that the release profile, as well as EE, can vary from one drug to another

depending on the affinity of the drug to the lipid matrix and to the aqueous media (15). TEM images revealed that (-) SCM-NLC was the most homogeneous formulation, as shown in Figure 1.

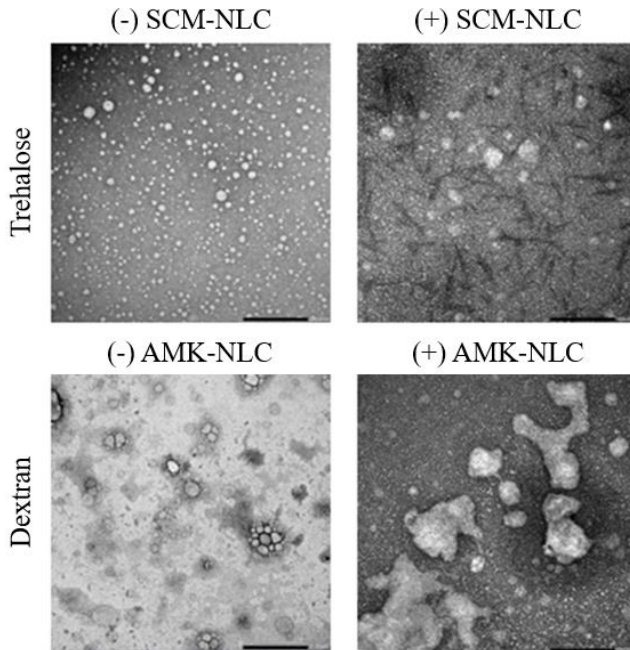


Figure 1. TEM images of antibiotic-loaded NLCs. Scale bar 450 nm.

After physicochemical characterization, we proceeded to determine which cryoprotectant was the most suitable to freeze-dry the lipid formulations. For that purpose, an *in vitro* activity assay was carried out in five *P. aeruginosa* strains. Results revealed that trehalose enhanced antibiotic activity, especially in the case of (+) SCM-NLC trehalose, since lower MIC, MBIC and MBEC values were obtained.

This finding is in accordance with the work carried out by Crowe *et al.*, who demonstrated that trehalose might be superior to other sugars preserving the structure of freeze-dried lipid carriers, and, consequently, the activity of the encapsulated drugs (16). After cryoprotectant selection, our next aim was to evaluate the suitability of chitosan for improving the nanoparticle antimicrobial activity. To this end, we evaluated the *in vitro* activity of the formulations lyophilized with trehalose in forty-two *P. aeruginosa*, *K. pneumoniae* and *A. baumannii* clinical isolates. No significant differences between positively and negatively charged formulations were found in

terms of *in vitro* activity. Therefore, taking into account that the efficacy of chitosan-coated formulations was not greater than the other formulations, and also considering that chitosan incorporation significantly hindered the manufacturing process from a cost-efficient and production-time point of view, positive coating was finally discarded. In addition, it was noticeable that (-) SCM-NLC trehalose showed the highest *in vitro* activity compared to the remaining formulations, concretely against *A. baumannii* strains. For all these reasons, (-) SCM-NLC trehalose was selected as the formulation of choice for further studies.

Next, we evaluated the efficacy of (-) SCM-NLC trehalose in a neutropenic murine acute pneumonia model, intending to simulate the poor health condition of chronic resistant infections. *A. baumannii* was selected for mouse infection since these bacteria resulted to be the most sensitive to SCM-NLCs.

NLCs were administered following intraperitoneal (IP) and intramuscular (IM) routes. IP administration was selected because it is an easy to handle route for rodents, and due to its pharmacokinetic, comparable to that of the clinical antibiotic rescue-treatments in humans. IM route was chosen as a more endurable and manageable administration method. The efficacy of SCM-NLCs administered by IP and IM routes was compared to that obtained from IM free SCM (60 mg/kg). IM route was chosen for free SCM administration because a previous internal pharmacokinetic study showed that IM administration of 60 mg/kg of free SCM reached drug plasma levels similar to that clinically recommended by the Sanford Guide To Antimicrobial Therapy (0.83 µg/ml colistin peak serum level) (17). The study design and SCM-NLC dosage are depicted in Table 2, along with the results of the study.

Table 2. Posology, administration route and results from *in vivo* efficacy study.

Route	Treatment	N	Log <sub>10</sub> cfu/g lung median (IQR <sub>25-75</sub> )
IM	Control 0.9 % NaCl (q6h)	10	6.33 (4.94-7.07)
	SCM 60 mg/kg (q6h)	8	3.58 (3.15-4.01) <sup>a</sup>
	(-) SCM-NLC 12 mg/kg (q12h)	8	5.91 (4.57-6.41)
	(-) SCM-NLC 12 mg/kg (q24h)	7	6.56 (5.37-7.09)
IP	(-) SCM-NLC 6 mg/kg (q12h)	7	3.35 (2.87-4.67) <sup>a</sup>
	(-) SCM-NLC 6 mg/kg (q24h)	8	3.02 (2.19-4.40) <sup>a</sup>

## *Nanostructured lipid carriers (NLCs) for multiresistant infections*

N; number of animals IQR; interquartile range, NaCl; sodium chloride, CFU; colony-forming units, SCM; sodium colistimethate, IM; intramuscular, IP; intraperitoneal; \*p value < 0.05 vs control

The *in vivo* study revealed that IP SCM-NLC administration was superior to the IM route and as effective as IM free SCM. IP (-) SCM-NLC 6 mg/kg q12h and IP (-) SCM-NLC 6 mg/kg q24h showed the same efficacy as free SCM using a 20- and 40-fold lower dose, respectively. In addition, it should be noted that the IP administration of (-) SCM-NLC 6 mg/kg administered once a day (q24h) achieved the same activity as free SCM 60 mg/kg administered every 6 h (q6h). These data are very remarkable because (-) SCM-NLCs may potentially improve current treatment efficacy and safety since the same effect is achieved using lower doses of SCM. In fact, frequency of administration could be considerably spaced and dose highly decreased, leading to safer treatments with reduced cost. This, undeniably, would significantly impact on patient's quality of life and healthcare systems' sustainability. From these data, also, it can be postulated that the encapsulation process enhanced the antimicrobial activity of SCM, probably because the lipid matrix of NLCs hinders drug degradation, which improves SCM stability and enhances its *in vivo* disposition. In this regard, several studies indicated that NLCs are capable of improving stability of different type of drugs, preserving their structure and avoiding its rapid degradation; it has also been proven that their composition allows the control of drug release, thereby drug concentration remains appropriate over time (18). All in all, IP (-) SCM-NLC 6 mg/kg administered once a day (q24h) could represent a promising option to fight against resistant pulmonary infections caused by *A. baumannii*. However, this study did not clarify the reason why IM SCM-NLCs showed lower efficacy. Since this route is an attractive and easy to handle way of administration in clinical practice, SCM-NLCs administered by IM route were further investigated in the next studies.

### **2. To evaluate SCM-NLC biodistribution, safety and efficacy in a murine acute pneumonia infection model caused by an extensively drug-resistant *P. aeruginosa* strain, following pulmonary and intramuscular routes.**

To evaluate the *in vivo* efficacy of the SCM-NLCs, a murine acute pneumonia model caused by an extensively drug-resistant *P. aeruginosa* strain was developed. Mice were kept under hyperoxia (O<sub>2</sub> 95 %) to better simulate the mechanical ventilation condition associated to the clinical context. *P. aeruginosa* was selected due to its

severity and incidence all over the world (19). In this study, treatments were administered through the IM and pulmonary route. On the one hand, the IM route was selected because it is an easy to handle administration route and, on the other hand, the pulmonary administration permits directly reaching the infected area. Finally, SCM-NLC dose was reduced compared to the previous *in vivo* study in order to further enhance antibiotic safety by means of nanotechnology. Doses, administration routes and results from the *in vivo* efficacy study are shown in Table 3.

Table 3. Posology, administration route and results from the *in vivo* efficacy study.

Route	Treatment	Pa 1016R (XDR)	
		Total dose ( $\mu\text{g}$ )	$\log_{10}$ cfu/g lung median (IQ <sub>25-75</sub> )
Pulmonary	Control NaCl (q12h)	0	6.66 (6.50-7.61)
	Free SCM 15mg/kg (q12h)	1,944	5.70 (5.03-6.61)*
	SCM-NLC 2.8mg/kg (q12h)	420	6.21 (4.97-6.74)*
	SCM-NLC 2.8mg/kg (q24h)	210	5.64 (5.24-6.14)*
IM	Free SCM 80mg/kg (q12h)	10,200	6.03 (4.90-6.44)*
	SCM-NLC 2.8mg/kg (q12h)	420	6.37 (5.85-7.43)
	SCM-NLC 2.8mg/kg (q24h)	210	5.85 (4.97-6.45)*

\*p<0.05 compared to the control group; hyperoxia condition (O<sub>2</sub> 95 %).

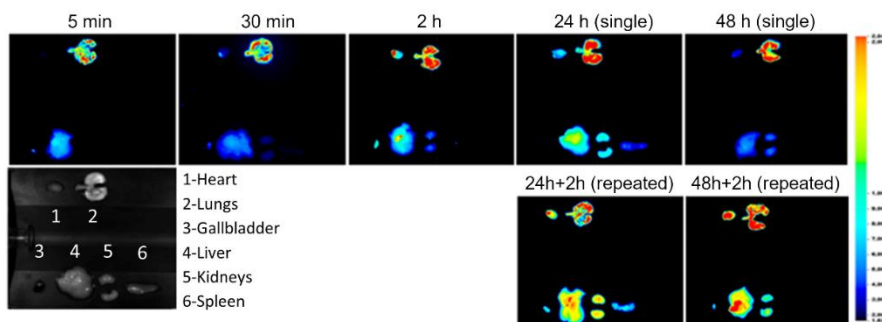
SCM-NLC efficacy was the same as that of the free SCM group, either using the pulmonary or the IM route. Accordingly, it is important to highlight that SCM-NLC doses were significantly lower than those used in the groups receiving the free drug; *i.e.* maximum daily dose for SCM-NLCs, given either pulmonary or intramuscularly, was 2.8-5.6 mg/kg, whereas daily nebulized free SCM dose was 15-30 mg/kg or daily IM free SCM was 80-160 mg/kg. These striking results demonstrated that *in vivo* SCM-NLCs were more active than free SCM, since the same effect was observed using at least a 5-fold or even a 60-fold lower dose when SCM is nanoencapsulated. All these results are in line with the data obtained in the previous *in vivo* study and suggest that the encapsulation process enhances the pharmacological effect of SCM, as lower doses are sufficient to achieve the same effect as free SCM.

### *Nanostructured lipid carriers (NLCs) for multiresistant infections*

Moreover, SCM-NLC safety was investigated through *in vivo* toxicity and biodistribution studies in healthy mice. The toxicity study following pulmonary or IM route demonstrated nanoparticle safety even at high doses. In fact, all the inflammatory states found were attributable to physiological or external events, such as the hyperoxia condition, which generally leads to lung inflammation and acute lung injury (20). Besides, phenomena such as splenic hematopoiesis, dark neuron, alveolar wall congestion and red blood extravasation, extramedullary hematopoietic process in spleen and granular deposits in liver were also found in all studied groups, including the control groups. Therefore, it might be stated that the toxicity effect of SCM-NLCs at different doses was negligible.

Finally, a biodistribution study was carried out using infrared labeled-NLCs (IR-NLCs) administered by IM or pulmonary routes. As shown in Figure 2, nebulization gave rise to a predominant NLC lung disposition, increased over the time, although signal could be slightly detected in other organs, suggesting a mild systemic absorption. As lungs display high vascularization, it is clear that part of the dose reached systemic circulation. Concretely, after pulmonary administration, IR-NLCs were mainly biodistributed in the lungs and to a lesser extent in the liver. After 48 h, the signal in the liver decreased, whereas the signal in the lung was still high and homogeneous. When repeated doses were administered at 24 and 48 h, signal in the lung increased. Interestingly, the signal detected in the kidneys was negligible, which could indicate a greater antibiotic safety due to nephrotoxicity reduction. Thus, this route may be interesting to use as maintenance therapy in the clinical practice. Conversely, biodistribution images after IM administration, revealed a notorious and fast systemic absorption of NLCs. Images from Figure 2 showed that IR-NLCs mainly remained at the injection site, even though the signal was also detected from the very beginning in other organs, such as the liver and gallbladder. When repeated doses were administered, the signal increased in all the studied organs. The immediacy of this distribution could make the IM route as an interesting approach for a rescue therapy in clinical settings.

## A IR-NLCs, Pulmonary



## B IR-NLCs, IM

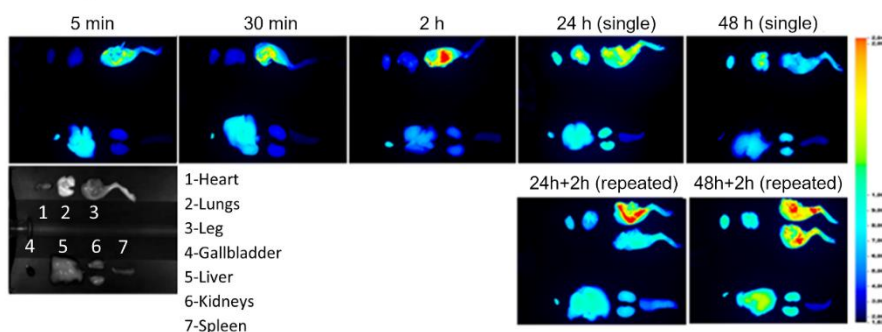


Figure 2. Biodistribution study. (A) IR-NLC distribution after nebulization by Microsprayer® aerosolizer. (B) IR-NLC biodistribution after IM administration.

In conclusion, SCM-NLCs represent a promising approach for fighting against MDR/XDR *P. aeruginosa* infections. It was confirmed that SCM-NLCs were active against XDR *P. aeruginosa* in a murine acute pneumonia model and, in addition, presented no toxic effect. Finally, it is particularly noteworthy to mention that, in accordance with the biodistribution studies, the pulmonary route might be selected when using maintenance therapy since its effect is mainly localized in lungs, decreasing SCM nephrotoxicity. On the other hand, the IM route may be more appropriate in an emergency as it showed faster absorption.

### 3. To evaluate blank-NLC biodistribution and safety after topical administration on impaired and intact skin, respectively.

As already mentioned, *P. aeruginosa*, *K. pneumonia* and *A. baumannii* are classified as principal responsible for multiresistant gram-negative bacterial infections, especially in skin and respiratory tract. In this regard, lipid-nanoparticles, especially

### *Nanostructured lipid carriers (NLCs) for multiresistant infections*

NLCs, have shown appropriate characteristics for enhancing wound recovery, such as, biodegradability, occlusive properties or wound moisture maintenance (21). However, to date, there are no safety-preclinical data for NLCs concerning topical application.

In this line, in the previous sections of this piece of work, NLCs have demonstrated to be absorbed after IP, IM or pulmonary administration, exerting a systemic effect. However, so far, NLC biodistribution through topical administration on impaired skin is still unknown. Thus, in order to efficiently treat infected wounds, we aim to avoid systemic absorption for the purpose of achieving a local effect of NLCs. With that in mind, NLCs with a size of  $133.48 \pm 4.40$  nm should exert a local effect on wounds, as it is well known that particles above 20 nm do not penetrate into damaged skin (22); therefore, no penetration of the developed formulation was expected.

Considering the foregoing, the last purpose of this doctoral thesis was to evaluate blank-NLC biodistribution and safety after topical administration. To this aim, firstly, *in vivo* and *ex vivo* biodistribution studies were carried out in a full-thickness wound model. Then, *in vitro* and *in vivo* toxicity was analyzed, following ISO 10993 standard (Biological evaluation of medical devices). *In vivo* toxicity studies were evaluated on intact skin.

For the *in vivo* and *ex vivo* biodistribution studies, NLCs were radiolabeled with  $^{99m}\text{Tc}$  (technetium-99m) since previous studies revealed that this radiomarker did not cause significant changes either in NLC morphology or in size (23,24). The *in vivo* biodistribution study performed by SPECT/CT revealed that  $^{99m}\text{Tc}$ -NLCs remained on the wound (almost 100 % of the signal appeared at the wound area) and no absorption was observed for at least 24 h. In control animals, free  $^{99m}\text{Tc}$  was quickly absorbed (7.3 % of the signal remained at the wound area), reaching the stomach and then the large intestine, which is compatible with the natural metabolism of  $^{99m}\text{Tc}$  (25). Biodistribution images are shown in Figure 3. Besides, data obtained *in vivo* were supported by *ex vivo* biodistribution studies, confirming that NLCs exerted a local effect (as no systemic absorption was detected). It should be noted that, since

this is the first reported study analyzing NLC biodistribution after topical administration on wounds, these results cannot be compared.

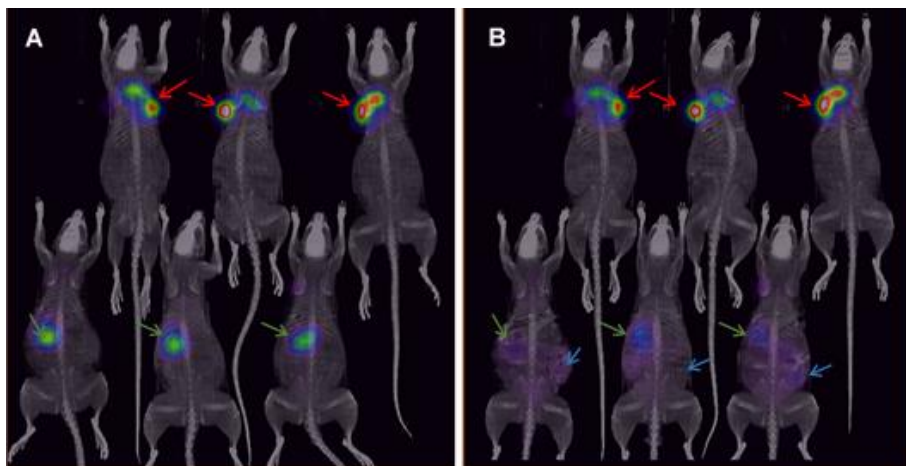


Figure 3. 3D images of the SPECT/ CT studies at 1 hour (A) and 24 hours (B). The three rats in the upper part of the image were treated with <sup>99m</sup>Tc-NLCs on the wound area (red arrow), producing a stable signal over time. The three rats at the bottom of the image were control animals receiving free <sup>99m</sup>Tc on the wound. The green arrows indicate the stomach area, more evident at early times, and the blue arrows point to the large intestine.

Regarding the toxicity studies, no relevant *in vitro* cytotoxicity was observed at a concentration equal to or lower than 1 mg/mL; thus, the developed NLCs were considered non-cytotoxic *in vitro*. Accordingly, *in vivo* sensitization and irritation/corrosion assays, based on ISO 10,993 standard, demonstrated that NLCs were neither sensitizing nor irritating since no erythema, edema or any other reactions were observed when topically applied on intact skin. These results were reasonably expected since the excipients used for NLC formulation are considered biodegradable, biocompatible and non-toxic carriers for human use by FDA and EMA (26).

All in all, the results suggested that NLCs are safe when topically applied and may potentially exert a local effect on wounds. In fact, *in vivo* and *ex vivo* biodistribution studies showed that NLCs remained at the wound area and were not absorbed for at least 24 h, probably due to their particle size, which does not allow penetration. *In vitro* cytotoxicity and *in vivo* sensitization and irritation/corrosion studies, demonstrated that nanoparticles were safe. Overall, results indicated that our NLCs might be a promising tool for local treatment of skin wounds. In this regard, it could be interesting to perform further studies to evaluate the antimicrobial effectiveness of

*Nanostructured lipid carriers (NLCs) for multiresistant infections*

SCM-NLCs topically administered on infected wounds in order to assess if this type of nanoformulation is as effective for impaired skin as for lung infections.

## References

- (1) Centers for Disease Control and Prevention. About Antimicrobial Resistance [article online], 2018. Available from <https://www.cdc.gov/drugresistance/about.html>
- (2) World Health Organization Europe. Antibiotic resistance [article online], 2019. Available from <http://www.euro.who.int/en/health-topics/disease-prevention/antimicrobial-resistance/antibiotic-resistance>
- (3) Luepke KH, Mohr JF. The antibiotic pipeline: reviving research and development and speeding drugs to market. *Expert Rev Anti Infect Ther* 2017;15(5):425-433
- (4) Arzanlou M, Chai WC, Venter H. Intrinsic, adaptive and acquired antimicrobial resistance in Gram-negative bacteria. *Essays Biochem* 2017 Mar 3;61(1):49-59
- (5) Pulcini C, Kahlmeter G, Kluytmans J, Carmeli Y, Ouellette M, Outterson K, Patel J, Cavaleri M, Cox EM, Houchens CR, Grayson ML, Hansen P, Singh N, Theuretzbacher U, Magrini N. WHO Pathogens Priority List Working Group. Discovery, research, and development of new antibiotics: the WHO priority list of antibiotic-resistant bacteria and tuberculosis. *Lancet Infect Dis* 2018;18(3):318-327
- (6) Global priority list of antibiotic-resistant bacteria to guide research, discovery, and development of new antibiotics [article online], 2017. Available from [https://www.who.int/medicines/publications/WHO-PPL-Short\\_Summary\\_25Feb-ET\\_NM\\_WHO.pdf?ua=1](https://www.who.int/medicines/publications/WHO-PPL-Short_Summary_25Feb-ET_NM_WHO.pdf?ua=1)
- (7) Kalhapure RS, Suleman N, Mocktar C, Seedat N, Govender T. Nanoengineered drug delivery systems for enhancing antibiotic therapy. *J Pharm Sci* 2015;104(3):872-905
- (8) Pastor M, Basas J, Vairo C, Gainza G, Moreno-Sastre M, Gomis X, *et al.* Safety and effectiveness of sodium colistimethate-loaded nanostructured lipid carriers (SCM-NLC) against *P. aeruginosa*: *in vitro* and *in vivo* studies following pulmonary and intramuscular administration. *Nanomedicine* 2019;18:101-111
- (9) Cui B, Feng L, Wang C, Yang D, Yu M, Zeng Z, *et al.* Stability and Biological Activity Evaluation of Chlorantraniliprole Solid Nanodispersions Prepared by High Pressure Homogenization. *PLoS ONE* 2016;11(8):e0160877

*Nanostructured lipid carriers (NLCs) for multiresistant infections*

(10) Sun W, Davidson P. Effect of dextran molecular weight on protein stabilization during freeze-drying and storage. *Cryo Letters* 2001; 22(5):285-92

(11) Ball RL, Bajaj P, Whitehead KA. Achieving long-term stability of lipid nanoparticles: examining the effect of pH, temperature, and lyophilization. *Int J Nanomedicine* 2017;12:305-315

(12) Kong M, Chen XG, Xing K, Park HJ. Antimicrobial properties of chitosan and mode of action: A state of the art review. *Int J Food Microbiol* 2010;144(1):51-63

(13) Gottenbos B, Grijpma DW, van der Mei HC, Feijen J, Busscher H. Antimicrobial effects of positively charged surface on adhering Gram-positive and Gram-negative bacteria. *J Antimicrob Chemother* 2001;48(1):7-13

(14) Danaei M, Dehghankhold M, Ataei S, Hasanzadeh Davarani F, Javanmard R, Dokhani A, Khorasani S, Mozafari MR. Impact of Particle Size and Polydispersity Index on the Clinical Applications of Lipidic Nanocarrier Systems. *Pharmaceutics* 2018 18;10(2):57

(15) zur Mühlen A, Schwarz C, Mehnert W. Solid lipid nanoparticles (SLN) for controlled drug delivery – Drug release and release mechanism. *Eur J Pharm Biopharm* 1998;45(2):149-155

(16) Crowe LM, Reid DS, Crowe JH. Is trehalose special for preserving dry biomaterials? *Biophys J* 1996 10;71(4):2087-2093

(17) Gilbert D, Chambers H, Eliopoulos G, Saag M, Pavia A. *The Sanford Guide to Antimicrobial Therapy* 2019. 49<sup>th</sup> ed. perryville, VA, USA:Antimicrobial Therapy, Inc.; 2019

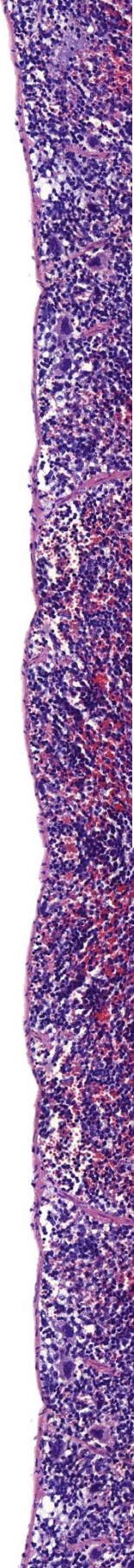
(18) Pastor M, Moreno-Sastre M, Esquisabel A, Sans E, Viñas M, Bachiller D, Asensio VJ, Pozo AD, Gainza E, Pedraz JL. Sodium colistimethate loaded lipid nanocarriers for the treatment of *Pseudomonas aeruginosa* infections associated with cystic fibrosis. *Int J Pharm* 2014;477(1):485-494

(19) Andrade F, Rafael D, Videira M, Ferreira D, Sosnik A, Sarmiento B. Nanotechnology and pulmonary delivery to overcome resistance in infectious diseases. *Adv Drug Deliv Rev* 2013;65(13):1816-1827

- (20) Lv R, Zheng J, Ye Z, Sun XJ, Tao Y, Liu K, *et al.* Advances in the therapy of hyperoxia-induced lung injury: Findings from animal models, 41(3); 2014:183-202
- (21) Pardeike J, Hommoss A, Müller RH. Lipid nanoparticles (SLN, NLC) in cosmetic and pharmaceutical dermal products. *Int J Pharm* 2009;366(1):170-184
- (22) Campbell CSJ, Contreras-Rojas LR, Delgado-Charro MB, Guy RH. Objective assessment of nanoparticle disposition in mammalian skin after topical exposure. *Journal of Controlled Release* 2012 20 August 2012;162(1):201-207
- (23) Esposito E, Boschi A, Ravani L, Cortesi R, Drechsler M, Mariani P, *et al.* Biodistribution of nanostructured lipid carriers: a tomographic study. *Eur J Pharm Biopharm* 2015;89:145-156
- (24) Ucar E, Teksoz S, Ichedef C, Kilcar AY, Medine EI, Ari K, *et al.* Synthesis, characterization and radiolabeling of folic acid modified nanostructured lipid carriers as a contrast agent and drug delivery system. *Appl Radiat Isot* 2017;119:72-79
- (25) Emamian SA, Shalaby-Rana EF, Majd M. The spectrum of heterotopic gastric mucosa in children detected by Tc-99m pertechnetate scintigraphy. *Clin Nucl Med.* 2001;26(6):529-535
- (26) Reinke JM, Sorg H. Wound repair and regeneration. *Eur Surg Res.* 2012;49(1):35-43



# Conclusions





On the basis of the results obtained in the experimental studies of this doctoral thesis, the following conclusions were derived:

1. NLCs were successfully produced by the hot-melt homogenization method, both at laboratory and large-scale. According to their physicochemical properties, the developed NLCs were suitable for IP and IM administration.
2. Both SCM and AMK were successfully encapsulated into NLCs. Trehalose was selected as cryoprotectant because it enhanced the activity of the encapsulated antibiotics. Conversely, chitosan positive coating was discarded since it did not improve antibiotic activity and was less cost-effective. Therefore, SCM-NLCs freeze-dried with trehalose was the formulation of choice to further assess their *in vivo* efficacy.
3. The *in vivo* study in a neutropenic murine acute pneumonia model caused by an extensively drug resistant *A. baumannii* strain revealed that SCM-NLC IP administration may potentially improve both efficacy and safety of the current SCM treatments since a 40-fold lower SCM dose can be used achieving the same outcomes.
4. The *in vivo* efficacy study in a murine acute pneumonia model caused by an extensively drug-resistant *P. aeruginosa* strain showed that SCM-NLCs were more effective than free SCM, either by pulmonary or IM administration. It should be noted that SCM-NLC doses were significantly lower than that used in the groups receiving free drug; 10-fold lower and 60-fold lower for the pulmonary route and the IM route, respectively.
5. The *in vivo* toxicity studies demonstrated that SCM-NLCs were safe even at high doses when administered following the pulmonary and IM routes
6. Biodistribution studies suggested that the pulmonary route might be selected in case of maintenance therapy since its main effect is exerted in the lungs, and its lower nephrotoxicity, whereas, IM route may be more suitable in an emergency as it showed faster absorption.
7. Blank-NLC intended to use topically for wound healing revealed to be safe when applied on intact skin. In addition, the *in vivo* biodistribution studies showed no

*Nanostructured lipid carriers (NLCs) for multiresistant infections*

systemic absorption of NLCs, suggesting their suitability to exert a local effect on wounds.





¡Por fin llega la parte de la tesis más fácil de escribir! La verdad es que no tenía pensado incluir esta sección, pero, hay que reconocer los buenos consejos cuando se nos presentan inesperadamente.

Muchas gracias **Silvia** por todo. Ya sabes que esta tesis es en gran parte tuya, no solo por haber mejorado sustancialmente ( $p < 0.05$ ) el contenido día tras día (y noches también), sino por siempre recordarme sacar lo mejor de mí, especialmente en los momentos más difíciles. Eso último, ya sabes que solo consiguen hacerlo los líderes y, por lo tanto, creo que ha llegado el momento de ascenderte de “starfish” a “leaderfish”. Mola, ¿verdad? No lo borres cuando me corrija los agradecimientos jaja

No puedo olvidarme de ti, **Marta**. Me dejaste una gran herencia y espero que te guste, tanto como a mí, todo el trabajo realizado y las conclusiones sacadas hasta ahora. Gracias por haberme enseñado la mayoría de las técnicas de laboratorio, siempre con paciencia y con tu gran sentido del humor.

**Garazi**, gracias por confiar en mí por primera vez años atrás, cuando solo entendía el 80 % de lo que se me decía y no podía expresarme como me hubiera gustado. Has sido el pilar de esta etapa especial de mi vida y un ejemplo a seguir en todos los aspectos.

Mil gracias **Rosa** y **Manoli**, por darme la posibilidad de realizar un Doctorado Industrial y por ayudarme a superar los obstáculos que se han presentado a lo largo de estos años, entre los cuales están mis crisis telefónicas.

Gracias **Eusebio** por tu manera de ser, por tu filosofía empresarial, por tu energía y por tu confianza en los “jóvenes talentos”. Ha sido un honor trabajar contigo y especialmente un placer compartir esas paellas vegetarianas tan ricas, sin mencionar el gazpacho de cerezas jeje

Ya sabes, **Amaia**, que voy a echar mucho pero mucho de menos nuestras comidas de desahogo en el Museo del Órgano. Gracias por escuchar pacientemente mis quejas y por intentar reducir en todo lo posible mi nivel de estrés. No tengo dudas de que tu futuro vaya a ser brillante. Te lo mereces.

### *Ringraziamenti*

Agradecer también a **Joan Gavalda** y a su grupo de investigación del VHIR. **Marta, Jana** y **Xavi** me habéis recibido con los brazos abiertos y no habéis dudado en solucionar todas mis dudas de microbiología. Infinitamente gracias.

En fin, resulta evidente que el apoyo que he tenido en todos estos años ha sido fundamental. Gracias a tod@s los que habéis tenido unas palabras de ánimo. *“Words are, in my not so humble opinion, our most inexhaustible source of magic, capable of both inflicting injury and remedying it”*. Gracias **Enara** y **Vanesa** por estar siempre ahí, preguntando y ofreciendo vuestra ayuda incondicional. Gracias a **Gloria** por recordarme que, de alguna forma, soy “una campeona”, aunque a veces se me olvide, y gracias a **Mikel** por repetirme mil veces “todo saldrá bien, cariño”. Si estáis leyendo estas palabras, es porque este camino ha llegado a su fin. Sin vosotr@s, no hubiese sido tan llevadero. Gracias de corazón.



Cari mamma, papà e sorella bella, grazie per credere sempre in me.

Grazie **mamma** per tutte quelle volte che hai cercato di capire cosa facevo a lavoro e di cosa parlava il dottorato. Non penso di aver risolto i tuoi dubbi pero l'importante é che ci abbiamo provato. Giusto? PS: scusa se mi sono innervosita molte volte <3

Grazie **papá** per aver, forse, accettato il fatto di avere una figlia lontana. Almeno potrai raccontare in giro che hai preso un aereo e che tua figlia é “international”.

Grazie **Manu**, per essere tanto orgogliosa di me da riferire a tutti quello che faccio. Tra poco potrai dire che hai una sorella con un dottorato, ma forse già lo dici XD

Vi voglio bene

Claudia





Antimicrobial resistance (AMR) is a serious problem that urgently needs to be addressed. Colistin and amikacin represent the last available weapons to fight against multiresistant gram-negative bacterial infections, despite their high neuro- and nephrotoxicity. In fact, clinicians are forced to choose between an effective or a safe dose, mostly leading to treatment failure. With that in mind, nanostructured lipid carriers (NLCs) offer a captivating strategy to reduce drug toxicity, due to their ability to release antibiotics in a sustained and controlled manner and allow dose reduction. In this doctoral thesis, colistin-NLCs have been developed, characterized and tested in murine pneumonia models with promising results, achieving an enhanced efficacy with a significant dose reduction and thus, a presumable lower toxicity. Moreover, safety of topically applied blank-NLC was tested on intact and impaired skin. NLCs resulted to be safe and not systemically absorbed, which may imply that these carriers can exert a local effect, becoming an interesting approach to be exploited for wound healing. In essence, NLCs could be the ultimate safe strategy for delivering effective but toxic antibiotics in the battle against drug-resistant gram-negative lung and wound infections.

